

The climate and vegetation of Europe, North Africa and the Middle East during the Last Glacial Maximum (21,000 years BP) based on pollen data

Basil A.S. Davis¹, Marc Fasel², Jed O. Kaplan³, Emmanuele Russo⁴, Ariane Burke⁵

¹Institute of Earth Surface Dynamics, University of Lausanne, Lausanne, 1015, Switzerland

²enviroSPACE lab, Institute for Environmental Sciences, University of Geneva, Geneva, 1211, Switzerland

³Department of Earth Sciences, The University of Hong Kong, Hong Kong, Peoples Republic of China

⁴Department of Environmental Systems Science, ETH Zurich, Zurich, 8092, Switzerland

⁵Laboratoire d'Ecomorphologie et de Paleoanthropologie, Departement d'Anthropologie, Universite de Montreal, Montreal, Quebec, H3C 3J7, Canada

Correspondence to: Basil A. S. Davis (basil.davis@unil.ch)

Abstract. Pollen data represents one of the most widely available and spatially-resolved sources of information about the past land cover and climate of the Last Glacial Maximum (21,000 years BP). Previous pollen data compilations for Europe, the Mediterranean and the Middle East however have been limited by small numbers of sites and poor dating control. Here we present a new compilation of pollen data from the region that improves on both the number of sites (63) and the quality of the chronological control. Data has been sourced from both public data archives and published (digitized) diagrams. Analysis is presented based on a standardized pollen taxonomy and sum, with maps shown for the major pollen taxa, biomes and total arboreal pollen, as well as quantitative reconstructions of forest cover and winter, summer and annual temperatures and precipitation. The reconstructions are based on the modern analogue technique (MAT) with a modern ~~calibration~~-pollen dataset taken from the latest Eurasian Modern Pollen Database (~8000 samples). A site-by-site comparison of MAT and Inverse Modelling methods shows little or no significant difference between the methods for the LGM, indicating that no-modern-analogue and low CO₂ conditions during the LGM do not appear to have had a major effect on MAT transfer function performance. Previous pollen-based climate reconstructions using modern pollen ~~calibration~~-datasets show a much colder and drier climate for the LGM than both Inverse Modelling and climate model simulations, but our new results suggest much greater agreement. Differences between our latest MAT reconstruction and those in earlier studies can be largely attributed to bias in the small modern ~~calibration~~-dataset previously used. We also find that quantitative forest cover reconstructions show more forest than that previously suggested by biome reconstructions, but less forest than that suggested by simple percentage arboreal pollen, although uncertainties remain large. Overall, we find that LGM climatic cooling/drying was significantly greater in winter than in summer, but with large site to site variance that emphasizes the importance of topography and other local factors in controlling the climate and vegetation of the LGM.

45 **1 Introduction**

46

47 During the Last Glacial Maximum (LGM) ~21,000 years BP (Mix et al., 2001), the climate,
48 vegetation and landscape of Europe and its surrounding regions were very different than
49 today. Scandinavia and a large part of the British Isles were covered by a single ice sheet,
50 with separate ice sheets covering the Alps and Pyrenees, while many smaller and lower
51 mountainous areas were also glaciated (Ehlers et al. 2011). As a result of this global build-up
52 of ice on land, sea levels were around 120 meters lower than today, resulting in the retreat of
53 Atlantic and Mediterranean coastlines and the emergence on land of the English Channel and
54 North Sea basin. Falling sea levels also led to the disconnection of the Black Sea from the
55 Mediterranean, and a subsequent drop in Black Sea water levels as evaporation exceeded
56 inflow (Arslanov et al. 2007). On land, permafrost and periglacial processes occurred
57 immediately to the south of the Scandinavian ice sheet, while the massive discharge of glacial
58 clays and sands provided material to be redeposited by the wind as belts of loess across
59 northern France, Benelux, Germany and central Europe (Lehmkuhl et al. 2021). Under these
60 cooler and drier climatic conditions, forests are thought to have retreated to the relative
61 shelter of Southern Europe and the Mediterranean, while relatively unproductive steppe and
62 tundra dominated the region north of the Alps (Grichuk 1992).

63

64 This traditional view of the LGM has been established for many years, but many details
65 concerning the climate and vegetation of the LGM remain debated. Much of this debate
66 concerns information derived from the pollen record, which represents one of the most
67 widely available and spatially-resolved sources of information concerning LGM vegetation
68 and climate, and the primary terrestrial proxy used to evaluate climate models in the
69 Palaeoclimate Modelling Intercomparison Project (PMIP) (Bartlein et al., 2011; Harrison et
70 al., 2014).

71

72 For example, climate model simulations continue to indicate a climate that is less cold and
73 more humid than pollen-based reconstructions (Jost et al., 2005). These results are similar to
74 reconstructions based on glaciological modelling (Allen et al., 2008b). On the other hand, the
75 pollen-based reconstructions that show the greatest disagreement with climate models have
76 themselves been criticized for not considering the possible effect of low atmospheric CO₂ on
77 the physiological relationship between plants and climate (Ramstein et al., 2007). Methods
78 that use modern pollen samples ~~for calibration purposes~~ are based on the assumption that the
79 relationship between vegetation and climate remains the same through time, and that this is
80 independent of change in CO₂ concentration. Studies have shown however that plant growth
81 processes and plant resilience are sensitive to CO₂ concentration, and particularly water-use
82 efficiency which would make plants more drought sensitive in low CO₂ environments
83 (Cowling & Sykes 1999). Atmospheric CO₂ during the LGM was around 190 ppm, some
84 100 ppm lower than the pre-industrial period, and 200 ppm lower than the levels experienced
85 in the last 50 years. Concerns about the effects of lower CO₂ during the LGM has directly led
86 to the development of pollen-climate reconstruction methods that can take account of CO₂
87 effects, either through use of a process-based vegetation model run in inverse mode (Guiot et
88 al. 2000, Guiot et al. 2009), or through the use of a correction algorithm (Prentice et al.
89 2017). Pollen-climate reconstructions based on inverse modelling that account for these low
90 CO₂ effects show less cooling and drying and consequently greater agreement with climate
91 models (Ramstein et al., 2007; Wu et al., 2007).

92

93 Further data-model discrepancies have also been highlighted concerning LGM vegetation
94 cover. Earlier pollen synthesis studies, especially those that applied the biomisation method

95 (Elenga et al., 2000) give the impression that non-glaciated areas of LGM Europe were
96 dominated by treeless steppe, while vegetation models driven by climate model simulations
97 indicate large areas of forest and woodlands (Binney et al., 2017; Kaplan et al., 2016;
98 Velasquez et al., 2021). The apparent data-model discrepancy associated with steppe has led
99 to the suggestion that early humans, which are not included in vegetation models, could have
100 reduced the forest cover with only a relatively moderate use of fire because of the cold
101 climate and slow speed of vegetation recovery (Kaplan et al., 2016). This debate is important
102 because of studies that have shown the sensitivity of the climate system to vegetation
103 boundary conditions during the LGM (Ludwig et al., 2017; Velasquez et al., 2021). This
104 suggests that accurate knowledge of the vegetation cover during the LGM is a necessary
105 prerequisite to understanding the role of other influences on the climate system at this time.
106

107 More recent pollen and macrofossil studies from eastern Central Europe have shown that at
108 least in this region there existed areas of open boreal forest and woodland with some
109 temperate broadleaf species (Kuneš et al., 2008; Willis and Van Andel, 2004). The evidence
110 of forest, and particularly elements of temperate broadleaf forest, north of the Alps has come
111 to represent a challenge to the traditional view that forest species only survived the LGM in
112 sheltered refugia far to the south of the Fenoscandian ice sheet and close to the moderating
113 influence of the Mediterranean Sea. The presence of micro-refugia north of the Alps is
114 important because it would represent a very different baseline for understanding the later rate
115 and route of plant migrations under the rapid warming that occurred during the Late Glacial
116 to Holocene transition (Douda et al., 2014; Giesecke, 2016; Krebs et al., 2019; Nolan et al.,
117 2018), as well as understanding patterns of present-day genetic diversity (Normand et al.,
118 2011; Svenning et al., 2008). Modelling studies have shown difficulty in supporting the very
119 high rates of postglacial expansion that would be necessary for southern refugia (Feurdean et
120 al., 2013, Nogués-Bravo et al. 2018).
121

122 Much of this debate has been informed by an increasing number of LGM pollen studies from
123 an ever-broader geographical area, and especially from an increasing number of studies from
124 north of the Alps. Nevertheless, the synthesis of these studies into a single narrative is made
125 difficult by several factors, for instance: different taxonomic definitions, pollen percentages
126 calculated from non-standardized pollen sums, and quantitative analyses such as climate
127 reconstructions that are based on different training sets and methodologies. This has led to
128 some modelling studies ignoring the pollen record completely, on the basis that data from the
129 LGM is too scarce (Janská et al., 2017). Where standardized methods have been applied to
130 multiple LGM pollen records, poor dating control has resulted in the inclusion of many
131 records that may not actually be from the selected LGM time window. This is particularly
132 important because the 21 ± 2.0 ka time slice commonly used to represent the LGM period in
133 PMIP data-model comparisons and other synthesis studies (MARGO members, 2009;
134 Bartlein et al., 2011) occurs immediately after the glacial maxima in the Alps around 26-23
135 ka (Heiri et al., 2014; Spötl et al., 2021) and Heinrich stadial HS-2 (24.3-26.5), whilst also
136 being closely followed by Heinrich stadial HS-1 (15.6-18.0 ka) (Sanchez-Goñi & Harrison,
137 2010). These closely associated time periods can therefore be expected to represent both a
138 different vegetation and climate than the LGM itself.
139

140 For example, of the 18 European pollen records used in the PMIP benchmarking dataset
141 (Bartlein et al., 2011), 10 fall into the worst class ('poor') in the COHMAP chronological
142 quality classification scheme if relative dating such as pollen correlation is excluded. More
143 recent synthesis studies have also relied heavily on records from the European Pollen
144 Database (EPD) which currently has 116 records with samples of LGM age (as of June

145 2022). Many of these records however are based on chronologies that are considered reliable
146 for the Holocene (Giesecke et al., 2014), but have large uncertainties for the LGM as a result
147 of 1) excessive extrapolation back in time from Holocene age dates, 2) the use of pollen
148 correlation or other relative dating despite poorly defined regional biostratigraphy, or 3) the
149 inappropriate use of radiocarbon dates contaminated with old carbon. We found that 104 of
150 these 116 EPD records (Neotoma, 2021) fall into the worst class ('poor') in the COHMAP
151 chronological quality classification.

152

153 Here we address these problems using a new synthesis of LGM pollen records from
154 throughout Europe, the Mediterranean and the Middle East (EurMedMidEst) based on
155 rigorous quality control criteria. Records were compiled from an extensive review of public
156 databases and archives, and the scientific literature. Pollen records were selected according to
157 the robustness of their chronological control around the PMIP LGM time-window (21 ± 2
158 ka), and combined into a single dataset based on a harmonized taxonomy and standardized
159 pollen sum. The dataset was then analysed so that standardised maps could be produced to
160 show the distribution of the major pollen taxa, biomes and total arboreal pollen at the LGM.
161 In addition, quantitative reconstructions of forest cover as well as winter, summer and annual
162 temperatures and precipitation were undertaken using the Modern Analogue Technique
163 (MAT), utilizing the latest Eurasian Modern Pollen Database v2 ~~calibration~~-dataset. These
164 climate reconstructions are compared and evaluated against previous LGM pollen-climate
165 reconstructions, as well as reconstructions based on other proxies. The dataset and results are
166 fully documented and the complete data files are provided in the supplementary information.

167

168 **2 Methods**

169

170 **2.1 Pollen Data**

171

172 LGM fossil pollen data from Europe and bordering regions including North Africa and the
173 Middle East were selected and collated into a single standardized project database. This data
174 was sourced from the EPD/Neotoma database (Williams et al., 2021), the Pangaea data
175 archive, publications in scientific journals, and from the original authors. We selected LGM
176 pollen sites/data according to strict quality control criteria. Where possible, primary raw
177 pollen counts were used where this was available. Where the original electronic data was not
178 available, the data was digitized from the published diagram. Overall we have included 63
179 records in our study, of which 35 were digitized and 28 consisted of the original pollen
180 counts (Table 1).

181

182 The distribution of the 63 sites reflects the distribution of suitable archives, with fewer
183 records available from climatically or environmentally challenging regions (Fig. 1). High
184 rates of erosion and a drier and colder climate during the LGM reduced the number of
185 suitable anoxic sediment sinks for pollen preservation, especially in Central Europe between
186 the Scandinavian and Alpine ice sheets. Nevertheless, our dataset includes sites from this
187 region, as well as North Africa and eastern Central Europe through to Iran, although most
188 sites are located in an arc across eastern Spain, the Alps, and Italy. Lakes sites are the most
189 numerous archive and tend to be located in the more sheltered and topographically favourable
190 regions of Southern Europe and the Mediterranean. Peat is the next most important archive,
191 followed by alluvial and colluvial sediments, as well as cave sites, the later also often being
192 known for their archaeological significance. Sites located at the ice margins that appear to be
193 under the ice reflect uncertainties in the location of the ice margin both in time and space
194 during the LGM, as well as the fact that the selected time window for this study (21 ± 2 ka) is

195 later than the maximum ice advance in some regions (Hughes and Gibbard, 2015). For
196 completeness, we also include 7 marine records which have the advantage of more
197 continuous deposition and often better dating over the LGM period, but which are prone to
198 taphonomic biases compared to terrestrial records. These biases are discussed later in this
199 section.

200

201 LGM pollen records were selected according to a number of quality control criteria, but
202 primary amongst these was the existence of sufficient independent chronological control
203 points to accurately identify samples that would fall within the 21 ± 2 ka BP time-slice of
204 interest. We have used all of the samples within this time frame where the samples have been
205 available in electronic form, else we have used the sample closest to the target time (21 ka
206 BP). For records taken from the EPD we have used the latest Bayesian age-depth models
207 where these were available (Giesecke et al., 2014), otherwise we have used the dates and
208 chronology proposed by the original authors. We classified chronologies according to the
209 COHMAP chronological quality scheme for the LGM period (Anderson et al., 1988; Yu and
210 Harrison, 1995), which classifies record quality from 1-6 depending on whether a date falls
211 within 2000 14C years (or less) of the time being assessed, or whether bracketing dates fall
212 within 6000 and 8000 14C years (or less) about the time being assessed (Table A1).

213 Chronologies based on dates that fall outside of these limits fall into COHMAP class 7, and
214 are regarded as ‘poorly dated’ with respect to the LGM. Importantly, we have only included
215 radiometric and other absolute dates (such as varves) in this assessment, and have excluded
216 dates based on correlation with regional pollen records. These pollen-based stratigraphic
217 dates have been widely used in previous LGM studies, but do not include estimates of
218 uncertainty and are generally regarded as unreliable at this time given the sparsity of well
219 dated pollen sites and samples on which to base any correlation (Giesecke et al., 2014).

220

221 All records that were classified as poorly dated (COHMAP class 7) were subsequently
222 excluded from our analysis. This has meant that many of the pollen records used in previous
223 studies were excluded, including 16 of the 26 LGM records used by PMIP and associated
224 studies in Europe (Bartlein et al., 2011; Elenga et al., 2000; Tarasov et al. 2000, Jost et al.,
225 2005; Peyron et al., 1998; Wu et al., 2007; Cleator et al., 2020). We also excluded 104 of the
226 116 records in the EPD with samples that fall within our LGM time window. Many of these
227 EPD pollen records have been used in more recent studies, although the exact record (EPD
228 Entity number) is often not stated. We estimate that we have excluded 16 of the 17 European
229 sites used by Binney et al. (2017) (this study only included sites above latitude 40N), 5 of the
230 6 European sites used by Allen et al. (2010), 28 of the 33 sites used by Cao et al. (2019) and
231 27 of the 71 sites used by Kaplan et al. (2016).

232

233 Other quality control criteria were also used in the selection of LGM pollen records.
234 Published pollen diagrams that only included a small part of the terrestrial pollen assemblage,
235 or only presented summary taxa, were excluded. Records were also excluded where the
236 dating information was incomplete, for instance where radiocarbon dating uncertainties were
237 not published or where it was not possible to determine if the date shown was in calibrated or
238 uncalibrated radiocarbon years.

239

240 The modern pollen data for the climate and tree cover reconstructions were sourced from the
241 latest version 2 of the Eurasian Modern Pollen Database (Davis et al., 2020), which is
242 managed as part of the EPD. The EMPD2 includes 8133 modern pollen samples from across
243 the Palearctic biogeographic region from Europe to the far East of Asia. The taxa from both
244 the fossil and modern pollen data were consolidated into 120 of the most commonly-

245 occurring terrestrial taxa types. This taxa list was designed to be compatible with the
246 biomisation scheme used in our study (Peyron et al., 1998; Tarasov et al., 2000) and that used
247 in the Holocene mapping study of Brewer et al. (2017). The count of *Larix* was amplified by
248 a factor of 10 due to its low pollen representation (Edwards et al. 2000, Bigelow et al. 2003,
249 Tarasov et al. 1998, 2000, 2013, Binney et al., 2017).

250

251 **2.2 Biomisation**

252

253 We converted pollen assemblages to biomes based on the European biomisation scheme of
254 Peyron et al (1998), which in turn is based on Prentice et al. (1996). The method is described
255 in detail in Collins et al. (2012). We expanded the number of taxa included in the biomisation
256 procedure proposed by Peyron et al (1998) to include taxa from the Northern Eurasian
257 biomisation procedure of Tarasov et al. (1998). The inclusion of additional Northern Eurasian
258 taxa reflects recent evidence that modern analogues of LGM vegetation occur in parts of
259 Siberia (Magyari et al., 2014a). The biomisation procedure (Prentice et al. 1996) assigns each
260 taxa to a plant functional type (PFT) and calculates a score for each of these PFT's based on
261 the sum of the square root of the percentage of each of the taxa included in that PFT. To
262 reduce the influence of long-distance transport, taxa below 0.5% are removed at the start of
263 the procedure. Each biome is then assigned one or more PFT's and a score for each biome is
264 calculated as the sum of the associated PFT scores. The biome with the highest score is then
265 viewed as the dominant biome. Where the highest score is the same for more than one biome,
266 the dominant biome is decided based on a hierarchy of unique PFT's. Peyron et al. (1998)
267 also included a procedure for distinguishing warm and cold steppe biomes based on re-
268 assigning certain steppe PFT's according to the presence or otherwise of PFT's indicative of
269 cold or warm conditions. Following the Biome6000 project (Elenga et al., 2000) and Allen et
270 al. (2010), we did not apply this additional procedure and present only the merged steppe
271 biome. In summary, the biomisation procedure categorised 39 arboreal pollen taxa and 39
272 non-arboreal taxa into 22 plant functional types (PFT's), which were then combined into 12
273 biomes.

274

275 **2.3 Quantitative climate reconstruction**

276

277 We reconstructed climate from pollen data based on a standard Modern Analogue Technique
278 (MAT) that used PFT scores to match fossil samples with modern ~~calibration~~ pollen samples
279 (as used by Davis et al., 2003). ~~This is a similar approach to that used by Peyron et al. (1998)~~
280 ~~and Jost et al. (2005) who also applied pollen PFT scores to reconstruct LGM climate from~~
281 ~~pollen data, but who used an artificial neural network technique (ANN) (Chevalier et al.,~~
282 ~~2020).~~ Other methods using PFT scores and artificial neural network techniques have been
283 developed to reconstruct the climate of Europe during the LGM from pollen data (Peyron et
284 al. (1998) and Jost et al (2005). PFT scores have been used in previous large-scale European
285 pollen-based climate reconstructions for the Holocene (Davis et al., 2003; Mauri et al., 2014,
286 2015), where performance was found to be better than the conventional approach based on
287 individual taxa (eg Marsicek et al., 2018). A particular advantage of the PFT approach for the
288 LGM is that it can help overcome problems associated with vegetation (pollen) assemblages
289 that may have no modern analogue (Davis et al. 2003). This can be a problem during the
290 LGM when the climate and environment could be expected to be very different from today,
291 and when many taxa formed unusual vegetation assemblages as a result of their forced retreat
292 to sheltered refugia locations. The problem of modern analogues is also addressed in our
293 reconstruction by using the latest EMPD2 modern pollen dataset ~~for calibration purposes.~~
294 The EMPD2 provides a large number of potential modern analogues for many different LGM

295 vegetation types and climates found today across the Palearctic region. PFT scores were
296 calculated according to the methods outlined already in the Biomisation section, then
297 normalized so that each sample was proportional to every other sample (Juggins and Birks,
298 2012).

299
300 The MAT method was applied using the Rioja program for R (Juggins, 2020). The modern
301 ~~calibration-pollen~~ data was taken from the latest version 2 of the EMPD (as detailed earlier).
302 The EMPD2 includes 8133 samples, which is considerably larger than the modern datasets
303 used in previous LGM pollen-based reconstructions. For instance, Peyron et al. (1998) used a
304 ~~calibration-modern pollen~~ dataset of 683 samples, which was updated by Jost et al (2005) to
305 include an additional 185 samples. These datasets were also mainly taken from the steppes of
306 Kazakstan and Mongolia, while the EMPD2 covers a much wider area, spanning most of the
307 Eurasian Palearctic region (Davis et al., 2020). The size and distribution of the modern
308 training set in climate and vegetation space is important because in order for the method to
309 work effectively, it is necessary to have samples representative of the likely vegetation and
310 climate space that could be occupied by the fossil assemblage (Turner et al. 2021, Chevalier
311 et al., 2020; Salonen et al. 2012, Juggins, 2013).

312
313 A known problem with MAT is the role of spatial auto-correlation in providing
314 unrealistically low estimates of uncertainty (Chevalier et al., 2020; Telford and Birks, 2009).
315 This results from the fact that closely analogous modern pollen samples can also be located
316 closely in physical space, and therefore in climate space. To reduce this problem it is possible
317 to exclude closely located samples from the analogue matching process using a filter based
318 on a set distance (h-block filter) (Telford and Birks, 2009). While this approach can help,
319 there are also three main problems associated with it. The first is error substitution, since
320 removing samples also reduces the number of potential analogues, creating a different source
321 of error that is not easy to categorise. Secondly, multiple samples taken from the same
322 location are actually a strength of pollen training sets, since they are more likely to capture
323 the full range of the assemblage diversity associated with a given climate. Thirdly, current
324 methods that limit spatial range such as the h-block filter only do so on the horizontal axis,
325 and do not consider the fact that samples can also be found at different elevations. In hilly or
326 mountainous regions samples can therefore be excluded because they are closely located in
327 horizontal space, but in fact they actually occupy very different climates and vegetation
328 associations, contradicting the logical premise of the h-block filter. It was therefore decided
329 not to apply this filter.

330
331 Uncertainties for the pollen-climate reconstructions were calculated using a standard method
332 for MAT (Juggins 2020) based on the spread of the climates associated with the best modern
333 pollen analogues used for each fossil sample. The closer the climates of the best modern
334 pollen analogues (6 in the case of this study) then the smaller are the calculated uncertainties
335 assigned to the reconstructed climate of the fossil pollen sample.

336
337 Climate reconstructions are presented as anomalies. These have been calculated with respect
338 to modern climate (1970-2000 average) at each core site location using WorldClim 2 (Fick
339 and Hijmans, 2017) (Table A2), which was also used to assign the modern climate for the
340 modern pollen samples in the transfer function (Davis et al., 2020).

341
342 **2.4 Quantitative tree cover reconstruction**

343

344 It has long been recognized that the proportional representation of individual pollen taxa in a
345 pollen assemblage does not necessarily reflect the proportion of land area covered by that
346 taxa in the pollen source area surrounding the sample site (Davis 1963, Gaillard et al. 2010,
347 Zanon et al. 2018). These differences can be caused by variations in pollen productivity,
348 differential transport, deposition and preservation of pollen grains, and even the ease or
349 otherwise of the identification of pollen grains themselves. This can make the interpretation
350 of pollen taxa percentages difficult, even for relatively simple questions such as the
351 proportion of forest to non-forest in the landscape.

352

353 There have been two main methods developed to account for this quantification problem, one
354 using a physical modelling technique (PMT) based on estimates of pollen production for
355 individual taxa (Gaillard et al., 2010), and the other using a MAT very similar to that used in
356 pollen-climate reconstructions (Williams and Jackson, 2003). Both approaches have been
357 widely applied during the Holocene in Europe (Zanon et al., 2018), but we know of no
358 previous study that has applied either of these approaches to the LGM. The LGM presents a
359 number of challenges, not least the problem of potential missing vegetation analogues, as
360 well as low atmospheric CO₂, which has been shown to influence pollen productivity (Leroy
361 and Arpe, 2007).

362

363 Here we use the MAT to provide quantitative estimates of forest cover, following the
364 approach of Zanon et al. (2018) who applied this method to the Holocene pollen record of
365 Europe. We apply MAT in exactly the same way as for the climate reconstructions described
366 earlier, including the use of PFT scores to match fossil and modern pollen samples. Instead of
367 modern climate values, we assigned an estimate of modern forest cover to each of our
368 modern pollen sites. To do this we use a high resolution (~100m) remote sensing dataset
369 derived from satellite observations (Hansen et al., 2013). Zanon et al. (2018) have shown that
370 the MAT calibrated in this way gives comparable results to the PMT approach in Europe, at
371 least for the Holocene. One of the main differences however is that the PMT is designed to
372 provide estimates of the proportions of different taxa, whereas the MAT (as applied here) is
373 designed to provide estimates of the proportion of forest cover. Where the PMT can only
374 reconstruct the proportion of forest forming trees, irrespective of their size, the MAT
375 (following Zanon et al. 2018) is calibrated specifically to reconstruct forest composed of trees
376 over 5m tall. This follows the FAO definition of forest as “land spanning more than 0.5
377 hectares with trees higher than 5 meters and a canopy cover of more than 10 percent, or trees
378 able to reach these thresholds in situ” (FAO Terms and definitions 2020
379 <http://www.fao.org/3/I8661EN/i8661en.pdf>).

380

381 **2.5 Maps**

382

383 We present our results in the form of maps that include the main physiographic features of
384 the LGM in the study area. The maps are based on the WGS84 projection. Coastlines reflect
385 LGM sea level at 120m below present, while ice sheets are based on Ehlers et al. (2011).
386 Modern national country boundaries are also included for reference.

387

388 **2.6 Marine pollen records**

389

390 We have included marine pollen records in our analysis for reasons explained below, but it is
391 important that these records should be viewed with caution, particularly when used for biome
392 and quantitative MAT reconstructions, and when compared with terrestrial records from
393 different archives. Biomisation methods have been applied to individual marine pollen

394 records (Combourieu Nebout et al., 2009), as well as multi-site synthesis studies such as the
395 ACER project (ACER project members et al., 2017). However, marine records were
396 specifically excluded from the Biome6000 project (Elenga et al., 2000). Similarly,
397 quantitative climate methods have been applied to individual marine pollen records
398 (Combourieu Nebout et al., 2009; Fletcher et al., 2010), as well as multi-site synthesis studies
399 (Sánchez Goñi et al., 2005; Brewer et al., 2008; Salonen et al., 2021). However, marine
400 records have also been specifically excluded from other major pollen-climate studies
401 (Cheddadi et al., 1996; Davis et al., 2003; Marsicek et al., 2018), as well as quantitative forest
402 cover reconstructions (Zanon et al. 2018).

403
404 Discussion on the advantages and problems associated with marine records can be found
405 elsewhere (Chevalier et al., 2020; Daniau et al., 2019), but are reviewed briefly here where
406 relevant to the methodologies applied in this study. Marine sedimentary records provide
407 continuous and well dated pollen records for the LGM that are often lacking from many
408 terrestrial regions, especially in arid areas with few alternative anaerobic sediment sinks.
409 Conversely however, pollen source areas for marine sites may be many hundreds of
410 kilometers from the coring site and may be liable to change through time in response to
411 changes in distance to the coastline, rates of river discharge and ocean and atmospheric
412 dynamics. This can theoretically give rise to changes in the vegetation shown in the pollen
413 assemblage recorded at the marine site without any actual change in climate or other
414 environmental pressure. The large and indeterminable source area of marine records also
415 mean that it is difficult to apply quantitative MAT reconstruction methods, not least because
416 the mean climate or forest cover of the source area is almost impossible to determine. In
417 addition, the fossil pollen record and the calibration-modern pollen dataset to which it is
418 being compared are composed largely of terrestrial lakes and bog sites with much smaller and
419 more homogeneous source areas. This creates a series of problems, the more obvious of
420 which is the calculation of anomalies, since we cannot assume that the modern climate at the
421 (marine) coring site location is representative of the (terrestrial) source area. In this study we
422 have taken the closest point on land as the modern climate for the calculation of anomalies,
423 but provide the absolute values for all sites so that these can be recalculated if necessary
424 (Table A2). The next problem is that the large source area may capture a combination of
425 different vegetation types that is not going to be represented in a calibration-modern pollen
426 dataset based on samples from terrestrial sites with much smaller source areas, for instance a
427 mixture of coastal and mountain vegetation, or even vegetation from different continents
428 (Magri and Parra, 2002). However, in our analysis we did not find any sample from a marine
429 record (or terrestrial record) that did not have a reasonable modern analogue in our training
430 set (chord distance <0.3)(Huntley, 1990), even though we did not adjust the pollen
431 assemblage for the over-representation of Pinus (and other Pinaceae) in the marine pollen
432 samples.

433
434 Typically, the Pinaceae component is excluded from the terrestrial pollen sum when
435 calculating percentages for marine pollen samples, and in some cases Pine has been excluded
436 entirely from the samples used in marine pollen-climate reconstructions (Combourieu Nebout
437 et al., 2009). The problem with excluding Pinus is two-fold, the first is that Pinus often
438 represents the main forest forming tree in the Koeppen Csb climate zone on the Atlantic coast
439 where many marine sites are located (García-Amorena et al., 2007), as well as representing
440 the most abundant tree taxa in Europe during the LGM (Figure A3c). Removing Pinus from
441 the assemblage would almost certainly create an artificially arid assemblage in these
442 circumstances, undermining the ability of the transfer function to reconstruct precipitation,
443 although temperature would likely be less affected since Pinus is a generalist found in both

444 ~~hot and cold temperature regions. The second problem is that the remaining terrestrial taxa~~
445 ~~often constitute a very small number of pollen grains in a typical marine pollen sample (<100~~
446 ~~grains), which can result in pollen assemblages that are not based on a statistically stable~~
447 ~~count of the pollen sample (Chevalier et al., 2020).~~
448

449 The effect of excluding Pinaceae on the biomisation algorithm and MAT climate
450 reconstruction process has not been widely investigated. We therefore decided to evaluate
451 this problem for 1) biomisation, and 2) pollen-climate reconstruction. In table S3 we show
452 the biomisation results for 8213 modern pollen samples taken from the EMPD2 modern
453 pollen database. Using this as the control, we then artificially varied the amount of Pinaceae
454 (*Pinus*, *Abies* and *Picea*) in the assemblage of each pollen sample and compiled the results
455 (Table S3). This shows quite clearly that removing all of the Pinaceae has a much more
456 profound effect on the biomisation process than artificially inflating the amount of Pinaceae
457 (as might be expected in a marine sample where Pinaceae can be over-represented). Even
458 when Pinaceae was artificially inflated by as much as 400% of the original value, the biomes
459 were changed in only 2348 samples, compared to 5860 samples if all the Pinaceae was
460 removed entirely. In terms of the effects on individual biomes, removing the Pinaceae
461 considerably increased the amount of CLDE, STEP and TUND, whilst greatly reducing the
462 amount of XERO, almost eliminating the amount of TAIG, and completely eliminating the
463 COCO biome. In contrast, the effect of inflating the amount of Pinaceae tended to be more
464 evenly distributed between the biomes, with the biggest increase seen in TUND and biggest
465 decrease in STEP. This suggests that even if the over-representation of Pinaceae was quite
466 extreme in marine pollen samples, the effect on biome classification (and by definition, the
467 underlying PFT scores) is less than removing Pinaceae completely from the pollen
468 assemblage.
469

470 In a second test, we compared the reconstruction of LGM climate from marine pollen
471 samples when Pinaceae was included, and excluded. The results are shown in table S4 and
472 indicate reconstructed temperatures are generally 1-2C cooler, and precipitation slightly
473 higher when Pinaceae is excluded. The differences between the two methods however are
474 small, and generally less than half of the uncertainties, suggesting that differences are
475 statistically indistinguishable when considered in the context of the overall uncertainties.
476

477 In summary we find that including Pinaceae in the biomisation process is less likely to lead to
478 miss-assignment of the biome than excluding Pinaceae, except in extreme cases of over-
479 representation. Percentages of Pinaceae in the LGM marine samples range on average
480 between 23-88%, suggesting that while Pinaceae was high at some sites, it does not appear to
481 completely overwhelm the assemblage as might be expected if over-representation was to be
482 a significant problem. We also find that including Pinaceae in the pollen assemblage of the
483 LGM marine pollen samples gives pollen-climate reconstructions that are statistically
484 indistinguishable from those obtained by excluding Pinaceae from the assemblage. Including
485 Pinaceae in marine samples also provides compatibility with terrestrial samples, particularly
486 when calculating and plotting pollen taxa percentages. For these reasons we have included
487 Pinaceae in the analysis of all marine pollen samples in this study, although it is important to
488 recognize that Pinaceae in such samples can be subject to over-representation and that the
489 results presented here from marine sites should consequently be viewed with caution.
490

491 **3. Results**

492
493

494 3.1 Vegetation & Biomes

495

496 Results of the biomisation analysis shows that steppe (STEP) was the most common biome at
497 the LGM across the study area, occurring at 36 out of 63 sites, indicating that the landscape
498 was largely dominated by cool temperate grasslands across much of western Central Europe,
499 central and eastern Mediterranean, as well as North Africa and the Middle East (Fig. 2).
500 However, at the same time we also find that there were a significant number of sites where
501 we find that woody and forest biomes occur, more particularly in southern and eastern Iberia,
502 northern Italy and central eastern Europe. The most dominant of these forest and woody
503 biomes are taiga (TAIG) in the north, and cool-mixed forest (COMX) and xerophytic
504 woodlands (XERO) in the south.

505

506 As would be expected, the dominance of STEP biomes is generally reflected in low arboreal
507 pollen percentages across the same areas/sites (Fig. 3 & 4). Exceptions to this rule can be
508 found at marine sites such as [MD99-2331 site #3] and [MD01-2430 site #58] where STEP is
509 reconstructed despite arboreal pollen percentages of 71 and 80 percent respectively. This
510 apparent contradiction illustrates some of the idiosyncrasies of the biomisation method,
511 especially when applying the method to marine pollen samples. In this case it is important to
512 remember that the AP% is calculated from the sum of the percentages of each relevant taxa,
513 but the score for each biome is the sum of the square root of the percentages of each of its
514 constituent taxa. This results in biomes with taxa with large percentage values scoring
515 proportionally smaller, and biomes with taxa with small percentage values scoring
516 proportionally larger. For example, a single taxa at 50% has a square root of 7.07, but the
517 sum of the square roots of 10 taxa each at 5% is 22.36 even though the sum of the
518 percentages is the same 50%. This effect can be particularly pronounced in marine pollen
519 samples because they are usually dominated by a single taxa (*Pinus*) that forms a high
520 percentage of the total assemblage. Since there are often more non-arboreal taxa than
521 arboreal taxa in a pollen assemblage, the non-arboreal taxa can dominate in the biomisation
522 process even if collectively their percentage of the assemblage is a lot less than the arboreal
523 taxa, resulting in a non-arboreal biome such as STEP having the highest biome score.

524

525 Of the main arboreal biomes, Taiga (TAIG) is the dominant biome at 3 sites at the eastern
526 end of the Alpine ice sheet, as well as at a site just to the north in northern Germany and a
527 site in Slovakia, while Cool Conifer Forest (COCO) is found at 1 site close to the
528 Scandinavian ice sheet in Lithuania. Cool Mixed Forest (COMX) is found much more widely
529 at 8 sites south of the Alps from south-west Iberia to Romania, with Xerophytic Scrub
530 (XERO) occurring at 8 sites with a similar distribution but not as far east or west. Cold
531 Mixed Forest (CLMX) occurs at just two sites in Georgia and the Alboran Sea at the far east
532 and west of the study area, while Warm Mixed Forest (WAMX) is the dominant biome at just
533 1 site in Southern Spain. We do not record Temperate Deciduous Forest (TEDE), Tundra
534 (TUND) or Desert (DESE) as the dominant biome at any site at the LGM, although they do
535 occur as sub-dominant biomes.

536

537 An alternative picture of LGM tree-cover is provided by the MAT reconstructions (Fig. 4).
538 MAT performance statistics for tree cover are shown in table 2, based on an evaluation using
539 the modern training set. This shows a relatively large root mean square error (RMSE) of
540 21.03. and an R2 of 0.52 that is not as good as for the MAT climate analysis, but overall the
541 results are comparable with previous MAT tree cover studies (Zanon et al., 2018). In general,
542 the MAT values (site average 34%) show forest-cover around 16% less than that suggested
543 from AP% (site average 50%) (Fig. A1), although sites with very low AP% also show higher

544 values based on MAT. These differences are consistent with comparisons between MAT and
545 AP% in Zanon et al (2018), although it should be noted that uncertainties related to the MAT
546 reconstructions are large ($\pm 23\%$). Zanon et al (2018) found that the differences between
547 MAT and AP% were greatest over Northern Europe and in Arctic and sub-Arctic climate
548 regions that are likely to be comparable to many areas of Europe during the LGM. These
549 regions today are associated with tree-forming taxa such as Birch that fail to grow to a height
550 of 5m or more, developing only as shrubs or krummholz forms.

551

552 Pollen taxa percentages are shown in supplementary figure A2, and distribution maps of the
553 33 most common taxa are shown in the supplementary figures A3a-f. Of the 21 arboreal taxa,
554 *Pinus* generally has the highest values and is the most widespread, being present at all 63
555 sites. Other acicular arboreal taxa include *Juniperus*, which also has a wide distribution
556 across EurMedMidEst although at lower values. The rest of the acicular arboreal taxa have
557 more regional distributions. *Picea* is found mainly to the north of the study region, away from
558 the Mediterranean, whilst *Abies* is generally found more to the south. *Larix* occurs only in the
559 central European area including the northern edge of the Po plain just south of the Alps,
560 whilst *Cedrus* is found mainly across south and west Europe in locations much further north
561 than its Holocene and modern distribution which is confined mainly to Morocco and Lebanon
562 (Collins et al., 2012). Temperate broadleaf arboreal taxa which also include cold-tolerant
563 species such as *Betula* and *Salix* are relatively widely spread across the EurMedMidEst
564 during the LGM, while less drought tolerant taxa such as *Alnus*, *Carpinus* and *Corylus* are
565 found more to the south-west through to the north-east. Other temperate broadleaf arboreal
566 taxa such as *Quercus* (deciduous) and *Ulmus* have a much more southern distribution, with
567 *Fraxinus*, *Olea*, and *Quercus* (evergreen) being more prevalent in the south-west. In contrast,
568 *Fagus* occurs more to centre and the east, while *Tilia* is found even in more northern
569 locations of central Europe. The remaining arboreal taxa are more shrubby and drought
570 adapted, with *Ephedra* and particularly *Ephedra fragilis* having a southern distribution,
571 whilst the more cold adapted *Hippophae* being found even in the north of central Europe
572 (similar to *Tilia*).

573

574 The main non-arboreal taxa generally indicate cool, dry and environmentally disturbed
575 conditions across much of the EurMedMidEst. The most widely distributed taxon is Poaceae,
576 which like *Pinus*, is found in all records. Other non-arboreal taxa with a widespread
577 distribution include Rubiaceae, Apiaceae and Asteraceae (Asteroideae), while *Plantago*,
578 Cayophyllaceae, Brassicaceae and Asteraceae (Cichorioideae) have a more southern and
579 western distribution. *Thalictrum* can be found mostly at sites in the centre of the
580 EurMedMidEst, along with *Helianthemum* which also extends to sites in the south-west.
581 Other taxa such as *Chenopodiaceae* and *Artemisia* have a more southern distribution,
582 reflecting their preference for drier and less cold climates.

583

584 **3.2 Climate reconstruction evaluation**

585

586 Evaluation of transfer function performance based on the modern training set is presented in
587 table 2. This shows that root mean square error predicted (RMSEP) values were smallest for
588 summer temperatures (2.21C), and largest for winter temperature (3.35C), with mean annual
589 temperatures in between (2.28C). The weaker performance for winter temperatures largely
590 reflects the much greater range of winter temperatures in the training set. In turn, this
591 contributes to a better R2 performance for winter temperatures (0.91) than annual
592 temperatures (0.9) and summer temperatures (0.81). Overall R2 performance for precipitation
593 is weaker than for temperature, which is typical because of the higher spatial variability of

594 precipitation compared to temperature. Summer precipitation has the strongest R2
595 performance (0.75) compared to winter and annual precipitation (both 0.69), as well as
596 smaller RMSE values (52mm) than winter (78mm).

597
598 Given the widespread occurrence of steppe during the LGM, we also undertook a separate
599 evaluation of transfer function performance in this type of environment. For this we used a
600 subset of 1588 pollen samples from the EMPD2 that are classified with the steppe pollen-
601 biome (Davis et al. 2020). The results indicate (Table A53) little difference in performance
602 compared to the full dataset, with a small decrease in performance in annual and summer
603 seasons in both precipitation and temperature, and a slight increase in performance in winter.

604
605 The results overall indicate good transfer function performance especially for temperature,
606 and are comparable with those found in other continental scale pollen-climate studies
607 (Bartlein et al., 2011). It is important to remember though that comparisons between studies
608 can only be made with caution because results are often heavily dependent on the nature of
609 the modern pollen dataset used as the training set, which is not the same in all studies
610 (Juggins, 2013).

611
612

613 **3.3 Climate reconstruction**

614

615 Reconstructed LGM temperatures indicate an overall mean annual cooling of $-7.2 \pm 3.3\text{C}$,
616 with a greater cooling of around $-9.3 \pm 4.5\text{C}$ in winter and $-5.0 \pm 3.2\text{C}$ in summer (Fig. 5). All
617 sites apart from Lake Van [site #62] in eastern Turkey show cooler temperatures at the LGM
618 compared to modern (Fig. 6), and even at this site cooler conditions fall within the
619 uncertainties. With greater cooling in winter compared to summer, the difference in
620 temperature between winter and summer also increased (shown by positive anomalies) at
621 most (but not all) sites (Fig. 6). This increase in continentality was around $+4.2\text{C}$ on average
622 across all sites (Fig. 5).

623

624 We reconstruct an overall decline in mean annual precipitation of around $-91 \pm 270\text{mm}$ (-
625 13%) at the LGM. Most of this decline is in winter ($-38 \pm 90\text{mm}$) (-21%), while in summer a
626 small increase is shown ($10 \pm 57\text{mm}$) (6%), although uncertainties are large (Fig. 7).

627 Compared to temperature there is significant seasonal and spatial variability in positive and
628 negative precipitation anomalies (Fig. 8). Positive anomalies appear more predominant in
629 eastern and southern Spain and in central eastern Europe in both summer and winter, while
630 positive anomalies are found more generally in summer across sites in Southern Europe and
631 the Mediterranean. These more positive summer anomalies also reflect a relative shift from
632 winter to summer in the seasonality of precipitation in this region.

633

634 **4.0 Discussion**

635

636 Before we consider the results of our analysis it is important to provide some context in terms
637 of European LGM geography and environment, which was very different from today (Fig. 1).
638 Major ice sheets covered Scandinavia and much of the UK, the Alps, and the Pyrenees. Sea
639 level was 120m lower, resulting in much of the North Sea and English Channel becoming dry
640 land, and the European coastline extending over 100 km out into the Atlantic and
641 Mediterranean, especially around the Bay of Biscay and Adriatic. The Black Sea was no
642 longer connected to the Mediterranean, and was smaller with a water level around 100m
643 lower than today (Genov, 2016). These changes in sea or water level had two main

644 consequences, the first being that the marine sites were closer to land, and therefore closer to
645 (low lying) terrestrial vegetation and (pollen carrying) river discharge points than they are
646 today. The second consequence of lower seas levels is that terrestrial pollen sites were
647 located further from the moderating effect of the ocean than they are today, resulting in a
648 localised modification of the climate experienced by the site irrespective of regional or global
649 changes (Geiger, 1960).

650

651 The maps used in our analysis shows the maximum ice sheet at $21k \pm 2k$ (Ehlers et al., 2011).
652 The precise geographical location of the ice sheet is difficult to resolve at a fine spatial scale,
653 however, which explains why some sites close to the ice margin appear to be actually located
654 under the ice (for example sites Kersdorf-Briesen site #46 & Mickunai site #54). The
655 resolution of the map also shows the occurrence of permanent ice not only to the north and
656 over the Alps, but also on many subsidiary areas of high ground across central and southern
657 Europe, including areas such as the Pyrenees, Massif Central, Vosges and Carpathian
658 Mountains. While global ice volume may have peaked ~ 21 ka individual ice sheets in Europe
659 and other areas are known to have reached their maximum extent at different times (Hughes
660 et al., 2016). The larger ice sheets are likely to have had a significant influence on regional
661 climate and environmental conditions across Europe, but the smaller ice sheets had similar if
662 more localized impacts as well. Surrounding each ice sheet would have been an unglaciated
663 area of active peri-glacial processes and newly created and unstable ground. This would
664 include outwash plains, impounded lakes and recently drained lake beds, seasonally and
665 sporadically flooded areas, moraines, kettle holes and other glaciological and peri-glacial
666 features. Soils in these areas would be non-existent or skeletal, and vegetation would find it
667 difficult to obtain nutrients and water for survival, irrespective of the prevailing climatic
668 conditions. Outside of these areas, permafrost is also likely to have been present, particularly
669 north of the Alps (Vandenberghe et al., 2014), which would also act as an impediment to
670 vegetation growth.

671

672 In terms of regional climate, the major ice sheets would have provided significant barriers to
673 westerly atmospheric circulation, or even north-south circulation in the case of the Alps and
674 Pyrenees. As well as representing a physical obstruction, the thermodynamic response of the
675 atmosphere to these high, cold obstructions would have been to encourage the formation of
676 areas of semi-permanent high pressure, similar to those found today for instance over the
677 Greenland ice sheet. In addition, the Laurentide ice sheet located over North America would
678 have generated downstream effects over Europe (COHMAP, 1988). These physical and
679 thermodynamic effects would have affected the direction of storm tracks, as well as more
680 local climatic effects commonly associated with ice sheets such as strong katabatic winds
681 (Kageyama, et al. 2021, Velasquez et al. 2021, Luetscher et al. 2015, Lefort et al. 2019)

682

683 **4.1 Vegetation Cover**

684

685 The nature and extent of forest cover during the LGM remains a matter of considerable
686 debate. Vegetation models driven by LGM climate model simulations generally indicate
687 extensive areas of boreal forest north of the Alps, and a mix of temperate and warm-
688 temperate woodland to the south across southern Europe and much of the Mediterranean.
689 Treeless areas such as steppe are mainly confined to those areas where it is also found today,
690 namely inland Iberia, Ukraine, southern Russia and Turkey, while Tundra is found to the
691 north close to the Scandinavian Ice Sheet (Allen et al., 2010; Cao et al., 2019; Prentice et al.,
692 2011; Velasquez et al., 2021).

693

694 Evaluation of these vegetation-model simulations against data has been largely based on
695 comparison with compilations of pollen-biome reconstructions (Prentice et al., 2011; Allen et
696 al., 2010; Cao et al., 2019; Velasquez et al., 2021). Early studies were based on only a limited
697 number of sites from southern Europe, and showed steppe at all sites in contradiction with
698 model simulations (Elenga et al. 2000). More recent pollen compilations have included more
699 sites especially to the north that have revealed a more mixed picture of vegetation cover, with
700 forest biomes at some sites both south and north of the Alps that appear more consistent with
701 model simulations (Binney et al., 2017; Cao et al., 2019). However, many of these pollen
702 sites used in these studies were assigned an LGM age based on poor or incorrect dating
703 control, and likely date to MIS3, the Late-Glacial or even the Holocene. Nevertheless, based
704 on our compilation of more securely dated LGM pollen sites, we also show a wider
705 distribution of forest biomes particularly in Iberia, northern Italy and Central Europe,
706 although with greater areas of steppe than suggested by the models over the remaining
707 regions.

708

709 However, the interpretation of biome reconstructions requires care since the forest cover and
710 vegetation composition may not be as clear as the dominant biome suggests. For instance, we
711 find that steppe is still reconstructed as the dominant biome at some sites despite arboreal
712 pollen forming 70-80% of the pollen assemblage. In addition, it is important to remember
713 that pollen-biomes are based only on the proportion of taxa that can form forest and
714 woodland, while these taxa may in fact exist only as shrubs or stunted krummholz forms in
715 the challenging climate and environment of the LGM. Alternatively, similar conditions may
716 favour low-lying non-arboreal taxa forms with poor pollen dispersion or even insect
717 pollinated taxa forms that may be poorly represented in the pollen assemblage, giving greater
718 prominence to arboreal taxa whose pollen may be the result of long-distance transport
719 particularly *Pinus*. However there also appear to be plenty of samples with low or even very
720 low (<20%) arboreal percentages, so not all sites in open areas may be affected by long-
721 distance transport of *Pinus* in the same way.

722

723 Quantitative MAT based reconstructions of forest cover can overcome some of these
724 problems, where they can be detected, based on the composition of the pollen assemblage
725 when compared with the modern land-cover. Chord-distance measurements of the match
726 between fossil and modern pollen assemblages indicate good LGM analogues exist in our
727 large Eurasian modern pollen dataset. The results of the MAT forest cover reconstruction
728 indicates that forest cover was low but not entirely devoid of woodland in most areas, similar
729 to the modern boreal forests of Siberia and consistent with a steppe-tundra-woodland mosaic
730 proposed by many authors (e.g. Birks and Willis, 2008; Willis and Van Andel, 2004). This is
731 confirmed in an analysis of the most commonly found modern analogue ecoregions for LGM
732 pollen samples at each site (Table A64). Uncertainties are large, but for comparison the MAT
733 site-average of 33% forest cover is slightly less than the average today over the Boreal region
734 of Europe (43%) and slightly more than the average today over Mediterranean region (27%)
735 (Zanon et al. 2018).

736

737 By calculating the percentage of each of the taxa in each LGM pollen sample using a
738 standardized pollen sum, we are able to make direct comparisons between different LGM
739 pollen records and their taxa percentages (Figure A2, A3). The results show a preponderance
740 of boreal forest taxa to the north of the Alps, consistent with biome results mentioned earlier.
741 *Pinus* is the most common forest forming taxa in this boreal zone, together with *Picea*, and
742 including *Larix* to the east and *Abies* to the west. The occurrence of *Betula* and *Juniperus*
743 also suggests shrubby elements consistent with arctic shrub-tundra, although high Poaceae

744 and other herbaceous taxa such as *Artemisia* and *Chenopodiaceae* indicate more steppe than
745 tundra. Other deciduous taxa found north of the Alps include cold tolerant generalists such as
746 *Corylus* and *Alnus*, as well as low percentages of relatively thermophilous taxa in the east,
747 such as *Carpinus* and *Tilia*.

748
749 These results are consistent with charcoal (Magyari et al., 2014a; Willis and Van Andel,
750 2004), malacological (Juříčková et al., 2014), biomarkers (Zech et al., 2010) and genetic
751 evidence (Stivrins et al., 2016; Willis and Van Andel, 2004) that the main forest region north
752 of the Alps was in the eastern region of Central Europe around the Carpathian basin. This
753 was also an area where cold and moisture sensitive deciduous taxa were also able to survive
754 (Magyari et al., 2014), although evidence of temperate taxa found in the pollen record has yet
755 to be supported by charcoal and macrofossil records (Feurdean et al., 2014). Our pollen
756 evidence indicates an open taiga or cool mixed forest that extended in central and eastern
757 Europe to areas close to the Scandinavian and Alpine ice caps, as proposed by Willis and Van
758 Andel (2004) and Huntley and Allen (2003), although whether this represents isolated
759 pockets of forest or an extended open steppe-forest is difficult to determine (Kuneš et al.,
760 2008). Even steppe or tundra areas in western Europe show a low but significant presence of
761 the pollen of tree taxa at sites close to the ice sheets that are unlikely to be solely the result of
762 long distance transport or reworking (Kelly et al., 2010). The presence of woodland in these
763 areas is also supported by mammalian remains, for instance at Kents Cavern in SW England
764 (Stewart and Lister, 2001).

765
766 Overall however, our results clearly show a much greater predominance of thermophilous
767 and moisture sensitive deciduous taxa south of the Alps, particularly in Iberia and Northern
768 Italy, where temperate broadleaf forests survived in sheltered refugia (Kaltenrieder et al.,
769 2009). Most of these appear to be in hilly areas with the ability to generate orographic rainfall
770 (Monegato et al., 2015), on south facing slopes to make the most of the sun's radiant energy
771 and located above the valley floor to escape frost and flooding. We might also expect these
772 areas to be sheltered from cold northerly winds, and benefit from relatively mild and moisture
773 laden winds coming from the Mediterranean Sea. For instance, the presence of woodland and
774 low glacier altitudes along the southern slopes of the Alps around the Po Valley and Trentino
775 region is consistent with strong orographic rains generated by southerly and easterly winds
776 that today can be generated by low pressure located south of the Alps in the Gulf of Genoa,
777 and consistent with a southerly storm track around the Alps (Kehrwald et al., 2010; Luetscher
778 et al., 2015). Generally, as might be expected, areas of forest reconstruct similar or increased
779 precipitation compared to today, and areas of steppe indicate decreased precipitation (see next
780 section).

781
782 Independent evidence of LGM vegetation is provided by archaeozoological data. This data
783 supports the palynological evidence for the existence of forest and woodland refugia across
784 the ice-free areas of Europe at latitudes north of the Alps. For instance, large vertebrates in
785 these areas show patterns of extirpation and extinction in response to shifts in climate and
786 vegetation cover that is different for different species, indicating a variety of environments
787 and niches (Lister and Stuart, 2008; Stewart and Lister, 2001). As with the pollen record, the
788 presence of temperate adapted large vertebrate taxa within the glacial landscape of Western
789 Europe also suggests the existence of temperate “micro-refugia” (Stewart and Lister, 2001) ,
790 consistent with suggestions that temperate arboreal taxa were not entirely extirpated from the
791 region during the LGM (Magri, 2010). Further east, mammal assemblages indicate
792 generalized loss of forest components in the East European Plain (Demay et al. 2021,
793 Puzachenko et al., 2021) which is consistent with our data indicating low forest cover in this

794 region. In other areas, evidence of the prevailing land cover at the LGM comes from studies
795 of small vertebrate communities, which have a closer affinity to the prevailing environment
796 than large vertebrates (López-García and Blain, 2020) that have the propensity to migrate
797 large distances, often on a seasonal basis. These studies of small vertebrate assemblages also
798 support the existence of temperate “micro-refugia” in France (Royer et al., 2016) and the
799 existence of woodland components in many regions across Southern Europe including parts
800 of Iberia (Bañuls-Cardona et al., 2014) Italy (Berto et al., 2019) and the Balkan Peninsula
801 (Mauch Lenardić et al., 2018).

802
803 Other paleobotanical evidence also supports our land cover reconstruction. Schafer et al.
804 (2016) suggest leaf wax patterns from palaeosols in Spain may indicate the presence of
805 drought intolerant deciduous trees and more humid conditions during the LGM. Significantly,
806 none of the pollen sites indicate that temperate broadleaf forests were dominant, and
807 broadleaf temperate taxa always appear part of a mixed woodland together with cold or
808 aridity adapted evergreen and needleleaf taxa, including typical Mediterranean taxa. This type
809 of mixed vegetation probably extended to the Balkans where the hilly terrain and proximity
810 to the Mediterranean would appear to have provided favourable climatic conditions, although
811 we still lack LGM sites from this region. At sites in central and southern Italy and east
812 through Greece and Turkey to the Middle East (and including North Africa), the vegetation
813 appears drier with a greater prevalence of steppe. Only a site in Georgia at the edge of the
814 Caucasian mountains indicates the presence of significant amounts of forest (mainly *Pinus*), a
815 result that was also found by Tarasov et al. (2000), and probably linked to favourable
816 orographic precipitation and proximity to the Black Sea.

817
818 Comparison with LGM land cover from vegetation modelling studies driven by climate
819 model simulations indicate a much wider presence of forest than that shown by the pollen
820 data (Kaplan et al., 2016). Data-model agreement appears to be closest over eastern-central
821 Europe where pollen indicates the presence of open Boreal forest, and over south-west
822 Europe with the presence of cool mixed temperate forest, including broadleaf deciduous and
823 thermophilous elements (Prentice et al., 2011; Allen et al., 2010; Cao et al., 2019; Velasquez
824 et al., 2021). Nevertheless, agreement still appears to be weak over western-central Europe
825 and Southern and Eastern Europe through to the Middle East, where pollen data continues to
826 indicate widespread steppe. One proposed explanation for this data-model discrepancy has
827 been the role of fire (including man-made fire) in maintaining forest openness, a factor
828 influencing forest cover that is not included in most vegetation models (Kaplan et al., 2016).
829 In the Carpathian basin Magyari et al. (2014a) noted that charcoal increased as forest cover
830 declined, suggesting that wildfires played a role in decreasing forest cover during the LGM.
831 Other studies have noted low levels of charcoal and therefore fires during the LGM, although
832 these tend to be from steppe areas with low biomass and fuel availability (Connor et al.,
833 2013; Kaltenrieder et al., 2009). Recent LGM vegetation simulations that include fire indicate
834 much lower values of forest cover than those without fire over western central Europe, while
835 forest remains in central eastern Europe (see figure 6 in Velasquez et al., 2021). This appears
836 closer to the data, but the values are perhaps too low compared with our MAT
837 reconstructions here (Figure 4).

838 839 **4.2 Climate**

840 841 **4.2.1 Comparison with previous pollen-based reconstructions**

842

843 The climate of the LGM is generally considered to have been cooler and drier than today, but
844 data-model comparisons continue to highlight important discrepancies, not only in the degree
845 of cooling and drying but also in their seasonal and spatial distribution. Data-model
846 comparisons over Europe have mainly used pollen-based climate reconstructions, especially
847 the Paleoclimate Modelling Intercomparison Project (PMIP/CMIP) (Kageyama et al., 2021,
848 Bartlein et al., 2011; Harrison et al., 2015; Kageyama et al., 2006). The most commonly used
849 reconstructions have been based on two main methods, a neural-network methodology
850 (ANN) of Peyron et al. (1998) and Jost et al. (2005), and an Inverse Modelling approach
851 (INV) applied by Wu et al. (2007). The ANN method uses modern pollen samples ~~for~~
852 ~~calibration~~ and does not include any correction for CO₂ effects, being similar in these
853 respects with the MAT method used in this study. In contrast the INV method does not use
854 modern pollen samples ~~for calibration~~, but instead uses a process-based vegetation model run
855 in inverse mode. Ordinarily, a vegetation model will use climate as an input to generate a
856 vegetation as an output, but in inverse mode the model is reconfigured to generate climate as
857 an output given a particular vegetation (pollen) assemblage as an input. One of the
858 advantages of the INV method is that CO₂ can also be varied as an input, and therefore the
859 effect of changes in CO₂ on the vegetation, and therefore reconstructed climate, can be
860 investigated. Comparison of these ANN and INV reconstructions have shown important
861 differences, with the INV reconstruction generally not as cold and somewhat drier than ANN
862 (Wu et al. 2007). These differences between pollen-climate methods have often been
863 attributed to CO₂ effects (Wu et al. 2007) but this is not clear since there may be other
864 factors, such as the size and location of the training set used in the ANN reconstruction.

865

866 We make a comparison with these earlier reconstructions based on 10 sites/records in our
867 dataset which we identified as also being included in these earlier studies (Fig. 9). While we
868 were able to identify the site and data source, as well as the time window, we were unable to
869 establish if the the data represented a single sample or the mean of multiple samples within a
870 time-window or the exact depth of those samples, or the actual sediment core in the case of
871 multiple cores from the same site. While these aspects are unknown, it seems likely that the
872 pollen data we used in our analysis was very similar if not identical in most cases, and
873 reconstructed biomes for these sites from our pollen dataset are identical to the biomes
874 reconstructed using the earlier pollen dataset (Elenga et al., 2000).

875

876 We compare our MAT with the ANN and INV reconstructions in figure 9. On average across
877 all 10 records, the MAT and INV methods give almost identical results for both anomalies of
878 mean annual temperature (MAT -6.6C, INV -7.2C) and precipitation (MAT 158mm, INV
879 165mm). Uncertainties are also similar for both methods. In contrast, the ANN method gives
880 much cooler mean annual temperature anomalies (ANN -13.9C) and drier precipitation
881 anomalies (ANN -474mm). On a site by site basis the MAT and INV methods show closer
882 agreement for temperatures than precipitation, although precipitation has proportionally
883 larger uncertainties. The reconstructions based on these two methods are close enough that
884 the uncertainties overlap at all sites for both temperature and precipitation, except the
885 precipitation reconstruction at Lac de Bouchet (site #25). The reason for this is not clear, but
886 there could easily be minor differences with the pollen data analysed by Wu et al. (2007) in
887 their INV reconstruction since the pollen record (Reille and de Beaulieu, 1988) includes
888 multiple cores each with many different samples covering the LGM period.

889

890 This comparison shows that our MAT reconstructions are very similar to the INV method,
891 but not as cold or dry as the ANN method. This has two main implications. The first is that
892 our reconstructions indicate greater agreement with the results of climate model simulations

893 since climate models indicate temperatures closer to the INV reconstructions (Latombe et al.,
894 2018) than the ANN reconstructions (Jost et al., 2005; Kageyama et al., 2006). The difference
895 between our MAT and earlier ANN reconstructions is likely the result of the modern
896 ~~calibration-pollen~~ datasets used, since the ANN reconstruction was based on a considerably
897 smaller number of samples taken mainly from the cold dry steppes of Kazakstan and
898 Mongolia.

899

900 The second implication is that the MAT method may not be significantly impacted by the
901 effects of lower CO₂ (Cowling and Sykes, 1999; Prentice and Harrison, 2009; Williams et
902 al., 2000) or indeed insolation changes during the LGM, since the MAT results are similar to
903 those based on the INV method which specifically takes account of these non-climatic factors
904 (Wu et al., 2007). This would suggest that MAT could also work well for pollen-based
905 climate reconstructions on longer glacial-interglacial timescales where insolation and CO₂
906 vary significantly from their modern values. This is consistent with the findings of Pini et al.
907 (2021) who applied a correction algorithm developed by Prentice et al. (2017) and Cleator et
908 al. (2020) to a MAT reconstruction of mean annual precipitation at Lake Fimon in Northern
909 Italy. This shows a very small correction of 0mm to 30mm for samples across the LGM time-
910 window, which indicates that CO₂ is not a very significant factor in influencing this type of
911 reconstruction, at least compared to the overall uncertainties (+/- 200mm) of the
912 reconstruction itself. The uncertainties associated with the correction algorithm are not
913 discussed, but given that inputs include estimates of both LGM temperature and cloud cover,
914 it seems likely that these could be significant. Importantly, both Pini et al (2021) and Cleator
915 et al (2020) specifically exclude the necessity of applying a correction algorithm to
916 temperature reconstructions, since they consider only hydrological variables to be affected by
917 changes in atmospheric CO₂.

918

919

920 **4.2.2 Comparison with climate reconstructions based on other proxies**

921

922 **4.2.2.1 Temperature**

923

924 Proxies that are not based on plants should remain unaffected by the CO₂ problem during the
925 LGM, and provide an alternative basis for evaluating pollen-based reconstructions. Samartin
926 et al. (2016) reconstructed LGM summer temperatures based on chironomid remains from
927 Lago della Costa (site #34) in Northern Italy. They also undertook pollen analysis on the
928 same samples down the core, allowing us to make a sample-by-sample comparison between
929 the chironomid temperature record and our MAT reconstruction (Fig. 10). Our pollen-climate
930 reconstruction is for JJA mean temperate, while the chironomid reconstruction is for July
931 mean temperature, with the anomalies based on the modern equivalent JJA and July mean
932 temperatures respectively. The average anomaly values for all 8 samples reconstructed by the
933 pollen-climate MAT are $-10.2 \pm 3.5\text{C}$, and for the chironomids $-9.5 \pm 3.0\text{C}$. This indicates
934 that pollen and chironomid average summer temperature reconstructions are very similar on
935 average, taking into account the overlapping uncertainties, while also showing a strong
936 similarity on a sample-by-sample basis throughout the time-series.

937

938 Other reconstructions based on other proxies provide a basis for more general regional
939 comparisons (Figure A4, A5). We reconstruct both summer and winter temperatures and
940 show that cooling in winter was greater than in summer at most sites, associated with an
941 increase in continentality (increased temperature difference between summer and winter). A
942 similar seasonal pattern of temperature change has also been shown in other studies that

943 reconstruct both summer and winter LGM temperatures, including Prud'homme et al. (2016)
944 using $\delta^{18}\text{O}$ analysis of earthworm calcite granules at Nussloch near the French-German
945 border, Bañuls-Cardona et al. (2014) using faunal remains of small mammals at 4 locations in
946 western Spain, and Ferguson et al. (2011) who examined seasonal temperature change using
947 $\delta^{18}\text{O}$ and Mg/Ca analysis of limpet shells at Gibraltar in southern Spain. The increase in
948 continentality at Nussloch (Prud'homme et al., 2016) was reconstructed at between 11.6 to
949 15.6 °C, comparable at the lower end with nearby pollen sites [La Grotte Walou site #28]
950 10.4 ± 5.8 °C and [Bergsee site #29] 7.9 ± 5.7 °C. The faunal sites in western Spain studied
951 by Bañuls-Cardona et al. (2014) gave much reduced increases in continentality, but
952 nevertheless similar to nearby pollen sites. For instance at Valdavara 5.1 °C [MD99-2331 site
953 #3] 5.2 ± 3.1 °C, El Miron 1.2 °C [Tourbiere de l'Estarres site #19] 5.1 ± 6.2 °C, El Portalon
954 0.9C [Torrecilla de Valmadrid site #16] 2.8 ± 1.8 °C and Cueva de Maltrvieso 6.1C [SU81-18
955 site #2] 4.8 ± 3.4 °C. Further south at Gibraltar the limpet-based study of Ferguson et al.
956 (2011) also shows a relatively small increase of 2 °C. The nearest pollen site [Gorham Cave
957 site #5] however shows a larger increase of 4.7 ± 2.3 °C, although differences could be
958 expected given the different temporal resolution of annual laminae on mollusk shells
959 compared to pollen assemblages that reflecting much slower changes in trees and other long-
960 lived flora.

961
962 Summer temperatures were warm enough during the LGM over the Alpine areas that Swiss
963 lakes were largely ice free in summer, while glacier ELA's around the time of the LGM
964 suggest summers were -6.5 to -7.7 °C cooler compared to the LIA (Heiri et al., 2014). This
965 cooling was similar to that found at Nussloch some 200km north of the Swiss border by
966 Prud'homme et al. (2016), who reconstructed anomalies of -6 to -8 ± 4 °C from $\delta^{18}\text{O}$
967 analysis of earthworm calcite granules (representing warm season May-September
968 temperatures). Slightly less cooling was found close by at the nearby site of Achenheim
969 where analysis of Mollusc assemblages gave summer (August) cooling estimates of -3.5 to -
970 6.5 °C based on MAT (Rousseau, 1991), and -5.5 to -9.5 °C based on the Mutual Climatic
971 Range method (Moine et al., 2002). These reconstructions appear somewhat cooler than
972 nearby pollen sites [La Grotte Walou site #28] -1.4 ± 3.6 °C and [Bergsee site #29] -2.7 ± 5.1
973 °C, although comparable with the pollen site [Pilsensee site #32] -7.3 ± 5.0 °C 200 km further
974 east. Similar differences also occur at the site of Les Echets on the western edge of the Alps
975 where a diatom based reconstruction of summer (July) temperatures (Ampel et al., 2010)
976 indicated a greater cooling (-10.5 to -11.5 °C) than our pollen reconstruction [Les Echets G
977 site #27] $(-4 \pm 2.7$ °C). However, the authors caution that the results were based on poor
978 analogues and rare taxa, as well as a small training set of only 90 lakes in Switzerland.

979
980 South of the Alps, other proxies show the opposite relationship with the pollen
981 reconstructions. For instance, at Lago della Costa in the Po valley, a summer (July)
982 temperature chironomid reconstruction by Samartin et al. (2016) is around 1-2 °C less cool
983 than the pollen reconstruction (JJA) for the same site [Lago della Costa site #34] $-11.4 \pm$
984 2.7 °C, although both reconstructions fall within their respective uncertainty ranges (Figure 8).
985 In the Pindus Mountains in Greece, Hughes et al. (2006) estimated LGM summer
986 temperature anomalies of -7 °C based on glacier modelling, which is comparable with that
987 reconstructed at the nearest pollen site [Ioannina site #51] -7.7 ± 2.8 °C. In Spain the analysis
988 of small mammal remains by Bañuls-Cardona et al. (2014) shows similarly less cooling in
989 summer or even warmer than present positive anomalies compared to the nearest pollen sites,
990 such as Valdavara 1.4 °C [MD99-2331 site #3] -2.3 ± 2.8 °C, El Miron -2.3 °C [Tourbiere de
991 l'Estarres site #19] -5.7 ± 5.4 °C, El Portalon 0.8 °C [Torrecilla de Valmadrid site #16] $-2.6 \pm$
992 1.1 °C and Cueva de Maltrvieso -1.1C [SU81-18 site #2] -10.4 ± 2.8 °C. Further south at

993 Gibraltar, the limpet-based study of Ferguson et al. (2012) suggests an anomaly of around -7
994 °C, which is a greater cooling than the pollen reconstruction from this location [Gorham Cave
995 site #5] -1.3 ± 2.2 °C, although comparable with other pollen sites slightly further east.
996

997 Winter temperature reconstructions from non-pollen proxies show a similar pattern in relation
998 to pollen reconstructions as for summer temperatures. North of the Alps at Achenheim,
999 Prud'homme et al. (2016) use $\delta^{18}O$ on earthworm remains to reconstruct particularly cold
1000 winter anomalies of -17.6 to -23.6 °C compared to nearby pollen sites [La Grotte Walou site
1001 #28] -11.8 ± 8.0 °C and [Bergsee site #29] -10.6 ± 6.3 °C. South of the Alps in Spain, the
1002 analysis by Bañuls-Cardona et al (2014) based on the remains of small mammals shows less
1003 cooling in winter compared to the nearest pollen sites, in particular Valdavara -3.7 °C
1004 [MD99-2331 site #3] -7.5 ± 3.4 °C, El Miron -3.5 °C [Tourbiere de l'Estarres site #19] -10.8
1005 ± 7.0 °C, El Portalon -0.1 °C [Torrecilla de Valmadrid #16] -5.4 ± 2.5 °C and Cueva de
1006 Maltrvieso -7.2 °C [SU81-18 site #2] -15.2 ± 4.0 °C. And again, in southern Spain at Gibraltar,
1007 analysis of limpet shells by Ferguson et al (2011) suggests winter cooling of around -9 °C
1008 while the pollen reconstruction suggests [Gorham Cave site #5] -6.0 ± 2.5 °C, although sites
1009 further east indicate cooler conditions.
1010

1011 A number of additional proxies have also been used to reconstruct LGM mean annual
1012 temperature. Heyman et al. (2013) applied glacier mass balance modelling at sites located in
1013 the smaller mountain regions north of the Alps. These are generally slightly cooler than our
1014 pollen-based reconstructions at sites close to the Vosge Mountains -12.7 ± 2.0 °C and Black
1015 Forest -11.4 ± 2.3 °C [Bergsee site #29] -8.2 ± 3.3 °C, Bavarian Forest -10.7 ± 2.2 [Pilsensee
1016 site #32] -9.2 ± 1.2 °C and Giant Mountains -8.5 ± 1.8 [Kersdorf-Briesen site #46] -7.3 ± 0.3
1017 °C. These values obtained by Heyman et al. (2013) are warmer than Prud'homme et al. (2016)
1018 who estimated annual mean temperature anomalies of -15.1 to -19.1 °C based on $\delta^{18}O$ of
1019 earthworm calcite at the Nussloch site just north of the Vosge and Black Forest. The annual
1020 temperatures reconstructed by Heyman et al. (2013) are also around 2°C warmer than Allen et
1021 al. (2008) who applied a similar, although simpler method to over 29 different mountainous
1022 regions across Europe that had been glaciated during the LGM. Since glacier mass balance is
1023 a function of both snowfall and temperature, these estimated temperatures vary according to
1024 estimated changes in precipitation. For instance, mean annual temperature estimates by Allen
1025 et al. (2008a) are much cooler than reconstructed by pollen, with an average anomaly of -13.2
1026 °C for the 29 sites assuming a 40% reduction in precipitation, but this is reduced to -11.8 °C
1027 assuming the same precipitation as modern. This compares with -7.2 °C for our 63 pollen
1028 sites. The glacier mass balance modelling by Allen et al. (2008a) assumes a seasonal
1029 distribution of precipitation that is similar to the present day, and does not consider increases
1030 in winter precipitation or mean annual precipitation above present day levels. Both of these
1031 are suggested by the pollen data in some regions, and both could explain glacier extent found
1032 during the LGM based on less extreme temperature anomalies more comparable with the
1033 pollen data.
1034

1035 To the east of the Alps in the Panonian basin, mean annual temperature anomaly estimates
1036 have been made from noble gas measurements on groundwater ranging from -2 to -4 °C
1037 (Stute and Deak, 1990) up to -9 °C (Varsányi et al., 2011). These are similar to estimates
1038 ranging from -2 to -9 °C from oxygen isotope ratios from mammoth tooth enamel (Kovács et
1039 al., 2012) and are comparable with nearby pollen sites [Feher Lake site #50] -8.2 ± 3.3 °C and
1040 [Kokad site #52] -4.5 ± 2.3 °C. On a broader scale, Sanchi et al (2014) estimated LGM
1041 cooling in the Danube and Dneiper basins based on Lipid biomarkers in a core from the
1042 Black Sea and came up with similar mean annual temperature anomalies between -6 to -10

1043 °C, which again are comparable with pollen sites from the region that range from
1044 [Nagymohos site #48] -10.5 ± 4.1 °C to [Straldzha site #57] -4.3 ± 5.8 °C.

1045
1046 Further south and west, García-Amorena et al. (2007) reported mean annual temperature
1047 anomalies of -2.0 to -11.3 °C at LGM sites along the Portuguese coast, based on an indicator
1048 species method using plant macrofossils. This is similar to the closest marine pollen sites off
1049 the coast, which recorded values of [MD95-2039 site #1] -10.5 ± 4.6 °C and [MD99-2331 site
1050 #3] -5.3 ± 2.9 °C. Meanwhile, in the far east of the study area, Zaarur et al. (2016) estimated a
1051 mean annual temperature anomaly of around -3 °C based on clumped isotope analysis of
1052 *Melanopsis* shells from LGM sediments in the Sea of Galilee. This limited cooling appears
1053 similar to the nearest pollen site [Lake Zeribar site #63] where we reconstruct a cooling of $-$
1054 2.2 ± 4.6 °C.

1055
1056 Reconstructions of LGM sea surface temperatures (SST's) provide yet another source of
1057 comparison with our terrestrial pollen-based reconstructions, although many of the physical
1058 processes controlling surface sea temperatures such as upwelling, surface mixing, surface
1059 currents, stratification and thermal inertia through the seasonal cycle, represent quite different
1060 processes to those controlling surface temperatures over land, particularly at the sub-regional
1061 scale. Nevertheless, the Atlantic coastal waters of Iberia and the waters throughout the
1062 Mediterranean Sea include many SST sites that lie in relative proximity to our terrestrial
1063 pollen-sites, allowing us to make a comparison at the largest scale. Within this area the
1064 MARGO database (MARGO Members, 2009) includes 13 Alkenone, 2 Mg/Ca and 41
1065 Foraminifera based SST records of mean annual temperature, with the Foraminifera records
1066 also providing an additional 41 winter (JFM) and summer (JAS) SST estimates. We compare
1067 the SST records with the 36 closest terrestrial pollen records which fall within a box of -11 to
1068 35 degrees longitude and 32 to 43 degrees latitude containing all of the SST records. A
1069 simple site average indicates a mean annual SST anomaly of -5.5 ± 1.0 °C which is relatively
1070 close to the value of -7.2 ± 3.4 °C obtained from the terrestrial pollen sites [sites #1-4, 5, 7-
1071 24, 25, 26, 30, 35-38, 41, 47, 51, 53, 56-59]. Interestingly the inter-site variance (standard
1072 deviation of the reconstructed temperatures across all sites) is almost identical for the two
1073 datasets, 2.57 °C for the SST sites and 2.63 °C for the pollen sites, despite representing very
1074 different environments, proxies and uncertainties. However, when we look at the seasonal
1075 temperature anomalies, we find very different results. Site averaged winter SST anomalies
1076 are -3.7 ± 1.1 °C compared to -9.3 ± 4.2 °C for winter temperatures from terrestrial pollen
1077 sites, while in summer the values are reversed, -7.0 ± 0.8 °C compared to -5.38 ± 3.3 °C
1078 respectively. This suggests that SST's experienced greater cooling in summer compared to
1079 winter, which is the opposite to that generally found in terrestrial seasonal temperature
1080 reconstructions throughout the region, although this is consistent with model simulations
1081 (Mikolajewicz, 2011).

1082 1083 **4.2.2.2 Precipitation**

1084
1085 Few proxies apart from pollen provide quantitative reconstructions of precipitation during the
1086 LGM. Glacier mass balance modelling includes assumptions about precipitation in order to
1087 derive temperatures (Allen et al., 2008a), but neither is independent of the other. Hughes et
1088 al. (2006) estimate from glacier modelling that mean annual precipitation during the LGM at
1089 sites in the Pindus mountains in Greece was around 2300 ± 200 mm, which they consider to
1090 be similar to the present day (>2000 mm). A small change in precipitation compared to
1091 modern values is also indicated by the nearest pollen site, which is around 47 km to the south
1092 [Ioannina #51], and indicates a mean annual precipitation anomaly of -152 ± 294 mm,

1093 representing just 15% of the modern value. A larger reduction in mean annual precipitation of
1094 -45% (maximum) is reconstructed by García-Amorena et al. (2007) based on plant
1095 macrofossil remains from sites on the Portuguese coast. In comparison, the closest pollen
1096 sites record values which are a little lower, ranging from [MD95-2039 site #1] -22% to
1097 [MD99-2331 site #3] -34%. Further north in south-west Germany, Prud'homme et al. (2018)
1098 reconstructed mean annual precipitation from the delta ^{13}C of earthworm calcite granules at
1099 Fussloch. They estimate a field site average of 333 (159-574) mm/yr at the LGM, which
1100 represents an anomaly of -503 mm/yr (-60%) relative to the modern precipitation of 836
1101 mm/yr. This is comparable with the closest pollen site [Bergsee #29] with an anomaly of -
1102 540 mm/yr.

1103
1104 As with glaciers, lake levels reflect changes in moisture balance that includes the effects of
1105 both temperature (via evapotranspiration) and precipitation, rather than just precipitation.
1106 They also represent semi-quantitative data at best, with changes often described relative to
1107 the modern or other baseline. There are few lake level records available north of the Alps, but
1108 to the south, many records indicate high lake levels in areas such as Spain (Lacey et al., 2016;
1109 Moreno et al., 2012; Vegas et al., 2010), Italy (Belis et al., 1999; Giraudi, 2017), Greece and
1110 Turkey (Harrison et al., 1996; Reimer et al., 2009) and the Middle East (Kolodny et al., 2005;
1111 Lev et al., 2019). These lake records are also supported by evidence of higher river levels in
1112 Morocco (El Amrani et al., 2008). The cause of the higher lake levels has been the subject of
1113 some debate, since many pollen records (and especially early biome reconstructions) show
1114 steppe vegetation that would suggest aridity that appears incompatible with higher lake
1115 levels. Prentice et al. (1992) proposed that the co-existence of steppe vegetation and high lake
1116 levels could be possible if precipitation increased outside of the summer growing season,
1117 while summers themselves were drier and cooler with decreased evaporation. However, the
1118 results of our analysis tend to indicate the opposite in regions with higher lake levels, with
1119 increased summer rainfall and decreased winter rainfall. In addition, the increase in summer
1120 precipitation was enough to compensate for the decrease in winter rainfall, leading to an
1121 overall increase in mean annual precipitation at many pollen sites in Spain and Greece for
1122 instance. This together with depressed temperatures and consequently decreased evaporation
1123 could explain the higher lake levels, whilst also limiting the growth of trees as a result of
1124 cooler temperatures and prolonged aridity outside of the summer season. Davis & Stevenson
1125 (2007) also note a differential hydrological response between summer and winter rainfall in
1126 the Mediterranean during the Holocene that may also provide an explanation. In this case
1127 sporadic summer storms may result in high rates of runoff that may fill run-off fed lakes, but
1128 low rates of soil moisture recharge that fails to benefit vegetation in the same way winter
1129 rainfall does.

1130
1131 Overall, we reconstruct only a small reduction in precipitation during the LGM of around
1132 91mm (13%) averaged over all sites, which is less than the ~200mm reduction based on the
1133 sites in the pollen-climate compilation used by PMIP (Bartlein et al., 2011). Since our
1134 precipitation reconstruction on average matches that of the INV reconstruction by Wu et al
1135 (2007), we can attribute much of the difference to the greater aridity shown in the ANN
1136 reconstruction by Peyron et al and Jost et al (2005) (see figure 9). As with temperature, this is
1137 probably a reflection of the modern training set used in the ANN reconstruction which is
1138 much smaller than our training set and is largely taken from the arid steppes of Kazakhstan
1139 and Mongolia. However, it is also important to recognize the significant spatial variability in
1140 precipitation, which means that a simple average of different sets of sites from different
1141 regions may not accurately reflect the change in LGM precipitation at the European scale.
1142 Nevertheless, one of the most consistent signals in our dataset is for an increase in summer

1143 precipitation over many areas of Southern Europe and the Mediterranean. This is also found
1144 in climate models, where it has been attributed to an increase in convection-driven
1145 precipitation, although the amount of precipitation generated by this mechanism varies
1146 significantly between models (Beghin et al., 2016). It may seem counter-intuitive to see an
1147 increase in reconstructed precipitation in the same regions where we also find a
1148 preponderance of steppe or xerophytic biomes and taxa, including *Artemisia* and
1149 *Chenopodiaceae*. This is attributable to the fact that climate can change quite markedly with
1150 necessarily invoking a major change in vegetation, and especially the pollen biome. For
1151 instance, a semi-arid climate ranges from 250-500mm rainfall a year, so we could expect a
1152 semi-arid vegetation to be dominant even if the rainfall increases 250mm (100%).
1153

1154 A more consistent response in models is for an increase in winter precipitation across
1155 Southern Europe and the Mediterranean related to a stronger and more southerly displaced jet
1156 stream, with winter precipitation also accounting for much of the change in mean annual
1157 precipitation (Beghin et al., 2016). Our reconstruction of winter precipitation however shows
1158 less support for this scenario with a more general decrease in winter precipitation apart from
1159 southern and eastern Iberia, and with summer precipitation generally more important in those
1160 sites that show an overall increase in mean annual precipitation. This may not necessarily
1161 contradict the models in terms of the strength and position of the winter jet stream, but may
1162 instead indicate that models over-estimate the amount of moisture being carried westward
1163 from the cold North Atlantic along the storm track, especially across the far northern
1164 Mediterranean. The increase in winter precipitation across southern and eastern Iberia is
1165 however entirely consistent with a strengthened and more southerly jet stream, which also
1166 brings increased winter precipitation to the region today as a result of blocking over northern
1167 Europe/Atlantic and a negative NAO (Vicente-Serrano et al., 2011).
1168

1169 Other areas that show an increase in winter precipitation include pollen sites around the
1170 eastern end of the Alps. This is consistent with a recent study by Spötl et al (2021) who
1171 argued, on the basis of cryogenic carbonates preserved in a cave in Austria, that heavy winter
1172 (and autumn) precipitation was a significant factor in driving LGM glaciation in the region.
1173 The seasonally specific nature of this precipitation is also supported by the same pollen sites,
1174 which do not show any increase in summer precipitation at this time.
1175

1176 **5.0 Conclusions**

1177

1178 We have reconstructed the climate and vegetation cover across Europe, North Africa and the
1179 Middle East at the time of the LGM based on 63 pollen records. These records were selected
1180 using strict quality control criteria, with particular attention paid to dating control, which led
1181 to the exclusion of many records that have been used in previous studies. This fully
1182 documented dataset represents the most chronologically precise and spatially resolved view
1183 of LGM climate and vegetation during the PMIP benchmarking time window at 21 ± 2 ka.
1184 Nevertheless, it is important to recognize that there are still significant spatial gaps in pollen
1185 sites especially north of the Alps, the Balkans, Turkey and the Middle East, and we continue
1186 to have only a partial understanding of the LGM over these areas.
1187

1188 One of the key questions concerning the vegetation landscape of the LGM in Europe has
1189 been the extent to which forest rather than steppe covered the continent, and to what extent
1190 temperate elements could be found north of the classical refugia areas of Southern Europe
1191 and the Mediterranean. Our results show that although steppe and tundra was extensive at the
1192 time of the LGM, areas of open forest also occurred in many regions, particularly (but not

1193 exclusively) in Iberia, northern Italy and Central Europe. These forest or woodland stands are
1194 likely to have been located in environmentally favourable areas, with good soils, elevated
1195 rainfall and shelter from cold, desiccating winds. In those areas where woodland existed,
1196 Boreal taxa generally dominated north and east of the Alps, while temperate and
1197 thermophilous (mainly drought adapted) taxa were generally confined to areas south of the
1198 Alps and around the Mediterranean. The temperate deciduous forests that compose the
1199 climax community in many areas of Europe today were displaced to the south and reduced to
1200 a partnership role with Boreal elements. Overall our new reconstruction indicates greater
1201 agreement with model land cover simulations, but models still appear to over-estimate the
1202 amount of forest and woodland over areas such as France and the Benelux, Greece, Turkey
1203 and the Far East.

1204
1205 Another key question about the LGM concerns the ability of climate models to simulate the
1206 climate of this period and whether pollen-based climate reconstructions which show
1207 disagreement with models have been biased by the effects of low CO₂ on plant physiology.
1208 We find that our new pollen-climate reconstruction shows much closer agreement with
1209 climate models than previous reconstructions that did not take account of low CO₂ effects.
1210 We also find close agreement with previous reconstructions that did take account of CO₂
1211 effects. Since our MAT method itself does not specifically take account of low CO₂ effects,
1212 this would suggest that this problem is not a significant hindrance to MAT performance at the
1213 time of the LGM, at least not compared to other uncertainties. Instead, we suggest that the
1214 main factor in the performance of pollen-climate transfer functions that use modern analogue
1215 methods is the provision of a large enough modern pollen dataset with suitable LGM
1216 analogues.

1217
1218 This conclusion is supported by comparison with climate reconstructions based on other
1219 proxies. We found little difference between our MAT reconstruction and a Chironomid-based
1220 summer temperature record based on a downcore sample by sample comparison, as well as
1221 comparisons with records from a variety of other proxies at a regional scale. However, it is
1222 notable that some studies using glacier mass balance modelling methods indicate LGM
1223 temperatures that are much cooler than our pollen-based reconstruction. The reasons behind
1224 this are not clear, but our pollen-based results indicate higher than present precipitation in
1225 some areas that could potentially explain low elevation glacier ELA's without the need for
1226 such cold temperatures.

1227
1228 We also find that although our pollen-based reconstruction and those of SST's generally
1229 agree in terms of mean annual temperatures, SST's indicate greater cooling in summer
1230 compared to winter, while terrestrial records indicate greater cooling in winter compared to
1231 summer. These seasonal differences are also reproduced in climate models, and probably
1232 reflect the different processes driving seasonal temperature change in the terrestrial and
1233 marine domain.

1234
1235 Our reconstructions of precipitation show large spatial and seasonal variability, but generally
1236 indicate less overall aridity than previously suggested from smaller scale studies which
1237 sampled less of the spatial domain. We find that in some regions of Southern Europe
1238 precipitation may actually have been greater than present, especially in summer, but also in
1239 winter in southern and eastern Iberia and around the southern slopes of the Alps. This may
1240 have important implications in understanding the development of LGM glaciation, which
1241 may be less a function of temperature than previously supposed. This could also help better
1242 explain the observed asynchronous nature of glaciation even within relatively small regions

1243 such as Europe, as a result of more localized controls on ice sheet development such as
1244 precipitation.

1245
1246 We hope that this new continental-scale dataset of climate and vegetation reconstructions will
1247 provide an improved baseline for data-model comparisons and other studies that will allow us
1248 to better understand the complex LGM environment.

1249
1250

1251 **Code/Data availability**

1252
1253 All of the data shown in the figures together with the fossil and modern pollen datasets will
1254 be made available on pangaea.de once the review process has been completed and these
1255 datasets are therefore no longer subject to change.

1256

1257 **Author contribution**

1258
1259 BASD designed the study, undertook the analysis and wrote the manuscript. MF and ER
1260 designed and prepared the maps. JOK and AB reviewed the manuscript and provided
1261 additional input.

1262

1263 **Competing interests**

1264

1265 The authors declare that they have no conflict of interest.

1266

1267 **Acknowledgements**

1268

1269 This work was supported by a grant from the Fonds de Recherche du Québec Société et
1270 Culture (2019-SE3-254686) to AB. Data were obtained from the European Pollen Database
1271 (EPD), based within the Neotoma Paleoecology Database (<http://www.neotomadb.org>). The
1272 work of data contributors, data stewards, and the Neotoma and EPD community is gratefully
1273 acknowledged. We dedicate this paper in memory of Eric Grimm, whose tireless work for the
1274 EPD and Neotoma helped make this study possible.

1275

1276
1277
1278

References

1279

1280 ACER project members, Goñi, M. F. S., Desprat, S., Daniau, A. L., Bassinot, F. C., Polanco-
1281 Martínez, J. M., Harrison, S. P., Allen, J. R. M., Scott Anderson, R., Behling, H., Bonnefille,
1282 R., Burjachs, F., Carrión, J. S., Cheddadi, R., Clark, J. S., Combourieu-Nebout, N., Mustaphi,
1283 C. J. C., Debusk, G. H., Dupont, L. M., Finch, J. M., Fletcher, W. J., Giardini, M., González,
1284 C., Gosling, W. D., Grigg, L. D., Grimm, E. C., Hayashi, R., Helmens, K., Heusser, L. E.,
1285 Hill, T., Hope, G., Huntley, B., Igarashi, Y., Irino, T., Jacobs, B., Jiménez-Moreno, G.,
1286 Kawai, S., Peter Kershaw, A., Kumon, F., Lawson, I. T., Ledru, M. P., Lézine, A. M., Mei
1287 Liew, P., Magri, D., Marchant, R., Margari, V., Mayle, F. E., Merna Mckenzie, G., Moss, P.,
1288 Müller, S., Müller, U. C., Naughton, F., Newnham, R. M., Oba, T., Pérez-Obiol, R., Pini, R.,
1289 Ravazzi, C., Roucoux, K. H., Rucina, S. M., Scott, L., Takahara, H., Tzedakis, P. C., Urrego,
1290 D. H., Van Geel, B., Guido Valencia, B., Vandergoes, M. J., Vincens, A., Whitlock, C. L.,
1291 Willard, D. A. and Yamamoto, M.: The ACER pollen and charcoal database: A global
1292 resource to document vegetation and fire response to abrupt climate changes during the last
1293 glacial period, *Earth Syst. Sci. Data*, 9(2), 679–695, doi:10.5194/essd-9-679-2017, 2017.

1294

1295 Allen, J. R. M., Hickler, T., Singarayer, J. S., Sykes, M. T., Valdes, P. J. and Huntley, B.:
1296 Last glacial vegetation of northern Eurasia, *Quat. Sci. Rev.*, 29(19–20), 2604–2618,
1297 doi:10.1016/j.quascirev.2010.05.031, 2010.

1298

1299 Allen, R., Siegert, M. J. and Payne, A. J.: Reconstructing glacier-based climates of LGM
1300 Europe and Russia – Part 2 : A dataset of LGM precipitation / temperature relations derived
1301 from degree-day modelling of palaeo glaciers, , 249–263, 2008a.

1302

1303 Allen, R., Siegert, M. J. and Payne, A. J.: Reconstructing glacier-based climates of LGM
1304 Europe and Russia – Part 3 : Comparison with previous climate reconstructions, , (1999),
1305 265–280, 2008b.

1306

1307 Ampel, L., Bigler, C., Wohlfarth, B., Risberg, J., Lotter, A. F. and Veres, D.: Modest summer
1308 temperature variability during DO cycles in western Europe, *Quat. Sci. Rev.*, 29(11–12),
1309 1322–1327, doi:10.1016/j.quascirev.2010.03.002, 2010.

1310

1311 El Amrani, M., Macaire, J. J., Zarki, H., Bréhéret, J. G. and Fontugne, M.: Contrasted
1312 morphosedimentary activity of the lower Kert River (northeastern Morocco) during the Late
1313 Pleistocene and the Holocene. Possible impact of bioclimatic variations and human action,
1314 *Comptes Rendus - Geosci.*, 340(8), 533–542, doi:10.1016/j.crte.2008.05.004, 2008.

1315

1316 Anderson, P. M., Barnosky, C. W., Bartlein, P. J., Behling, P. J., Brubaker, L., Cushing, E. J.,
1317 Dodson, J., Dworetsky, B., Guetter, P. J., Harrison, S. P., Huntley, B., Kutzbach, J. E.,
1318 Markgraf, V., Marvel, R., McGlone, M. S., Mix, A., Moar, N. T., Morley, J., Perrott, R. A.,
1319 Peterson, G. M., Prell, W. L., Prentice, I. C., Ritchie, J. C., Roberts, N., Ruddiman, W. F.,
1320 Salinger, M. J., Spaulding, W. G., Street-Perrott, F. A., Thompson, R. S., Wang, P. K., Webb,
1321 T., Winkler, M. G. and Wright, H. E.: Climatic changes of the last 18,000 years:
1322 Observations and model simulations, *Science* (80-.), 241(4869), 1043–1052,
1323 doi:10.1126/science.241.4869.1043, 1988.

1324

- 1325 Arpe, K., Leroy, S. A. G. and Mikolajewicz, U.: A comparison of climate simulations for the
 1326 last glacial maximum with three different versions of the ECHAM model and implications
 1327 for summer-green tree refugia, *Clim. Past*, 91–114, doi:10.5194/cp-7-91-2011, 2011.
 1328
- 1329 Arslanov, K. A., Dolukhanov, P. M. and Gei, N. A.: Climate, Black Sea levels and human
 1330 settlements in Caucasus Littoral 50,000-9000 BP, *Quat. Int.*, 167–168, 121–127,
 1331 doi:10.1016/j.quaint.2007.02.013, 2007.
 1332
- 1333 Bañuls-Cardona, S., López-García, J. M., Blain, H. A., Lozano-Fernández, I. and Cuenca-
 1334 Bescós, G.: The end of the Last Glacial Maximum in the Iberian Peninsula characterized by
 1335 the small-mammal assemblages, *J. Iber. Geol.*, 40(1), 19–27,
 1336 doi:10.5209/rev_JIGE.2014.v40.n1.44085, 2014.
 1337
- 1338 Bartlein, P. J., Harrison, S. P., Brewer, S., Connor, S., Davis, B. A. S., Gajewski, K., Guiot,
 1339 J., Harrison-Prentice, T. I., Henderson, A., Peyron, O., Prentice, I. C., Scholze, M., Seppä, H.,
 1340 Shuman, B., Sugita, S., Thompson, R. S., Viau, A. E., Williams, J. and Wu, H.: Pollen-based
 1341 continental climate reconstructions at 6 and 21 ka: A global synthesis, *Clim. Dyn.*, 37(3),
 1342 775–802, doi:10.1007/s00382-010-0904-1, 2011.
 1343
- 1344 de Beaulieu, J.-L. and Reille, M.: Pollen analysis of a long upper Pleistocene continental
 1345 sequence in a Velay maar (Massif Central, France), *Palaeogeogr. Palaeoclimatol. Palaeoecol.*,
 1346 80(1), 35–48, 1990.
- 1347 Beghin, P., Charbit, S., Kageyama, M., Combourieu-Nebout, N., Hatté, C., Dumas, C. and
 1348 Peterschmitt, J. Y.: What drives LGM precipitation over the western Mediterranean? A study
 1349 focused on the Iberian Peninsula and northern Morocco, *Clim. Dyn.*, 46(7–8), 2611–2631,
 1350 doi:10.1007/s00382-015-2720-0, 2016.
 1351
- 1352 Belis, C. A., Lami, A., Guilizzoni, P., Ariztegui, D. and Geiger, W.: The late Pleistocene
 1353 ostracod record of the crater lake sediments from Lago di Albano (Central Italy): Changes in
 1354 trophic status, water level and climate, *J. Paleolimnol.*, 21(2), 151–169,
 1355 doi:10.1023/A:1008095805748, 1999.
 1356
- 1357 Berto, C., López-García, J. M. and Luzi, E.: Changes in the Late Pleistocene small-mammal
 1358 distribution in the Italian Peninsula, *Quat. Sci. Rev.*, 225,
 1359 doi:10.1016/j.quascirev.2019.106019, 2019.
 1360
- 1361 Bigelow, N.H., Brubaker, L.B., Edwards, M.E., Harrison, S.P., Prentice, I.C., Anderson,
 1362 P.M., Andreev, A.A., Bartlein, P.J., Christiansen, T.R., Cramer, W., Kaplan, J.O., Lozhkin,
 1363 A.V., Matveyeva, N.V., Murray, D.F., McGuire, A.D., Razzhivin, V.Y., Ritchie, J.C., Smith,
 1364 B., Walker, D.A., Gajewski, K., Wolf, V., Holmqvist, B.H., Igarashi, Y., Kremenetskii, K.,
 1365 Paus, A., Pisaric, M.F.J., Volkova, V.S.: Climate change and arctic ecosystems: 1. Vegetation
 1366 changes north of 55 N between the last glacial maximum, mid-Holocene, and present. *J.*
 1367 *Geophys. Res.* 108 (D19), 8170. doi.org/10.1029/2002JD002558, 2013.
 1368
- 1369 Binney, H., Edwards, M., Macias-Fauria, M., Lozhkin, A., Anderson, P., Kaplan, J. O.,
 1370 Andreev, A., Bezrukova, E., Blyakharchuk, T., Jankovska, V., Khazina, I., Krivonogov, S.,
 1371 Kremenetski, K., Nield, J., Novenko, E., Ryabogina, N., Solovieva, N., Willis, K. and
 1372 Zernitskaya, V.: Vegetation of Eurasia from the last glacial maximum to present: Key
 1373 biogeographic patterns, *Quat. Sci. Rev.*, 157, 80–97, doi:10.1016/j.quascirev.2016.11.022,
 1374 2017.

1375
1376 Birks, H. J. B. and Willis, K. J.: Alpines, trees, and refugia in Europe, *Plant Ecol. Divers.*,
1377 1(2), 147–160, doi:10.1080/17550870802349146, 2008.
1378
1379 Bonatti, E.: Pollen sequence in the lake sediments. In: *Ianula: an account of the history and*
1380 *development of the Lago di Monterosi, Latium, Italy*, in *Trans. Am. phil. Soc.*, vol. 60, edited
1381 by G. E. Hutchinson, pp. 26–31., 1970.
1382
1383 Brewer, S., Guiot, J., Sánchez-Goñi, M. F. and Klotz, S.: The climate in Europe during the
1384 Eemian: a multi-method approach using pollen data, *Quat. Sci. Rev.*, 27(25–26), 2303–2315,
1385 doi:10.1016/j.quascirev.2008.08.029, 2008.
1386
1387 Brewer, S., Giesecke, T., Davis, B. A. S., Finsinger, W., Wolters, S., Binney, H., de
1388 Beaulieu, J. L., Fyfe, R., Gil-Romera, G., Köhl, N., Kuneš, P., Leydet, M. and Bradshaw, R.
1389 H.: Mapping Lateglacial and Holocene European pollen data: The maps, *J. Maps*, 13(2), 921–
1390 928, doi:10.1080/17445647.2016.1197613, 2017.
1391
1392 Camuera, J., Jiménez-Moreno, G., Ramos-Román, M. J., García-Alix, A., Toney, J. L.,
1393 Anderson, R. S., Jiménez-Espejo, F., Bright, J., Webster, C., Yanes, Y. and Carrión, J. S.:
1394 Vegetation and climate changes during the last two glacial-interglacial cycles in the western
1395 Mediterranean: A new long pollen record from Padul (southern Iberian Peninsula), *Quat. Sci.*
1396 *Rev.*, 205, 86–105, doi:10.1016/j.quascirev.2018.12.013, 2019.
1397
1398 Cao, X., Tian, F., Dallmeyer, A. and Herzschuh, U.: Northern Hemisphere biome changes
1399 (>30°N) since 40 cal ka BP and their driving factors inferred from model-data comparisons,
1400 *Quat. Sci. Rev.*, 220, 291–309, doi:10.1016/j.quascirev.2019.07.034, 2019.
1401
1402 Carrión, J. S.: Late quaternary pollen sequence from Carihuela Cave, southern Spain, *Rev.*
1403 *Palaeobot. Palynol.*, 71(1–4), doi:10.1016/0034-6667(92)90157-C, 1992.
1404
1405 Carrión, J. S.: Patterns and processes of Late Quaternary environmental change in a montane
1406 region of southwestern Europe, *Quat. Sci. Rev.*, 21, 2047–2066, 2002.
1407
1408 Carrión, J. S., Finlayson, C., Fernández, S., Finlayson, G., Allué, E., López-Sáez, J. A.,
1409 López-García, P., Gil-Romera, G., Bailey, G. and González-Sampériz, P.: A coastal reservoir
1410 of biodiversity for Upper Pleistocene human populations: palaeoecological investigations in
1411 Gorham’s Cave (Gibraltar) in the context of the Iberian Peninsula, *Quat. Sci. Rev.*, 27(23–
1412 24), 2118–2135, doi:10.1016/j.quascirev.2008.08.016, 2008.
1413
1414 Cheddadi, R., Yu, G., Guiot, J., Harrison, S. P. and Colin Prentice, I.: The climate of Europe
1415 6000 years ago, *Clim. Dyn.*, 13(1), 1–9, 1996.
1416
1417 Chevalier, M., Davis, B. A. S., Heiri, O., Seppä, H., Chase, B. M., Gajewski, K., Lacourse,
1418 T., Telford, R. J., Finsinger, W., Guiot, J., Köhl, N., Maezumi, S. Y., Tipton, J. R., Carter, V.
1419 A., Brussel, T., Phelps, L. N., Dawson, A., Zanon, M., Vallé, F., Nolan, C., Mauri, A., de
1420 Vernal, A., Izumi, K., Holmström, L., Marsicek, J., Goring, S., Sommer, P. S., Chaput, M.
1421 and Kupriyanov, D.: Pollen-based climate reconstruction techniques for late Quaternary
1422 studies, *Earth-Science Rev.*, 210, doi:10.1016/j.earscirev.2020.103384, 2020.
1423

- 1424 Cleator, S. F., Harrison, S. P., Nichols, N. K., Colin Prentice, I. and Roulstone, I.: A new
 1425 multivariable benchmark for Last Glacial Maximum climate simulations, *Clim. Past*, 16(2),
 1426 699–712, doi:10.5194/cp-16-699-2020, 2020.
- 1427
 1428 COHMAP,: Climatic changes of the last 18,000 years: observations and model
 1429 simulations. *Science*, 241, 1043-1052, 1988.
- 1430
 1431 Collins, P. M., Davis, B. A. S. and Kaplan, J. O.: The mid-Holocene vegetation of the
 1432 Mediterranean region and southern Europe, and comparison with the present day, *J.*
 1433 *Biogeogr.*, 39(10), doi:10.1111/j.1365-2699.2012.02738.x, 2012.
- 1434
 1435 Combourieu Nebout, N., Peyron, O., Dormoy, I., Desprat, S., Beaudouin, C., Kotthoff, U.
 1436 and Marret, F.: Rapid climatic variability in the west Mediterranean during the last 25 000
 1437 years from high resolution pollen data, *Clim. Past*, 5(3), 503–521, doi:10.5194/cp-5-503-
 1438 2009, 2009.
- 1439
 1440 Connor, S. E., Ross, S. A., Sobotkova, A., Herries, A. I. R., Mooney, S. D., Longford, C. and
 1441 Iliev, I.: Environmental conditions in the SE Balkans since the Last Glacial Maximum and
 1442 their influence on the spread of agriculture into Europe, *Quat. Sci. Rev.*, 68, 200–215,
 1443 doi:10.1016/j.quascirev.2013.02.011, 2013.
- 1444
 1445 Cowling, S. A. and Sykes, M. T.: Physiological significance of low atmospheric CO₂ for
 1446 plant-climate interactions, *Quat. Res.*, 52(2), 237–242, doi:10.1006/qres.1999.2065, 1999.
- 1447
 1448 Damblon, F.: L'enregistrement palynologique de la sequence pléistocène et holocène de la
 1449 grotte Walou, in *La grotte Walou à Trooz (Belgique)*, edited by C. Draily, S. Pirson, and M.
 1450 Toussaint, pp. 84–129, Service public de Wallonie (Etudes et Documents, Archéologie, 21).,
 1451 2011.
- 1452
 1453 Daniau, A.-L., Desprat, S., Aleman, J. C., Bremond, L., Davis, B., Fletcher, W., Marlon, J.
 1454 R., Marquer, L., Montade, V., Morales-Molino, C., Naughton, F., Rius, D. and Urrego, D. H.:
 1455 Terrestrial plant microfossils in palaeoenvironmental studies, pollen, microcharcoal and
 1456 phytolith. Towards a comprehensive understanding of vegetation, fire and climate changes
 1457 over the past one million years, *Rev. Micropaleontol.*, 63, doi:10.1016/j.revmic.2019.02.001,
 1458 2019.
- 1459
 1460 Davis, B. A. S. and Stevenson, A. C.: The 8.2 ka event and Early-Mid Holocene forests, fires
 1461 and flooding in the Central Ebro Desert, NE Spain, *Quat. Sci. Rev.*, 26(13–14),
 1462 doi:10.1016/j.quascirev.2007.04.007, 2007.
- 1463
 1464 Davis, B. A. S., Brewer, S., Stevenson, A. C., Guiot, J., Allen, J., Almqvist-Jacobson, H.,
 1465 Ammann, B., Andreev, A. A., Argant, J., Atanassova, J., Balwierz, Z., Barnosky, C. D.,
 1466 Bartley, D. D., De Beaulieu, J. L., Beckett, S. C., Behre, K. E., Bennett, K. D., Berglund, B.
 1467 E. B., Beug, H.-J., Bezusko, L., Binka, K., Birks, H. H., Birks, H. J. B., Björck, S.,
 1468 Bliakhartchouk, T., Bogdel, I., Bonatti, E., Bottema, S., Bozilova, E. D. B., Bradshaw, R.,
 1469 Brown, A. P., Brugiapaglia, E., Carrion, J., Chernavskaya, M., Clerc, J., Clet, M., Coûteaux,
 1470 M., Craig, A. J., Cserny, T., Cwynar, L. C., Dambach, K., De Valk, E. J., Digerfeldt, G.,
 1471 Diot, M. F., Eastwood, W., Elina, G., Filimonova, L., Filipovitch, L., Gaillard-Lemdhal, M.
 1472 J., Gauthier, A., Göransson, H., Guenet, P., Gunova, V., Hall, V. A. H., Harmata, K., Hicks,
 1473 S., Huckerby, E., Huntley, B., Huttunen, A., Hyvärinen, H., Ilves, E., Jacobson, G. L., Jahns,

1474 S., Jankovská, V., Jóhansen, J., Kabailiene, M., Kelly, M. G., Khomutova, V. I., Königsson,
1475 L. K., Kremenetski, C., Kremenetskii, K. V., Krisai, I., Krisai, R., Kvavadze, E., Lamb, H.,
1476 Lazarova, M. A., Litt, T., Lotter, A. F., Lowe, J. J., Magyari, E., Makohonienko, M.,
1477 Mamakowa, K., Mangerud, J., Mariscal, B., Markgraf, V., McKeever, Mitchell, F. J. G.,
1478 Munuera, M., Nicol-Pichard, S., Noryskiewicz, B., Odgaard, B. V., Panova, N. K.,
1479 Pantaleon-Cano, J., Paus, A. A., Pavel, T., Peglar, S. M., Penalba, M. C., Pennington, W.,
1480 Perez-Obiol, R., et al.: The temperature of Europe during the Holocene reconstructed from
1481 pollen data, *Quat. Sci. Rev.*, 22(15–17), doi:10.1016/S0277-3791(03)00173-2, 2003.

1482
1483 Davis, B. A. S., Chevalier, M., Sommer, P., Carter, V. A., Finsinger, W., Mauri, A., Phelps,
1484 L. N., Zanon, M., Abegglen, R., Åkesson, C. M., Alba-Sánchez, F., Scott Anderson, R.,
1485 Antipina, T. G., Atanassova, J. R., Beer, R., Belyanina, N. I., Blyakharchuk, T. A., Borisova,
1486 O. K., Bozilova, E., Bukreeva, G., Jane Bunting, M., Clò, E., Colombaroli, D., Combourieu-
1487 Nebout, N., Desprat, S., Di Rita, F., Djamali, M., Edwards, K. J., Fall, P. L., Feurdean, A.,
1488 Fletcher, W., Florenzano, A., Furlanetto, G., Gaceur, E., Galimov, A. T., Gałka, M., García-
1489 Moreiras, I., Giesecke, T., Grindean, R., Guido, M. A., Gvozdeva, I. G., Herzs Schuh, U.,
1490 Hjelle, K. L., Ivanov, S., Jahns, S., Jankovska, V., Jiménez-Moreno, G., Karpińska-Kołodziej,
1491 M., Kitaba, I., Kołodziej, P., Lapteva, E. G., Latałowa, M., Lebreton, V., Leroy, S., Leydet,
1492 M., Lopatina, D. A., López-Sáez, J. A., Lotter, A. F., Magri, D., Marinova, E., Matthias, I.,
1493 Mavridou, A., Mercuri, A. M., Mesa-Fernández, J. M., Mikishin, Y. A., Milecka, K.,
1494 Montanari, C., Morales-Molino, C., Mrotzek, A., Sobrino, C. M., Naidina, O. D., Nakagawa,
1495 T., Nielsen, A. B., Novenko, E. Y., Panajiotidis, S., Panova, N. K., Papadopoulou, M.,
1496 Pardoe, H. S., Pędziszewska, A., Petrenko, T. I., Ramos-Román, M. J., Ravazzi, C., Rösch,
1497 M., Ryabogina, N., Ruiz, S. S., Sakari Salonen, J., Sapelko, T. V., Schofield, J. E., Seppä, H.,
1498 Shumilovskikh, L., Stivrins, N., Stojakowits, P., Svitavska, H. S., Święta-Musznicka, J.,
1499 Tantau, I., Tinner, W., Tobolski, K., Tonkov, S., Tsakiridou, M., et al.: The Eurasian Modern
1500 Pollen Database (EMPD), version 2, *Earth Syst. Sci. Data*, 12(4), 2423–2445,
1501 doi:10.5194/essd-12-2423-2020, 2020.

1502
1503 Davis M.B.: On the theory of pollen analysis. *American Journal of Sciences*, 26, 897–912,
1504 1963.

1505
1506 Demay, L., Julien, M.A., Anghelinu, M., Shydlovskiy, P.S., Koulakovska, L.V., P’ean, S.,
1507 Stupak, D.V., Vasyliiev, P.M., Obřada, T., Wojtal, P., Belyaeva, V.I.: Study of human
1508 behaviors during the Late Pleniglacial in the East European Plain through their relation to the
1509 animal world. *Quat. Int.* <https://doi.org/10.1016/j.quaint.2020.10.047>, 2021.

1510
1511 Douada, J., Doudová, J., Drařnarová, A., Kuneř, P., Hadincová, V., Krak, K., Zákra vský, P.
1512 and Mandák, B.: Migration patterns of subgenus *Alnus* in Europe since the last glacial
1513 maximum: A systematic review, *PLoS One*, 9(2), doi:10.1371/journal.pone.0088709, 2014.

1514
1515 Duprat-Oualid, F., Rius, D., Bégeot, C., Magny, M., Millet, L., Wulf, S. and Appelt, O.:
1516 Vegetation response to abrupt climate changes in Western Europe from 45 to 14.7k cal a BP:
1517 the Bergsee lacustrine record (Black Forest, Germany), *J. Quat. Sci.*, 32(7), 1008–1021,
1518 doi:10.1002/jqs.2972, 2017.

1519
1520 Dupre Ollivier, M.: *Palinología y paleoambiente- nuevos datos españoles referencias*,
1521 Universidad de Valencia., 1988.

1522

1523 Edwards, M. E., Anderson, P. M., Brubaker, L. B., Ager, T., Andreev, A. A., Bigelow, N. H.,
1524 Cwynar, L. C., Eisner, W. R., Harrison, S. P., Hu, F.-S., Jolly, D., Lozhkin, A. V.,
1525 MacDonald, G. M., Mock, C. J., Ritchie, J. C., Sher, A. V., Spear, R. W., Williams, J. & Yu,
1526 G.: Pollen-based biomes for Beringia 18,000, 6000 and 0 14C yr bp. *Journal of*
1527 *Biogeography*, **27**, 521– 554, doi: [10.1046/j.1365-2699.2000.00426.x](https://doi.org/10.1046/j.1365-2699.2000.00426.x), 2000.
1528
1529 Ehlers, J., Gibbard, P. L. and Hughes, P. D.: Quaternary Glaciations - Extent and Chronology
1530 A Closer Look, edited by J. Ehlers, P. L. Gibbard, and P. D. Hughes, Elsevier., 2011.
1531
1532 Elenga, H., Peyron, O., Bonnefille, R., Jolly, D., Cheddadi, R., Guiot, J., Andrieu, V.,
1533 Bottema, S., Buchet, G., De Beaulieu, J. L., Hamilton, A. C., Maley, J., Marchant, R., Perez-
1534 Obiol, R., Reille, M., Riollet, G., Scott, L., Straka, H., Taylor, D., Van Campo, E., Vincens,
1535 A., Laarif, F. and Jonson, H.: Pollen-based biome reconstruction for southern Europe and
1536 Africa 18,000 yr BP, *J. Biogeogr.*, **27**(3), 621–634, doi:10.1046/j.1365-2699.2000.00430.x,
1537 2000.
1538
1539 Ferguson, J. E., Henderson, G. M., Fa, D. A., Finlayson, J. C. and Charnley, N. R.: Increased
1540 seasonality in the Western Mediterranean during the last glacial from limpet shell
1541 geochemistry, *Earth Planet. Sci. Lett.*, **308**(3–4), 325–333, doi:10.1016/j.epsl.2011.05.054,
1542 2011.
1543
1544 Feurdean A, Bhagwat SA, Willis KJ, Birks HJB, Lischke H, Hickler T.: Tree migration-rates:
1545 narrowing the gap between inferred post-glacial rates and projected rates. *PLoS ONE* **8**:
1546 e71797, 2013.
1547
1548 Feurdean, A., Perşoiu, A., Tanţău, I., Stevens, T., Magyari, E. K., Onac, B. P., Marković, S.,
1549 Andrič, M., Connor, S., Fărcaş, S., Gałka, M., Gaudeny, T., Hoek, W., Kolaczek, P., Kuneš,
1550 P., Lamentowicz, M., Marinova, E., Michezyńska, D. J., Perşoiu, I., Płóciennik, M.,
1551 Słowiński, M., Stancikaite, M., Sumegi, P., Svensson, A., Tămaş, T., Timar, A., Tonkov, S.,
1552 Toth, M., Veski, S., Willis, K. J. and Zernitskaya, V.: Climate variability and associated
1553 vegetation response throughout Central and Eastern Europe (CEE) between 60 and 8ka, *Quat.*
1554 *Sci. Rev.*, **106**, 206–224, doi:10.1016/j.quascirev.2014.06.003, 2014.
1555
1556 Fick, S. E. and Hijmans, R. J.: WorldClim 2: new 1-km spatial resolution climate surfaces for
1557 global land areas, *Int. J. Climatol.*, **37**(12), 4302–4315, doi:10.1002/joc.5086, 2017.
1558
1559 Fletcher, W. J., Goni, M. F. S., Peyron, O. and Dormoy, I.: Abrupt climate changes of the last
1560 deglaciation detected in a Western Mediterranean forest record, *Clim. Past*, **6**(2), 245–264,
1561 doi:10.5194/cp-6-245-2010, 2010.
1562
1563 Gaillard, M. J., Sugita, S., Mazier, F., Trondman, A. K., Broström, A., Hickler, T., Kaplan, J.
1564 O., Kjellström, E., Kokfelt, U., Kuneš, P., Lemmen, C., Miller, P., Olofsson, J., Poska, A.,
1565 Rundgren, M., Smith, B., Strandberg, G., Fyfe, R., Nielsen, A. B., Alenius, T., Balakauskas,
1566 L., Barnekow, L., Birks, H. J. B., Bjune, A., Björkman, L., Giesecke, T., Hjelle, K., Kalnina,
1567 L., Kangur, M., Van Der Knaap, W. O., Koff, T., Lageras, P., Latałowa, M., Leydet, M.,
1568 Lechterbeck, J., Lindbladh, M., Odgaard, B., Peglar, S., Segerström, U., Von Stedingk, H.
1569 and Seppä, H.: Holocene land-cover reconstructions for studies on land cover-climate
1570 feedbacks, *Clim. Past*, **6**(4), 483–499, doi:10.5194/cp-6-483-2010, 2010.
1571

1572 García-Amorena, I., Gómez Manzaneque, F., Rubiales, J. M., Granja, H. M., Soares de
1573 Carvalho, G. and Morla, C.: The Late Quaternary coastal forests of western Iberia: A study of
1574 their macroremains, *Palaeogeogr. Palaeoclimatol. Palaeoecol.*, 254(3–4), 448–461,
1575 doi:10.1016/j.palaeo.2007.07.003, 2007.

1576
1577 Genov, I.: The Black Sea level from the Last Glacial Maximum to the present time, *Geol.*
1578 *Balc.*, 45(1–3), 3–19, 2016.

1579
1580 Giesecke, T.: Did thermophilous trees spread into central Europe during the Late Glacial?,
1581 *New Phytol.*, 212(1), 15–18, doi:10.1111/nph.14149, 2016.

1582
1583 Giesecke, T., Davis, B., Brewer, S., Finsinger, W., Wolters, S., Blaauw, M., de Beaulieu, J.-
1584 L., Binney, H., Fyfe, R. M., Gaillard, M.-J., Gil-Romera, G., van der Knaap, W. O., Kuneš,
1585 P., Köhl, N., van Leeuwen, J. F. N., Leydet, M., Lotter, A. F., Ortu, E., Semmler, M. and
1586 Bradshaw, R. H. W.: Towards mapping the late Quaternary vegetation change of Europe,
1587 *Veg. Hist. Archaeobot.*, 23(1), doi:10.1007/s00334-012-0390-y, 2014.

1588
1589 Geiger, R.: *The climate near the ground*. Cambridge: Blue Hill Met. Observ. Harvard
1590 University 1960

1591
1592 Giraudi, C.: Lake levels and climate for the last 30,000 years in the fucino area (Abruzzo-
1593 Central Italy) - A review, *Palaeogeogr. Palaeoclimatol. Palaeoecol.*, 70(1–3), 249–260,
1594 doi:10.1016/0031-0182(89)90094-1, 1989.

1595
1596 Giraudi, C.: Climate evolution and forcing during the last 40 ka from the oscillations in
1597 Apennine glaciers and high mountain lakes, Italy, *J. Quat. Sci.*, 32(8), 1085–1098,
1598 doi:10.1002/jqs.2985, 2017.

1599
1600 Guido, M. A., Molinari, C., Moneta, V., Branch, N., Black, S., Simmonds, M., Stastney, P.
1601 and Montanari, C.: Climate and vegetation dynamics of the Northern Apennines (Italy)
1602 during the Late Pleistocene and Holocene, *Quat. Sci. Rev.*, 231,
1603 doi:10.1016/j.quascirev.2020.106206, 2020.

1604 Hansen, M. C., Potapov, P. V., Moore, R., Hancher, M., Turubanova, S. A., Tyukavina, A.,
1605 Thau, D., Stehman, S. V., Goetz, S. J., Loveland, T. R., Kommareddy, A., Egorov, A., Chini,
1606 L., Justice, C. O. and Townshend, J. R. G.: High-resolution global maps of 21st-century
1607 forest cover change, *Science (80-.)*, 342(6160), 850–853, doi:10.1126/science.1244693,
1608 2013.

1609
1610 Grichuk, V. P.: Main types of vegetation (ecosystems) for the maximum cooling of the last
1611 glaciation. B. Frenzel, B. Pecs, A.A. Velichko (Eds.), *Atlas of Palaeoclimates and*
1612 *Palaeoenvironments of the Northern Hemisphere*, NQUA/Hungarian Academy of
1613 Sciences, Budapest, pp. 123-124, doi: [10.2307/1551555](https://doi.org/10.2307/1551555), 1992.

1614
1615 Guiot, J., Torre, F., Jolly, D., Peyron, O., Boreux, J.J., Cheddadi, R.: Inverse vegetation
1616 modeling by Monte Carlo sampling to reconstruct palaeoclimates under changed precipitation

1617 seasonality and CO₂ conditions: application to glacial climate in Mediterranean region. *Ecol.*
1618 *Model.* 127, 119–140. doi: 10.1016/
1619 S0304-3800(99)00219-7, 2000.
1620
1621 Harrison, S. P., Yu, G. E. and Tarasov, P. E.: Late Quaternary Lake-Level Record from
1622 Northern Eurasia, *Quat. Res.*, 45(2), 138–159, doi:10.1006/qres.1996.0016, 1996.
1623
1624 Harrison, S. P., Bartlein, P. J., Brewer, S., Prentice, I. C., Boyd, M., Hessler, I., Holmgren,
1625 K., Izumi, K. and Willis, K.: Climate model benchmarking with glacial and mid-Holocene
1626 climates, *Clim. Dyn.*, 43(3–4), 671–688, doi:10.1007/s00382-013-1922-6, 2014.
1627
1628 Harrison, S. P., Bartlein, P. J., Izumi, K., Li, G., Annan, J., Hargreaves, J., Braconnot, P. and
1629 Kageyama, M.: Evaluation of CMIP5 palaeo-simulations to improve climate projections, *Nat.*
1630 *Clim. Chang.*, 5(8), 735–743, doi:10.1038/nclimate2649, 2015.
1631
1632 Heiri, O., Koinig, K. A., Spötl, C., Barrett, S., Brauer, A., Drescher-Schneider, R., Gaar, D.,
1633 Ivy-Ochs, S., Kerschner, H., Luetscher, M., Moran, A., Nicolussi, K., Preusser, F., Schmidt,
1634 R., Schoeneich, P., Schwörer, C., Sprafke, T., Terhorst, B. and Tinner, W.: Palaeoclimate
1635 records 60–8 ka in the Austrian and Swiss Alps and their forelands, *Quat. Sci. Rev.*, 106,
1636 186–205, doi:10.1016/j.quascirev.2014.05.021, 2014.
1637
1638 Heyman, B. M., Heyman, J., Fickert, T., Harbor, J. M. and Forest, B.: Paleo-climate of the
1639 central European uplands during the last glacial maximum based on glacier mass-balance
1640 modeling Bavarian Forest Republic, *Quat. Res.*, 79(1), 49–54,
1641 doi:10.1016/j.yqres.2012.09.005, 2013.
1642
1643 Hughes, A. L. C., Gyllencreutz, R., Lohne, Ø. S., Mangerud, J. and Svendsen, J. I.: The last
1644 Eurasian ice sheets - a chronological database and time-slice reconstruction, *DATED-1,*
1645 *Boreas*, 45(1), 1–45, doi:10.1111/bor.12142, 2016.
1646
1647 Hughes, P. D. and Gibbard, P. L.: A stratigraphical basis for the Last Glacial Maximum
1648 (LGM), *Quat. Int.*, 383(June 2014), 174–185, doi:10.1016/j.quaint.2014.06.006, 2015.
1649
1650 Hughes, P. D., Woodward, J. C. and Gibbard, P. L.: Late Pleistocene glaciers and climate in
1651 the Mediterranean, *Glob. Planet. Change*, 50(1–2), 83–98,
1652 doi:10.1016/j.gloplacha.2005.07.005, 2006.
1653
1654 Huntley, B.: Dissimilarity mapping between fossil and contemporary pollen spectra in
1655 Europe for the past 13,000 years, *Quat. Res.*, 33(3), 360–376, doi:10.1016/0033-
1656 5894(90)90062-P, 1990.
1657
1658 Huntley B.: Dissimilarity mapping between fossil and contemporary pollen spectra in Europe
1659 for the past 13,000 years. *Quaternary Research* 33:360–376, 1990.
1660
1661 Huntley, B. and Allen, J. R. M.: Glacial environments III. Palaeovegetation patterns in late
1662 glacial Europe, in Neanderthals and modern humans in the European landscape during the
1663 last glaciation, edited by T. H. Van Andel and H. C. Davies, pp. 79–102, McDonald Institute
1664 for Archaeological Research, Cambridge., 2003.

- 1665 Huntley, B. and Birks, H. J. B.: An Atlas of Past and Present Pollen Maps for Europe: 0–
1666 13,000 B.P. years ago, Cambridge University Press, Cambridge., 1983.
1667
- 1668 Jalut, G., Andrieu, V., Delibrias, G., Fontaugne, M. and Pages, P.: Palaeoenvironment of the
1669 valley of Ossau (Western French Pyrenees) during the last 27 000 year, *Pollen et Spores*,
1670 30(3–4), 357–393, 1988.
1671
- 1672 Jalut, G., Marti, J. M., Fontugne, M., Delibrias, G., Vilaplana, J. M. and Julia, R.: Glacial to
1673 interglacial vegetation changes in the northern and southern Pyrénées: Deglaciation,
1674 vegetation cover and chronology, *Quat. Sci. Rev.*, 11(4), 449–480, doi:10.1016/0277-
1675 3791(92)90027-6, 1992.
1676
- 1677 Jankovska, V.: Vegetation cover in West Carpathians during the Last Glacial period -
1678 analogy of present day siberian forest-tundra nad taiga, *Palynol. Stratigr. geoecology*,
1679 (SEPTEMBER 2008), 282–289, 2008.
1680
- 1681 Janská, V., Jiménez-Alfaro, B., Chytrý, M., Divíšek, J., Anenkhonov, O., Korolyuk, A.,
1682 Lashchinskyi, N. and Culek, M.: Palaeodistribution modelling of European vegetation types
1683 at the Last Glacial Maximum using modern analogues from Siberia: Prospects and
1684 limitations, *Quat. Sci. Rev.*, 159, 103–115, doi:10.1016/j.quascirev.2017.01.011, 2017.
1685
- 1686 Jost, A., Lunt, D., Abe-Ouchi, A., Abe-Ouchi, A., Peyron, O., Valdes, P. J. and Ramstein, G.:
1687 High-resolution simulations of the last glacial maximum climate over Europe: A solution to
1688 discrepancies with continental palaeoclimatic reconstructions?, *Clim. Dyn.*, 24(6), 577–590,
1689 doi:10.1007/s00382-005-0009-4, 2005.
1690
- 1691 Juggins, S.: Quantitative reconstructions in palaeolimnology : new paradigm or sick
1692 science ?, *Quat. Sci. Rev.*, 64, 20–32, doi:10.1016/j.quascirev.2012.12.014, 2013.
1693
- 1694 Juggins, S.: Rioja: Analysis of Quaternary Science Data, [online] Available from:
1695 <https://cran.r-project.org/package=rioja>, 2020.
1696
- 1697 Juggins, S. and Birks, H. J. B.: Quantitative Environmental Reconstructions from Biological
1698 Data, in *Developments in Palaeoenvironmental Research 5*, edited by H. J. B. Birks, pp. 431–
1699 494, Springer ScienceCBusiness Media B.V., 2012.
1700
- 1701 Juříčková, L., Horáčková, J. and Ložek, V.: Direct evidence of central European forest
1702 refugia during the last glacial period based on mollusc fossils, *Quat. Res. (United States)*,
1703 82(1), 222–228, doi:10.1016/j.yqres.2014.01.015, 2014.
1704
- 1705 Kageyama, M., Laine, A., Abe-Ouchi, A., Braconnot, P., Cortijo, E., Crucifix, M., de Vernal,
1706 A., Guiot, J., Hewitt, C. D., Kitoh, A., Kucera, M., Marti, O., Ohgaito, R., Otto-Bliesner, B.,
1707 Peltier, W. R., Rosell-Melé, A., Vettoretti, G., Weber, S. L. and Yu, Y.: Last Glacial
1708 Maximum temperatures over the North Atlantic, Europe and western Siberia: a comparison
1709 between PMIP models, MARGO sea-surface temperatures and pollen-based reconstructions,
1710 *Quat. Sci. Rev.*, 25(17–18), 2082–2102, doi:10.1016/j.quascirev.2006.02.010, 2006.
1711
- 1712 Kageyama, M., Harrison, S. P., Kapsch, M. L., Lofverstrom, M., Lora, J. M., Mikolajewicz,
1713 U., ... & Zhu, J. The PMIP4 Last Glacial Maximum experiments: preliminary results and
1714 comparison with the PMIP3 simulations. *Climate of the Past*, 17(3), 1065-1089, 2021.

1715
1716 Kaltenrieder, P., Belis, C. A., Hofstetter, S., Ammann, B., Ravazzi, C. and Tinner, W.:
1717 Environmental and climatic conditions at a potential Glacial refugial site of tree species near
1718 the Southern Alpine glaciers. New insights from multiproxy sedimentary studies at Lago
1719 della Costa (Euganean Hills, Northeastern Italy), *Quat. Sci. Rev.*, 28(25–26), 2647–2662,
1720 doi:10.1016/j.quascirev.2009.05.025, 2009.
1721
1722 Kaplan, J. O., Pfeiffer, M., Kolen, J. C. A. and Davis, B. A. S.: Large scale anthropogenic
1723 reduction of forest cover in last glacial maximum Europe, *PLoS One*, 11(11),
1724 doi:10.1371/journal.pone.0166726, 2016.
1725
1726 Kehrwald, N. M., McCoy, W. D., Thibeault, J., Burns, S. J. and Oches, E. A.: Paleoclimatic
1727 implications of the spatial patterns of modern and LGM European land-snail shell $\delta^{18}\text{O}$,
1728 *Quat. Res.*, 74(1), 166–176, doi:10.1016/j.yqres.2010.03.001, 2010.
1729
1730 Kelly, A., Charman, D. J. and Newnham, R. M.: A last glacial maximum pollen record from
1731 bodmin moor showing a possible cryptic Northern refugium in Southwest England, *J. Quat.*
1732 *Sci.*, 25(3), 296–308, doi:10.1002/jqs.1309, 2010.
1733
1734 Kolodny, Y., Stein, M. and Machlus, M.: Sea-rain-lake relation in the Last Glacial East
1735 Mediterranean revealed by $\delta^{18}\text{O}$ - $\delta^{13}\text{C}$ in Lake Lisan aragonites, *Geochim. Cosmochim.*
1736 *Acta*, 69(16), 4045–4060, doi:10.1016/j.gca.2004.11.022, 2005.
1737
1738 Kovács, J., Moravcová, M., Újvári, G. and Pintér, A. G.: Reconstructing the
1739 paleoenvironment of East Central Europe in the Late Pleistocene using the oxygen and
1740 carbon isotopic signal of tooth in large mammal remains, *Quat. Int.*, 276–277, 145–154,
1741 doi:10.1016/j.quaint.2012.04.009, 2012.
1742
1743 Krebs, P., Pezzatti, G. B., Beffa, G., Tinner, W. and Conedera, M.: Revising the sweet
1744 chestnut (*Castanea sativa* Mill.) refugia history of the last glacial period with extended pollen
1745 and macrofossil evidence, *Quat. Sci. Rev.*, 206, 111–128,
1746 doi:10.1016/j.quascirev.2019.01.002, 2019.
1747
1748 Kuneš, P., Pelánková, B., Chytrý, M., Jankovská, V., Pokorný, P. and Petr, L.: Interpretation
1749 of the last-glacial vegetation of eastern-central Europe using modern analogues from southern
1750 Siberia, *J. Biogeogr.*, 35(12), 2223–2236, doi:10.1111/j.1365-2699.2008.01974.x, 2008.
1751
1752 Küster, H.: Postglaziale Vegetationsgeschichte Südbayerns. Geobotanische Studien zur
1753 Prähistorischen Landschaftskunde, Akademie Verlag, Berlin., 1995.
1754
1755 Lacey, J. H., Leng, M. J., Höbig, N., Reed, J. M., Valero-Garcés, B. and Reicherter, K.:
1756 Western Mediterranean climate and environment since Marine Isotope Stage 3: a 50,000-year
1757 record from Lake Banyoles, Spain, *J. Paleolimnol.*, 55(2), 113–128, doi:10.1007/s10933-015-
1758 9868-9, 2016.
1759
1760 Latombe, G., Burke, A., Vrac, M., Levavasseur, G. and Dumas, C.: Comparison of spatial
1761 downscaling methods of general circulation model results to study climate variability during
1762 the Last Glacial Maximum, , 2563–2579, 2018.
1763

- 1764 Lefort J.P., Monnier J.L., Danukalova G.: Transport of Late Pleistocene loess particles by
1765 katabatic winds during the lowstands of the English Channel. *Journal of the Geological*
1766 *Society* 176: 1169–1181, doi: [10.1144/jgs2019-07](https://doi.org/10.1144/jgs2019-07), 2019.
- 1767
1768 Lehmkuhl, F., Nett, J.J., Pöfner, S., Schulte, P., Sprafke, T., Jary, Z., Antoine, P., Wacha, L.,
1769 Wolf, D., Zerboni, A., Hošek, J., Marković, S.B., Obrecht, I., Sümeği, P., Veres, D.,
1770 Zeeden, C., Boemke, B., Schaubert, V., Viehweger, J., Hambach, U.: Loess landscapes of
1771 Europe re-mapping, geomorphology, and zonal differentiation. *Earth Sci. Rev.* 215, 103496.
1772 <https://doi.org/10.1016/j.earscirev.2020.103496>, 2021.
- 1773
1774 Leroy, S. A. G. and Arpe, K.: Glacial refugia for summer-green trees in Europe and south-
1775 west Asia as proposed by ECHAM3 time-slice atmospheric model simulations, *J. Biogeogr.*,
1776 34(12), 2115–2128, doi:10.1111/j.1365-2699.2007.01754.x, 2007.
- 1777
1778 Lev, L., Stein, M., Ito, E., Fruchter, N., Ben-Avraham, Z. and Almogi-Labin, A.:
1779 Sedimentary, geochemical and hydrological history of Lake Kinneret during the past 28,000
1780 years, *Quat. Sci. Rev.*, 209, 114–128, doi:10.1016/j.quascirev.2019.02.015, 2019.
- 1781
1782 Lister, A. M. and Stuart, A. J.: The impact of climate change on large mammal distribution
1783 and extinction: Evidence from the last glacial/interglacial transition, *Comptes Rendus -*
1784 *Geosci.*, 340(9–10), 615–620, doi:10.1016/j.crte.2008.04.001, 2008.
- 1785
1786 López-García, J. M. and Blain, H. A.: Quaternary small vertebrates: State of the art and new
1787 insights, *Quat. Sci. Rev.*, 233, doi:10.1016/j.quascirev.2020.106242, 2020.
- 1788
1789 Ludwig, P., Pinto, J. G., Raible, C. C. and Shao, Y.: Impacts of surface boundary conditions
1790 on regional climate model simulations of European climate during the Last Glacial
1791 Maximum, *Geophys. Res. Lett.*, 44(10), 5086–5095, doi:10.1002/2017GL073622, 2017.
- 1792
1793
1794 Luetscher, M., Boch, R., Sodemann, H., Spötl, C., Cheng, H., Edwards, R. L., Frisia, S., Hof,
1795 F. and Müller, W.: North Atlantic storm track changes during the Last Glacial Maximum
1796 recorded by Alpine speleothems, *Nat. Commun.*, 6, 27–32, doi:10.1038/ncomms7344, 2015.
- 1797
1798 Magri, D.: Persistence of tree taxa in Europe and Quaternary climate changes, *Quat. Int.*,
1799 219(1–2), 145–151, doi:10.1016/j.quaint.2009.10.032, 2010.
- 1800
1801 Magri, D. and Parra, I.: Late Quaternary western Mediterranean pollen records and African
1802 winds, *Earth Planet. Sci. Lett.*, 200(3–4), 401–408, doi:10.1016/S0012-821X(02)00619-2,
1803 2002.
- 1804
1805 Magri, D. and Sadori, L.: Late Pleistocene and Holocene pollen stratigraphy at Lago di Vico,
1806 central Italy, *Veg. Hist. Archaeobot.*, 8(4), 247–260, doi:10.1007/BF01291777, 1999.
- 1807
1808 Magyari, E., Jakab, G., Rudner, E. and Sümeği, P.: Palynological and plant macrofossil data
1809 on Late Pleistocene short-term climatic oscillations in NE-Hungary, *Acta Palaeobot. Suppl.*,
1810 2(January), 491–502, 1999.
- 1811
1812 Magyari, E. K., Kuneš, P., Jakab, G., Sümeği, P., Pelánková, B., Schäbitz, F., Braun, M. and
1813 Chytrý, M.: Late Pleniglacial vegetation in eastern-central Europe: Are there modern

1814 analogues in Siberia?, *Quat. Sci. Rev.*, 95, 60–79, doi:10.1016/j.quascirev.2014.04.020,
1815 2014a.

1816

1817 Magyari, E. K., Veres, D., Wennrich, V., Wagner, B., Braun, M., Jakab, G., Karátson, D.,
1818 Pál, Z., Ferenczy, G., St-Onge, G., Rethemeyer, J., Francois, J. P., von Reumont, F. and
1819 Schäbitz, F.: Vegetation and environmental responses to climate forcing during the Last
1820 Glacial Maximum and deglaciation in the East Carpathians: Attenuated response to
1821 maximum cooling and increased biomass burning, *Quat. Sci. Rev.*, 106, 278–298,
1822 doi:10.1016/j.quascirev.2014.09.015, 2014b.

1823

1824 Magyari, E. K., Pál, I., Vincze, I., Veres, D., Jakab, G., Braun, M., Szalai, Z., Szabó, Z. and
1825 Korponai, J.: Warm Younger Dryas summers and early late glacial spread of temperate
1826 deciduous trees in the Pannonian Basin during the last glacial termination (20-9 kyr cal BP),
1827 *Quat. Sci. Rev.*, 225, doi:10.1016/j.quascirev.2019.105980, 2019.

1828

1829 Margari, V., Gibbard, P. L., Bryant, C. L. and Tzedakis, P. C.: Character of vegetational and
1830 environmental changes in southern Europe during the last glacial period; evidence from
1831 Lesvos Island, Greece, *Quat. Sci. Rev.*, 28(13–14), 1317–1339,
1832 doi:10.1016/j.quascirev.2009.01.008, 2009.

1833

1834 Marsicek, J., Shuman, B. N., Bartlein, P. J., Shafer, S. L. and Brewer, S.: Reconciling
1835 divergent trends and millennial variations in Holocene temperatures, *Nature*, 554(7690), 92–
1836 96, doi:10.1038/nature25464, 2018.

1837

1838 Mauch Lenardić, J., Oros Sršen, A. and Radović, S.: Quaternary fauna of the Eastern Adriatic
1839 (Croatia) with the special review on the Late Pleistocene sites, *Quat. Int.*, 494, 130–151,
1840 doi:10.1016/j.quaint.2017.11.028, 2018.

1841

1842 Mauri, A., Davis, B. A. S., Collins, P. M. and Kaplan, J. O.: The influence of atmospheric
1843 circulation on the mid-Holocene climate of Europe: A data-model comparison, *Clim. Past*,
1844 10(5), 1925–1938, doi:10.5194/cp-10-1925-2014, 2014.

1845

1846 Mauri, A., Davis, B. A. S., Collins, P. M. and Kaplan, J. O.: The climate of Europe during the
1847 Holocene: A gridded pollen-based reconstruction and its multi-proxy evaluation, *Quat. Sci.*
1848 *Rev.*, 112, doi:10.1016/j.quascirev.2015.01.013, 2015.

1849

1850 MARGE Project Members.: Constraints on the magnitude and patterns of ocean cooling at
1851 the Last Glacial Maximum, , (January), 1–6, doi:10.1038/ngeo411, 2009.

1852

1853 Mikolajewicz, U.: Modeling mediterranean ocean climate of the last glacial maximum, *Clim.*
1854 *Past*, 7(1), 161–180, doi:10.5194/cp-7-161-2011, 2011.

1855

1856 Miola, A., Bondesan, A., Corain, L., Favaretto, S., Mozzi, P., Piovan, S. and Sostizzo, I.:
1857 Wetlands in the Venetian Po Plain (northeastern Italy) during the Last Glacial Maximum:
1858 Interplay between vegetation, hydrology and sedimentary environment, *Rev. Palaeobot.*
1859 *Palynol.*, 141(1–2), 53–81, doi:10.1016/j.revpalbo.2006.03.016, 2006.

1860

1861 Mix, A. C., Bard, E. and Schneider, R.: Environmental processes of the ice age: Land,
1862 oceans, glaciers (EPILOG), *Quat. Sci. Rev.*, 20(4), 627–657, doi:10.1016/S0277-
1863 3791(00)00145-1, 2001.

- 1864 Moine, O., Rousseau, D. D., Jolly, D. and Vianey-Liaud, M.: Paleoclimatic reconstruction
 1865 using mutual climatic range on terrestrial mollusks, *Quat. Res.*, 57(1), 162–172,
 1866 doi:10.1006/qres.2001.2286, 2002.
- 1867
 1868 Monegato, G., Ravazzi, C., Donegana, M., Pini, R., Calderoni, G. and Wick, L.: Evidence of
 1869 a two-fold glacial advance during the last glacial maximum in the Tagliamento end moraine
 1870 system (eastern Alps), *Quat. Res.*, 68(2), 284–302, doi:10.1016/j.yqres.2007.07.002, 2007.
- 1871
 1872 Monegato, G., Ravazzi, C., Culiberg, M., Pini, R., Bavec, M., Calderoni, G., Jež, J. and
 1873 Perego, R.: Sedimentary evolution and persistence of open forests between the south-eastern
 1874 Alpine fringe and the Northern Dinarides during the Last Glacial Maximum, *Palaeogeogr.*
 1875 *Palaeoclimatol. Palaeoecol.*, 436, 23–40, doi:10.1016/j.palaeo.2015.06.025, 2015.
- 1876
 1877 Moreno, A., González-Sampériz, P., Morellón, M., Valero-Garcés, B. L. and Fletcher, W. J.:
 1878 Northern Iberian abrupt climate change dynamics during the last glacial cycle: A view from
 1879 lacustrine sediments, *Quat. Sci. Rev.*, 36, 139–153, doi:10.1016/j.quascirev.2010.06.031,
 1880 2012.
- 1881
 1882 Nogues-Bravo D, Rodríguez-Sánchez F, Orsini L, de Boer E, Jansson R, Morlon, H.,
 1883 Fordham, D.A., Jackson, S.T.: Cracking the code of biodiversity responses to past climate
 1884 change. *Trends Ecol. Evol.* 33:765–76, 2018.
- 1885
 1886
 1887 Nolan, C., Overpeck, J. T., Allen, J. R. M., Anderson, P. M., Betancourt, J. L., Binney, H. A.,
 1888 Brewer, S., Bush, M. B., Chase, B. M., Cheddadi, R., Djamali, M., Dodson, J., Edwards, M.
 1889 E., Gosling, W. D., Haberle, S., Hotchkiss, S. C., Huntley, B., Ivory, S. J., Kershaw, A. P.,
 1890 Kim, S. H., Latorre, C., Leydet, M., Lézine, A. M., Liu, K. B., Liu, Y., Lozhkin, A. V.,
 1891 McGlone, M. S., Marchant, R. A., Momohara, A., Moreno, P. I., Müller, S., Otto-Bliesner, B.
 1892 L., Shen, C., Stevenson, J., Takahara, H., Tarasov, P. E., Tipton, J., Vincens, A., Weng, C.,
 1893 Xu, Q., Zheng, Z. and Jackson, S. T.: Past and future global transformation of terrestrial
 1894 ecosystems under climate change, *Science* (80-.), 361(6405), 920–923,
 1895 doi:10.1126/science.aan5360, 2018.
- 1896
 1897 Normand, S., Treier, U. A. and Odgaard, B. V.: Tree refugia and slow forest development in
 1898 response to post - LGM warming in North - Eastern European Russia, , 2(4), 2–5, 2011.
- 1899
 1900 Paganelli, A.: Evolution of vegetation and climate in the Veneto-Po Plain during the Late-
 1901 Glacial and Early Holocene using pollen-stratigraphical data, *Alp. Mediterr. Quat.*, 9(2),
 1902 581–589, 1996.
- 1903
 1904 Peyron, O., Guiot, J., Cheddadi, R., Tarasov, P., Reille, M., De Beaulieu, J. L., Bottema, S.
 1905 and Andrieu, V.: Climatic Reconstruction in Europe for 18,000 YR B.P. from Pollen Data,
 1906 *Quat. Res.*, 49(2), 183–196, doi:10.1006/qres.1997.1961, 1998a.
- 1907
 1908 Pons, A. and Reille, M.: The Holocene- and upper Pleistocene pollen record from Padul
 1909 (Granada, Spain): A new study, *Palaeogeogr. Palaeoclimatol. Palaeoecol.*, 66(3–4),
 1910 doi:10.1016/0031-0182(88)90202-7, 1988.
- 1911
 1912 Potì, A., Kehl, M., Broich, M., Carrión Marco, Y., Hutterer, R., Jentke, T., Linstädter, J.,
 1913 López-Sáez, J. A., Mikdad, A., Morales, J., Pérez-Díaz, S., Portillo, M., Schmid, C., Vidal-

- 1914 Matutano, P. and Weniger, G. C.: Human occupation and environmental change in the
 1915 western Maghreb during the Last Glacial Maximum (LGM) and the Late Glacial. New
 1916 evidence from the Iberomaurusian site Ifri El Baroud (northeast Morocco), *Quat. Sci. Rev.*,
 1917 220, 87–110, doi:10.1016/j.quascirev.2019.07.013, 2019.
- 1918
- 1919 Prentice, I. C., Cleator, S. F., Huang, Y. H., Harrison, S. P., and Roulstone, I.: Reconstructing
 1920 ice-age palaeoclimates: Quantifying low-CO₂ effects on plants, *Global Planet. Change*, 149,
 1921 166–176, <https://doi.org/10.1016/j.gloplacha.2016.12.012>, 2017.
- 1922
- 1923 Prentice, I. C. and Harrison, S. P.: Ecosystem effects of CO₂ concentration: Evidence from
 1924 past climates, *Clim. Past*, 5(3), 297–307, doi:10.5194/cp-5-297-2009, 2009.
- 1925
- 1926 Prentice, I. C., Guiot, J. and Harrison, S. P.: Mediterranean vegetation, lake levels and
 1927 palaeoclimate at the Last Glacial Maximum, *Nature*, 360(6405), 658–660,
 1928 doi:10.1038/360658a0, 1992.
- 1929
- 1930 Prentice, I. C., Guiot, J., Huntley, B., Jolly, D. and Cheddadi, R.: Reconstructing biomes
 1931 from palaeoecological data: A general method and its application to European pollen data at
 1932 0 and 6 ka, *Clim. Dyn.*, 12(3), 185–194, doi:10.1007/BF00211617, 1996.
- 1933
- 1934 Prentice, I. C., Harrison, S. P. and Bartlein, P. J.: Global vegetation and terrestrial carbon
 1935 cycle changes after the last ice age, *New Phytol.*, 189(4), 988–998, doi:10.1111/j.1469-
 1936 8137.2010.03620.x, 2011.
- 1937
- 1938 Prud'homme, C., Lécuyer, C., Antoine, P., Moine, O., Hatté, C., Fourel, F., Martineau, F. and
 1939 Rousseau, D. D.: Palaeotemperature reconstruction during the Last Glacial from $\delta^{18}\text{O}$ of
 1940 earthworm calcite granules from Nussloch loess sequence, Germany, *Earth Planet. Sci. Lett.*,
 1941 442, 13–20, doi:10.1016/j.epsl.2016.02.045, 2016.
- 1942
- 1943 Prud'homme, C., Lécuyer, C., Antoine, P., Hatté, C., Moine, O., Fourel, F., Amiot, R.,
 1944 Martineau, F. and Rousseau, D. D.: $\delta^{13}\text{C}$ signal of earthworm calcite granules: A new proxy
 1945 for palaeoprecipitation reconstructions during the Last Glacial in western Europe, *Quat. Sci.*
 1946 *Rev.*, 179, 158–166, doi:10.1016/j.quascirev.2017.11.017, 2018.
- 1947
- 1948 Puzachenko, A. Y., Markova, A. K. and Pawłowska, K.: Evolution of Central European
 1949 regional mammal assemblages between the late Middle Pleistocene and the Holocene (MIS7–
 1950 MIS1), *Quat. Int.*, (November), doi:10.1016/j.quaint.2021.11.009, 2021.
- 1951
- 1952 Ramstein, G., Kageyama, M., Guiot, J. and Wu, H.: How cold was Europe at the Last Glacial
 1953 Maximum? A synthesis of the progress achieved since the first PMIP model-data
 1954 comparison, , 331–339, 2007.
- 1955
- 1956 Reille, M. and Andrieu, V.: The late Pleistocene and Holocene in the Lourdes Basin, Western
 1957 Pyrénées, France: new pollen analytical and chronological data, *Veg. Hist. Archaeobot.*, 4(1),
 1958 1–21, doi:10.1007/BF00198611, 1995.
- 1959
- 1960 Reille, M. and de Beaulieu, J. L.: History of the Würm and Holocene vegetation in western
 1961 velay (Massif Central, France): A comparison of pollen analysis from three corings at Lac du
 1962 Bouchet, *Rev. Palaeobot. Palynol.*, 54(3–4), 233–248, doi:10.1016/0034-6667(88)90016-4,
 1963 1988.

1964

1965 Reimer, A., Landmann, G. and Kempe, S.: Lake Van, Eastern Anatolia, hydrochemistry and

1966 history, *Aquat. Geochemistry*, 15(1–2), 195–222, doi:10.1007/s10498-008-9049-9, 2009.

1967

1968 Rousseau, D. D.: Climatic transfer function from quaternary molluscs in European loess

1969 deposits, *Quat. Res.*, 36(2), 195–209, doi:10.1016/0033-5894(91)90025-Z, 1991.

1970

1971 Royer, A., Montuire, S., Legendre, S., Discamps, E., Jeannet, M. and Lécuyer, C.:

1972 Investigating the influence of climate changes on rodent communities at a regional-scale

1973 (MIS 1-3, Southwestern France), *PLoS One*, 11(1), 1–25, doi:10.1371/journal.pone.0145600,

1974 2016.

1975

1976 Ruiz-Zapata, M. B., Vegas, J., Garcia-Cortes, A., Gil Garcia, M. J., Torres, T., Ortiz, J. E.

1977 and Perez-Gonzalez, A.: Vegetation evolution during the Last Maximum Glacial Period in

1978 FU-1 sequence (Fuentillejo Lacustrin Maar, Campo de Calatrava, Ciudad Real), *Polen*, 18,

1979 37–49, 2008.

1980

1981 Salonen, J., Sanchez Goñi, M.F., Renssen, H. and Plikk, A.: Contrasting northern and

1982 southern European winter climate trends during the Last Interglacial. *Geology* 49.

1983 10.1130/G49007.1. 2021

1984

1985 Salonen, J.S., Ilvonen, L., Seppä, H., Holmström, L., Telford, R.J., Gaidamavicius, A.,

1986 Stancikaite, M., Subetto, D. Comparing different calibration methods (WA/WA-PLS

1987 regression and Bayesian modelling) and different-sized calibration sets in pollen-based

1988 quantitative climate reconstruction. *The Holocene* 22, 413–424, 2012.

1989

1990 Samartin, S., Heiri, O., Kaltenrieder, P., Köhl, N. and Tinner, W.: Reconstruction of full

1991 glacial environments and summer temperatures from Lago della Costa, a refugial site in

1992 Northern Italy, *Quat. Sci. Rev.*, 143, 107–119, doi:10.1016/j.quascirev.2016.04.005, 2016.

1993

1994 Sánchez Goñi, M.F., Loutre, M.F., Crucifix, M., Peyron, O., Santos, L., Duprat, J., Malaizé,

1995 B., Turon, J.-L., and Peypouquet, J.-P.: Increasing vegetation and climate gradient in western

1996 Europe over the Last Glacial inception (122–110 ka): Data–model comparison. *Earth and*

1997 *Planetary Science Letters*, 231, 111–130, doi: 10.1016/j.epsl.2004.12.010, 2005.

1998

1999 Sanchez Goñi, M.F., Harrison, S.P.: Millennial-scale climate variability and vegetation

2000 changes during the Last Glacial: concepts and terminology. *Quaternary Science*

2001 *Reviews* 29, 2823–2827, doi: [10.1016/j.quascirev.2009.11.014](https://doi.org/10.1016/j.quascirev.2009.11.014), 2010.

2002

2003 Sanchi, L., Ménot, G. and Bard, E.: Insights into continental temperatures in the northwestern

2004 Black Sea area during the Last Glacial period using branched tetraether lipids, *Quat. Sci.*

2005 *Rev.*, 84, 98–108, doi:10.1016/j.quascirev.2013.11.013, 2014.

2006

2007 Satkūnas, J. and Grigienė, A.: Eemian-Weichselian palaeoenvironmental record from the

2008 Mickūnai glacial depression (Eastern Lithuania), *Geologija*, 54(2), 35–51,

2009 doi:10.6001/geologija.v54i2.2482, 2012.

2010 Schäfer, I. K., Bliedtner, M., Wolf, D., Faust, D. and Zech, R.: Evidence for humid

2011 conditions during the last glacial from leaf wax patterns in the loess-paleosol sequence El

2012 Paraíso, Central Spain, *Quat. Int.*, 407, 64–73, doi:10.1016/j.quaint.2016.01.061, 2016.

2013

2014 Scourse, J. D.: Late Pleistocene stratigraphy and palaeobotany of the Isles of Scilly, *Philos.*
2015 *Trans. - R. Soc. London, B*, 334(1271), 405–448, doi:10.1098/rstb.1991.0125, 1991.

2016

2017 Spötl, C., Koltai, G., Jarosch, A. H. and Cheng, H.: Increased autumn and winter
2018 precipitation during the Last Glacial Maximum in the European Alps, *Nat. Commun.*, 12(1),
2019 doi:10.1038/s41467-021-22090-7, 2021.

2020

2021 Stewart, J. R. and Lister, A. M.: Cryptic northern refugia and the origins of the modern biota,
2022 *Trends Ecol. Evol.*, 16(11), 608–613, doi:10.1016/S0169-5347(01)02338-2, 2001.

2023

2024 Stivrins, N., Soininen, J., Amon, L., Fontana, S. L., Gryguc, G., Heikkilä, M., Heiri, O.,
2025 Kisielienė, D., Reitalu, T., Stančikaitė, M., Veski, S. and Seppä, H.: Biotic turnover rates
2026 during the Pleistocene-Holocene transition, *Quat. Sci. Rev.*, 151, 100–110,
2027 doi:10.1016/j.quascirev.2016.09.008, 2016.

2028

2029 Strahl, J.: Zur Pollenstratigraphie des Weichselspätglazials von Berlin-Brandenburg [On the
2030 palynostratigraphy of the Late Weichselian in Berlin-Brandenburg], *Brand.*
2031 *Geowissenschaftliche Beiträge*, 12, 87–112, 2005.

2032

2033 Stute, M. and Deak, J.: Environmental isotope study (¹⁴C, ¹³C, ¹⁸O, D, noble gases) on
2034 deep groundwater circulation systems in Hungary with reference to paleoclimate,
2035 *Radiocarbon*, 31(3), 902–918, doi:10.1017/s0033822200012522, 1990.

2036

2037 Svenning, J., Normand, S. and Kageyama, M.: Glacial refugia of temperate trees in Europe :
2038 insights from species distribution modelling, , (Svenning 2003), 1117–1127,
2039 doi:10.1111/j.1365-2745.2008.01422.x, 2008.

2040

2041 Tarasov, P. E., Webb, T., Andreev, A. A., Afanas'eva, N. B., Berezina, N. A., Bezusko, L.
2042 G., Blyakharchuk, T. A., Bolikhovskaya, N. S., Cheddadi, R., Chernavskaya, M. M.,
2043 Chernova, G. M., Dorofeyuk, N. I., Dirksen, V. G., Elina, G. A., Filimonova, L. V., Glebov,
2044 F. Z., Guiot, J., Gunova, V. S., Harrison, S. P., Jolly, D., Khomutova, V. I., Kvavadze, E. V.,
2045 Osipova, I. M., Panova, N. K., Prentice, I. C., Saarse, L., Sevastyanov, D. V., Volkova, V. S.
2046 and Zernitskaya, V. P.: Present-day and mid-Holocene biomes reconstructed from pollen and
2047 plant macrofossil data from the former Soviet Union and Mongolia, *J. Biogeogr.*, 25(6),
2048 1029–1053, doi:10.1046/j.1365-2699.1998.00236.x, 1998.

2049

2050 Tarasov, P. E., Volkova, V. S., Webb, T., Guiot, J., Andreev, A. A., Bezusko, L. G.,
2051 Bezusko, T. V., Bykova, G. V., Dorofeyuk, N. I., Kvavadze, E. V., Osipova, I. M., Panova,
2052 N. K. and Sevastyanov, D. V.: Last glacial maximum biomes reconstructed from pollen and
2053 plant macrofossil data from northern Eurasia, *J. Biogeogr.*, 27(3), 609–620,
2054 doi:10.1046/j.1365-2699.2000.00429.x, 2000.

2055

2056 Tarasov, P.E., Andreev, A.A., Anderson, P.M., Lozhkin, A.V., Haltia-Hovi, E., Nowaczyk,
2057 N.R., Wennrich, V., Brigham-Grette, J., Melles, M.: A pollen-based biome reconstruction
2058 over the last 3.562 million years in the Far East Russian Arctic e new insights on climate-
2059 vegetation relationships at the regional scale. *Clim. Past* 9, 2759-2775, doi: 10.5194/cp-9-
2060 2759-2013, 2013.

2061

- 2062 Telford, R. J. and Birks, H. J. B.: Evaluation of transfer functions in spatially structured
 2063 environments, *Quat. Sci. Rev.*, 28(13–14), 1309–1316, doi:10.1016/j.quascirev.2008.12.020,
 2064 2009.
- 2065
- 2066 Turner, M. G., Wei, D., Prentice, I. C., & Harrison, S. P. The impact of methodological
 2067 decisions on climate reconstructions using WA-PLS. *Quaternary Research*, 99, 341-356,
 2068 2021.
- 2069
- 2070 Valero-Garcés, B. L., González-Sampériz, P., Navas, A., Machin, J., Delgado-Huertas, A.,
 2071 Pena-Monné, J. L., Sancho-Marcén, C., Stevenson, T. and Davis, B.: Paleohydrological
 2072 fluctuations and steppe vegetation during the last glacial maximum in the central Ebro valley
 2073 (NE Spain), *Quat. Int.*, 122(1 SPEC. ISS.), doi:10.1016/j.quaint.2004.01.030, 2004.
- 2074
- 2075 Valsecchi, V., Sanchez Goñi, M. F. and Londeix, L.: Vegetation dynamics in the
 2076 Northeastern Mediterranean region during the past 23 000 yr: Insights from a new pollen
 2077 record from the Sea of Marmara, *Clim. Past*, 8(5), 1941–1956, doi:10.5194/cp-8-1941-2012,
 2078 2012.
- 2079
- 2080 Vandenberghe, J., French, H. M., Gorbunov, A., Marchenko, S., Velichko, A. A., Jin, H.,
 2081 Cui, Z., Zhang, T. and Wan, X.: The Last Permafrost Maximum (LPM) map of the Northern
 2082 Hemisphere: Permafrost extent and mean annual air temperatures, 25-17ka BP, *Boreas*,
 2083 43(3), 652–666, doi:10.1111/bor.12070, 2014.
- 2084
- 2085 Varsányi, I., Palcsu, L. and Kovács, L. Ó.: Groundwater flow system as an archive of
 2086 palaeotemperature: Noble gas, radiocarbon, stable isotope and geochemical study in the
 2087 Pannonian Basin, Hungary, *Appl. Geochemistry*, 26(1), 91–104,
 2088 doi:10.1016/j.apgeochem.2010.11.006, 2011.
- 2089
- 2090 Vegas-Vilarrúbia, T., González-Sampériz, P., Morellón, M., Gil-Romera, G., Pérez-Sanz, A.
 2091 and Valero-Garcés, B.: Diatom and vegetation responses to late glacial and early holocene
 2092 climate changes at lake estanya (southern pyrenees, NE spain), *Palaeogeogr. Palaeoclimatol.*
 2093 *Palaeoecol.*, 392, 335–349, doi:10.1016/j.palaeo.2013.09.011, 2013.
- 2094
- 2095 Vegas, J., Ruiz-Zapata, B., Ortiz, J. E., Galán, L., Torres, T., García-Cortés, Á., Gil-García,
 2096 M. J., Pérez-González, A. and Gallardo-Millán, J. L.: Identification of arid phases during the
 2097 last 50 cal. ka BP from the Fuentillejo maar-lacustrine record (Campo de Calatrava Volcanic
 2098 Field, Spain), *J. Quat. Sci.*, 25(7), 1051–1062, doi:10.1002/jqs.1262, 2010.
- 2099
- 2100 Velasquez, P., Kaplan, J. O., Messmer, M., Ludwig, P. and Raible, C. C.: The role of land
 2101 cover in the climate of glacial Europe, *Clim. Past*, 17(3), 1161–1180, doi:10.5194/cp-17-
 2102 1161-2021, 2021.
- 2103
- 2104 Vicente-Serrano, S. M., Trigo, R. M., López-Moreno, J. I., Liberato, M. L. R., Lorenzo-
 2105 Lacruz, J., Beguería, S., Morán-Tejeda, E. and El Kenawy, A.: Extreme winter precipitation
 2106 in the Iberian Peninsula in 2010: Anomalies, driving mechanisms and future projections,
 2107 *Clim. Res.*, 46(1), 51–65, doi:10.3354/cr00977, 2011.
- 2108
- 2109 Williams, J.W., Grimm, E.G., Blois, J., Charles, D.F., Davis, E., Goring, S.J., Graham, R.,
 2110 Smith, A.J., Anderson, M., Arroyo-Cabrales, J., Ashworth, A.C., Betancourt, J.L., Bills,
 2111 B.W., Booth, R.K., Buckland, P., Curry, B., Giesecke, T., Hausmann, S., Jackson, S.T.,

2112 Latorre, C., Nichols, J., Purdum, T., Roth, R.E., Stryker, M., Takahara, H. :The Neotoma
2113 Paleocology Database: A multi-proxy, international community-curated data resource. *Quat.*
2114 *Res.* 89, 156-177, doi:10.1017/qua.2017.105, 2018.
2115

2116 Williams, J. W. and Jackson, S. T.: Palynological and AVHRR observations of modern
2117 vegetational gradients in eastern North America, *J. Quat. Geol.*, 4, 485–497, 2003.
2118

2119 Williams, J. W., Webb, T., Shurman, B. N. and Bartlein, P. J.: Do Low CO₂ Concentrations
2120 Affect Pollen-Based Reconstructions of LGM Climates? A Response to “Physiological
2121 Significance of Low Atmospheric CO₂ for Plant–Climate Interactions” by Cowling and
2122 Sykes, *Quat. Res.*, 53(3), 402–404, doi:10.1006/qres.2000.2131, 2000.
2123

2124 Willis, K. J. and Van Andel, T. H.: Trees or no trees? The environments of central and
2125 eastern Europe during the Last Glaciation, *Quat. Sci. Rev.*, 23(23–24), 2369–2387,
2126 doi:10.1016/j.quascirev.2004.06.002, 2004.
2127

2128 Wu, H., Guiot, J., Brewer, S. and Guo, Z.: Climatic changes in Eurasia and Africa at the last
2129 glacial maximum and mid-Holocene: Reconstruction from pollen data using inverse
2130 vegetation modelling, *Clim. Dyn.*, 29(2–3), 211–229, doi:10.1007/s00382-007-0231-3, 2007.
2131

2132 Yu, G. and Harrison, S. P.: Lake status records from Europe: data base documentation,
2133 NOAA Paleoclimatology Publications Series, Boulder, Colorado., 1995.
2134

2135 Zaarur, S., Affek, H. P. and Stein, M.: Last glacial-Holocene temperatures and hydrology of
2136 the Sea of Galilee and Hula Valley from clumped isotopes in *Melanopsis* shells, *Geochim.*
2137 *Cosmochim. Acta*, 179, 142–155, doi:10.1016/j.gca.2015.12.034, 2016.
2138

2139 Zanon, M., Davis, B. A. S., Marquer, L., Brewer, S. and Kaplan, J. O.: European forest cover
2140 during the past 12,000 years: A palynological reconstruction based on modern analogs and
2141 remote sensing, *Front. Plant Sci.*, 9, doi:10.3389/fpls.2018.00253, 2018.
2142

2143 Zech, M., Buggle, B., Leiber, K., Marković, S., Glaser, B., Hambach, U., Huwe, B., Stevens,
2144 T., Sümegi, P., Wiesenberg, G. and Zöller, L.: Reconstructing Quaternary vegetation history
2145 in the Carpathian Basin, SE-Europe, using n-alkane biomarkers as molecular fossils:
2146 Problems and possible solutions, potential and limitations, *Quat. Sci. J.*, 58(2), 148–155,
2147 doi:10.3285/eg.58.2.03, 2010.
2148
2149

2150
2151
2152

Tables

| Site | Site Name | Country/Ocean | Latitude | Longitude | Elevation | Site Type | Data Type | Samples | Source | Reference |
|------|--------------------------------|----------------|------------|------------|-----------|--------------|-----------|---------|------------------|------------------------------|
| 1 | MD95-2039 (M) | Atlantic | 40.578333 | -10.348333 | -3381 | Marine | Raw Count | 21 | EPD (E#1472) | Roucoux et al. 2005 |
| 2 | SU81-18 (M) | Atlantic | 37.77 | -9.82 | -3135 | Marine | Raw Count | 10 | ACER | Turon et al. 2003 |
| 3 | MD99-2331 (M) | Atlantic | 41.15 | -9.68 | -2110 | Marine | Raw Count | 41 | ACER | Naughton et al. 2006 |
| 4 | Carn Morval | United Kingdom | 49.926111 | -6.313889 | 5 | Lake | Digitised | 1 | Publication | Scourse 1991 |
| 5 | Gorham Cave | Spain | 36.132826 | -5.347358 | 0 | Cave | Digitised | 1 | Publication | Carrion et al. 2008 |
| 6 | Dozmary Pool | United Kingdom | 50.5347222 | -4.5358333 | 265 | Lake | Raw Count | 32 | Author | Kelly et al. 2010 |
| 7 | Bajondillo | Spain | 36.619722 | -4.496389 | 20 | Cave | Raw Count | 1 | EPD (E#1570) | Cortes-Sanchez et al. 2011 |
| 8 | Laguna del maar de Fuentillejo | Spain | 38.937996 | -4.0539 | 637 | Lake | Digitised | 1 | Publication | Ruiz-Zapata et al. 2009 |
| 9 | Padul-1 | Spain | 37.016338 | -3.608503 | 785 | Peat Bog | Digitised | 13 | Publication | Pons & Reille 1988 |
| 10 | Padul-2 | Spain | 37.010833 | -3.603889 | 726 | Peat Bog | Digitised | 1 | Publication | Camuera et al. 2019 |
| 11 | Cova di Carihuela | Spain | 37.4489 | -3.4297 | 1020 | Cave | Digitised | 1 | Publication | Carrion 1992 |
| 12 | Ifri El Baroud | Morocco | 34.75 | -3.3 | 539 | Cave | Digitised | 1 | Publication | Poti et al. 2019 |
| 13 | MD95-2043 (M) | Mediterranean | 36.14 | -2.621 | -1841 | Marine | Raw Count | 7 | ACER | Fletcher et al. 2008 |
| 14 | San Rafael | Spain | 36.773611 | -2.601389 | 0 | Peat Bog | Raw Count | 2 | EPD (E#574) | Pantaléon-Cano 1997 |
| 15 | Siles | Spain | 38.24 | -2.3 | 1320 | Lake | Digitised | 1 | Publication | Carrion 2002 |
| 16 | Torreçilla de Valmadrid | Spain | 41.4469444 | -0.895 | 570 | Colluvium | Digitised | 1 | Publication | Valero-Garces et al. 2004 |
| 17 | Navarrés-1 | Spain | 39.1 | -0.683333 | 225 | Peat Bog | Raw Count | 1 | EPD (E#469) | Carrion & Dupré-Olivier 1996 |
| 18 | Navarrés-2 | Spain | 39.1 | -0.683333 | 225 | Peat Bog | Raw Count | 1 | EPD (E#470) | Carrion & Dupré-Olivier 1996 |
| 19 | Tourbiere de l'Estarrès | France | 43.0933 | -0.3792 | 356 | Lake | Digitised | 1 | Publication | Jalut et al. 1988 |
| 20 | Cova de les Malladetes | Spain | 39.058 | -0.321 | 20 | Cave | Digitised | 1 | Publication | Dupré-Olivier 1988 |
| 21 | Lourdes | France | 43.033333 | -0.075 | 430 | Lake | Digitised | 15 | Publication | Reille & Andrieu 1995 |
| 22 | Lake Estanya | Spain | 42.0333333 | 0.53333333 | 670 | Lake | Digitised | 1 | Publication | Vegas-Villarubia et al. 2013 |
| 23 | Freychinede | France | 42.7833 | 1.4333 | 1350 | Lake | Digitised | 1 | Publication | Jalut et al. 1992 |
| 24 | Banyoles | Spain | 42.133333 | 2.75 | 173 | Lake | Raw Count | 13 | EPD (E#931) | Pérez-Obiol & Julia 1994 |
| 25 | Lac du Bouchet B5 | France | 44.916667 | 3.783333 | 1200 | Lake | Digitised | 14 | Publication | Reille & de Beaulieu 1988 |
| 26 | MD99-2348 (103) (M) | Mediterranean | 42.692778 | 3.841667 | -296 | Marine | Raw Count | 41 | EPD (E#1474) | Beaudouin et al. 2007 |
| 27 | Les Echets G | France | 45.9 | 4.93 | 267 | Peat Bog | Digitised | 136 | ACER | de Beaulieu & Reille 1984 |
| 28 | La Grotte Walou | Belgium | 50.585278 | 5.536389 | 252 | Cave | Digitised | 1 | Publication | Dambon 2011 |
| 29 | Bergsee | Germany | 47.5722222 | 7.93638889 | 382 | Lake | Digitised | 1 | Publication | Duprat-Oualid et al. 2017 |
| 30 | Garaat El-Ouez | Algeria | 36.818333 | 8.33333 | 45 | Peat Bog | Raw Count | 6 | EPD (E#1501) | Benslama et al. 2010 |
| 31 | Pian del Lago | Italy | 44.321561 | 9.485682 | 833 | Lake | Digitised | 1 | Publication | Guido et al. 2020 |
| 32 | Pilsensee | Germany | 48.0267 | 11.1883 | 534 | Lake | Digitised | 1 | Publication | Küster 1995 |
| 33 | Orgiano | Italy | 45.29 | 11.43 | 19 | Peat Bog | Digitised | 1 | Publication | Paganelli 1996 |
| 34 | Lago della Costa | Italy | 45.2702778 | 11.7430556 | 7 | Lake | Digitised | 8 | Publication | Kaltenrieder et al. 2009 |
| 35 | Lagaccione | Italy | 42.566667 | 11.85 | 355 | Lake | Raw Count | 7 | ACER | Magri 1999 |
| 36 | Lago Vico | Italy | 42.3166667 | 12.166667 | 510 | Lake | Digitised | 15 | Publication | Magri & Sadori 1999 |
| 37 | Stracciaccia | Italy | 42.13 | 12.32 | 220 | Lake | Raw Count | 2 | ACER | Giardini 2007 |
| 38 | Lago di Monterosi | Italy | 42.2166667 | 12.4333333 | 237 | Lake | Raw Count | 1 | Publication | Bonatti 1970 |
| 39 | Venice | Italy | 45.629523 | 12.654086 | 0 | Peat Bog | Digitised | 1 | Publication | Miola et al. 2006 |
| 40 | Azzano Decimo | Italy | 45.8833 | 12.7165 | 10 | Alluvial Fan | Raw Count | 6 | ACER | Pini et al. 2009 |
| 41 | Valle di Castiglione | Italy | 41.89 | 12.75 | 44 | Lake | Raw Count | 2 | ACER | Follieri et al. 1989 |
| 42 | Travesio | Italy | 46.2 | 12.87 | 220 | Lake | Digitised | 1 | Publication | Monegato et al. 2007 |
| 43 | Orvenco | Italy | 46.252088 | 13.169771 | 380 | Alluvial Fan | Digitised | 1 | Publication | Monegato et al. 2007 |
| 44 | Rio Doidis | Italy | 46.12 | 13.19 | 152 | Lake | Digitised | 1 | Publication | Monegato et al. 2007 |
| 45 | Billerio | Italy | 46.22 | 13.21 | 300 | Lake | Digitised | 1 | Publication | Monegato et al. 2007 |
| 46 | Kersdorf-Briesen | Germany | 52.333704 | 14.269142 | 44 | Lake | Digitised | 1 | Publication | Strahl 2005 |
| 47 | Lago Grande di Monticchio | Italy | 40.944444 | 15.6 | 1326 | Lake | Raw Count | 6 | EPD (E#932) | Watts et al. 1996 |
| 48 | Nagymohos | Hungary | 48.326944 | 20.436389 | 297 | Peat Bog | Raw Count | 14 | Publication | Magyari et al. 1999 |
| 49 | Safarka | Slovakia | 48.8819444 | 20.575 | 600 | Peat Bog | Digitised | 1 | Publication | Jankovska 2008 |
| 50 | Fehér Lake | Hungary | 46.45 | 20.65 | 86 | Lake | Raw Count | 10 | Publication | Magyari et al. 2014 |
| 51 | Ioannina | Greece | 39.75 | 20.85 | 470 | Peat Bog | Raw Count | 20 | ACER | Tzedakis et al. 2004 |
| 52 | Kokad | Hungary | 47.4027778 | 21.9286111 | 112 | Peat Bog | Raw Count | 2 | Publication | Magyari et al. 2019 |
| 53 | Lake Xinias | Greece | 39.05 | 22.27 | 500 | Lake | Raw Count | 5 | EPD (E#976) | Bottema 1979 |
| 54 | Mickunai | Lithuania | 54.722114 | 25.532218 | 143 | Lake | Digitised | 1 | Publication | Satkunas & Grigiene 2012 |
| 55 | Lake Sfanta Anna | Romania | 46.1263889 | 25.880556 | 946 | Lake | Digitised | 1 | Publication | Magyari et al. 2014 |
| 56 | Megali Limni | Greece | 39.1 | 26.3 | 323 | Lake | Digitised | 1 | Publication | Margari et al. 2009 |
| 57 | Straldzha | Bulgaria | 42.630278 | 26.77 | 138 | Peat Bog | Raw Count | 3 | Publication | Connor et l. 2013 |
| 58 | MD01-2430 (M) | Turkey | 40.796833 | 27.725166 | -580 | Marine | Digitised | 1 | Publication | Valsecchi et al. 2012 |
| 59 | Lake Iznik | Turkey | 40.433889 | 29.533056 | 88 | Lake | Raw Count | 7 | EPD (E#714) | Miebach et al. 2016 |
| 60 | M72/5 628-1 (M) | Black Sea | 42.1035 | 36.62383 | -418 | Marine | Raw Count | 6 | Pangaea (833387) | Shumilovskikh et al. 2014 |
| 61 | Dziguta | Georgia | 42.99 | 41.07 | 35 | Peat Bog | Digitised | 1 | Publication | Arslanov et al. 2007 |
| 62 | Lake Van LG | Turkey | 38.667 | 42.669 | 1649 | Lake | Raw Count | 10 | Pangaea (853779) | Pickarski et al. 2015 |
| 63 | Lake Zeribar | Iran | 35.533333 | 46.116667 | 1286 | Lake | Raw Count | 17 | EPD (E#714) | van Zeist & Bottema 1977 |

2153
2154
2155
2156
2157
2158

Table 1. List of selected sites

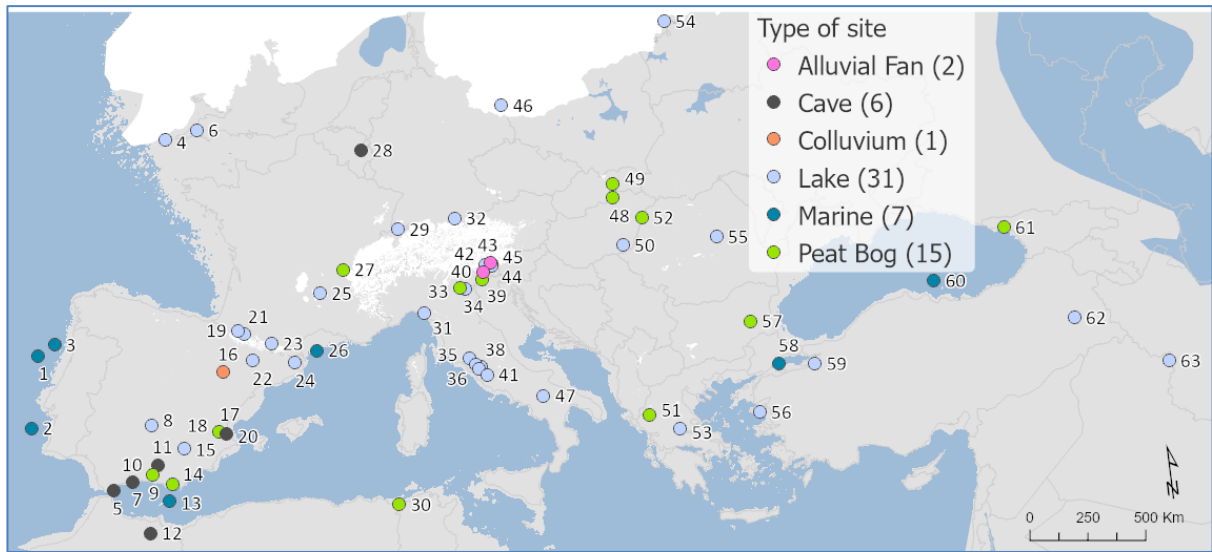
2159
2160
2161
2162
2163

| | RMSE | R2 |
|-------------------|-------------|-----------|
| TANN | 2.28 | 0.9 |
| TDJF | 3.35 | 0.91 |
| TJJA | 2.21 | 0.81 |
| PANN | 224.94 | 0.69 |
| PDJF | 78.51 | 0.69 |
| PJJA | 52.49 | 0.75 |
| Tree Cover | 21.03 | 0.52 |

2164
2165
2166
2167
2168
2169
2170
2171
2172
2173

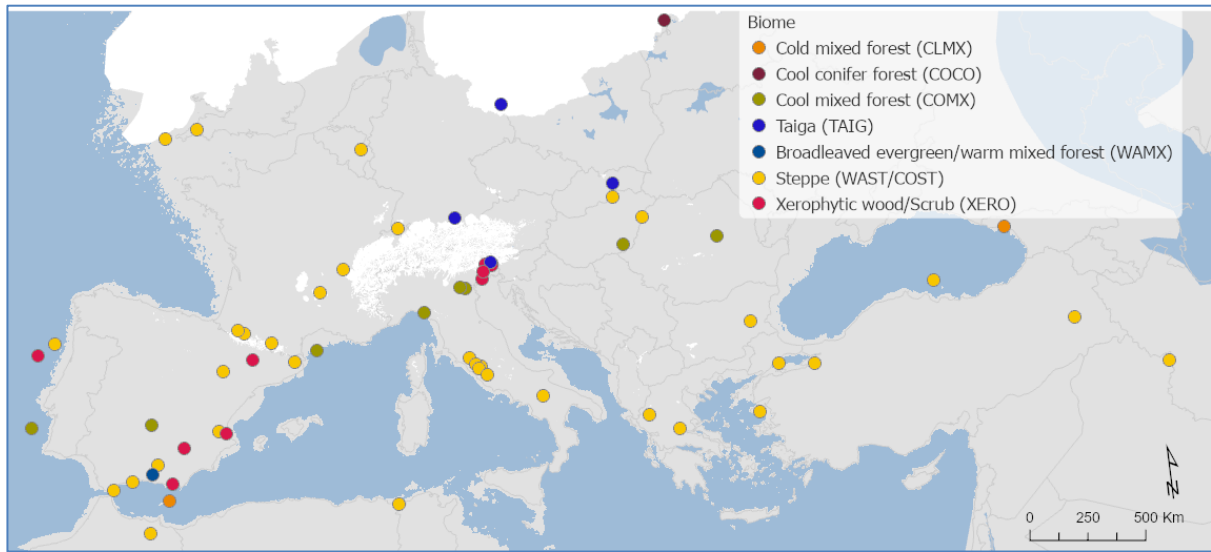
Table 2. MAT performance statistics based on the modern pollen sample training set. This includes Mean Annual Temperature and Precipitation (TANN and PANN), Mean Winter Temperature and Precipitation (TDJF and PDJF) and Mean Summer Temperature and Precipitation (TJJA and PJJA).

2174 **Figures**
2175
2176
2177



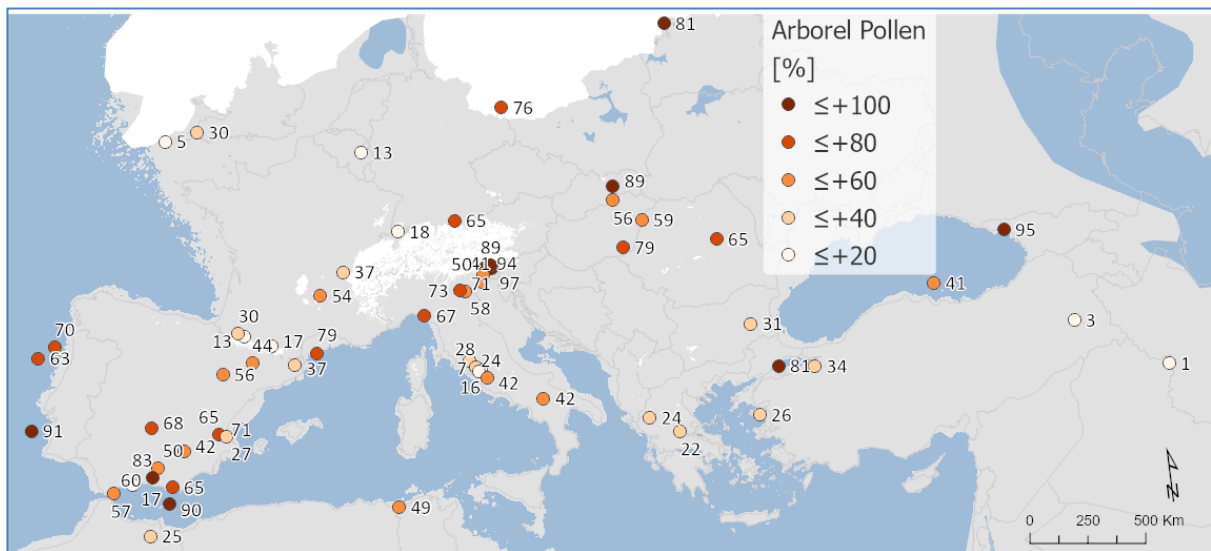
2178
2179
2180 Figure 1. Site locations and archives (Site numbers are as shown in Table 1)
2181
2182
2183

2184



2185
2186
2187
2188
2189

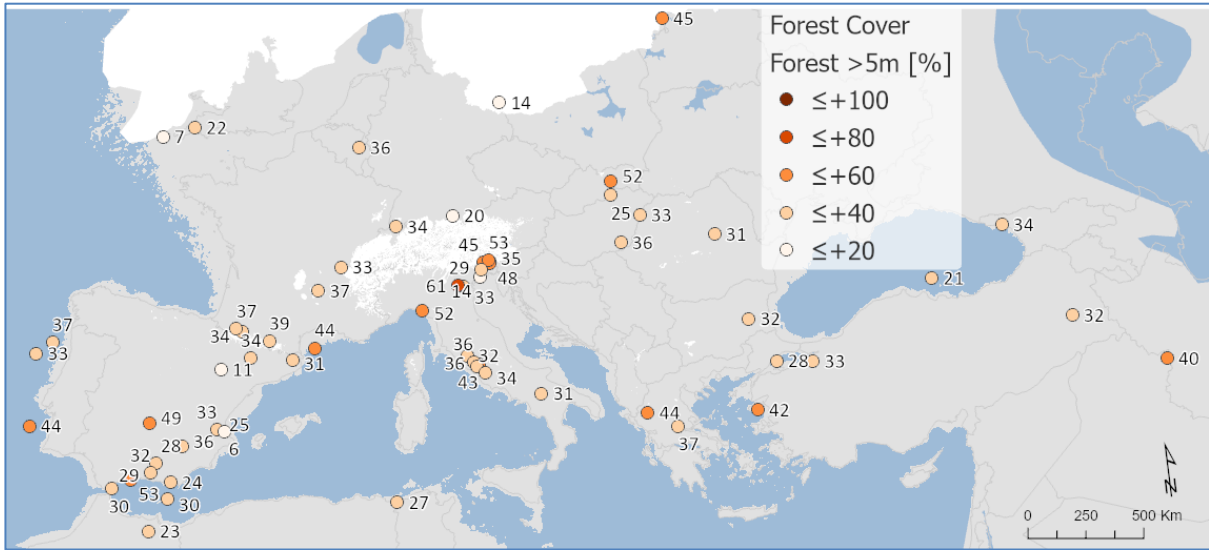
Figure 2. Pollen biomes



2190
2191
2192
2193
2194

Figure 3. Arboreal Pollen (AP) % forest cover

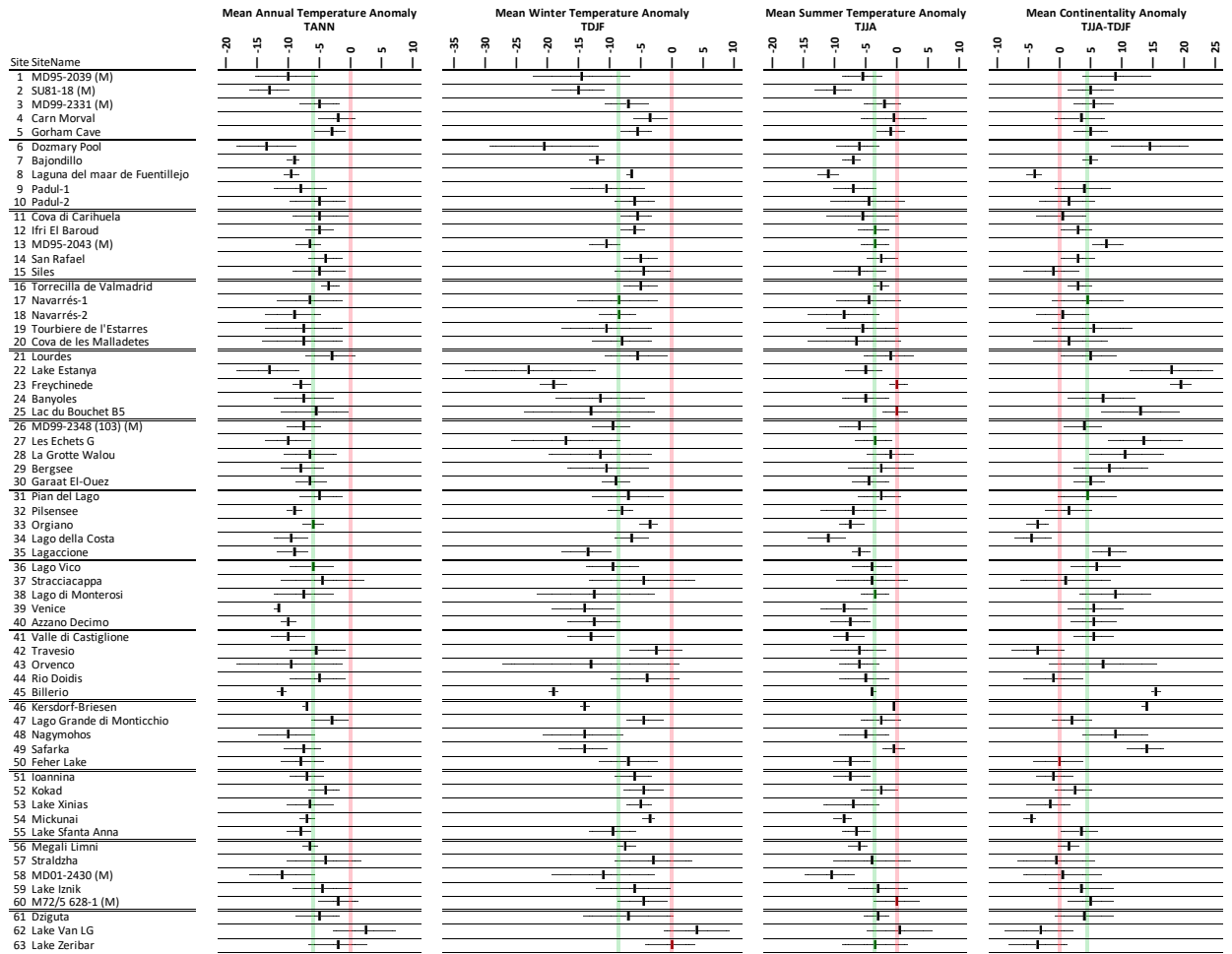
2195



2196
2197
2198
2199
2200

Figure 4. Modern Analogue Technique (MAT) % forest cover

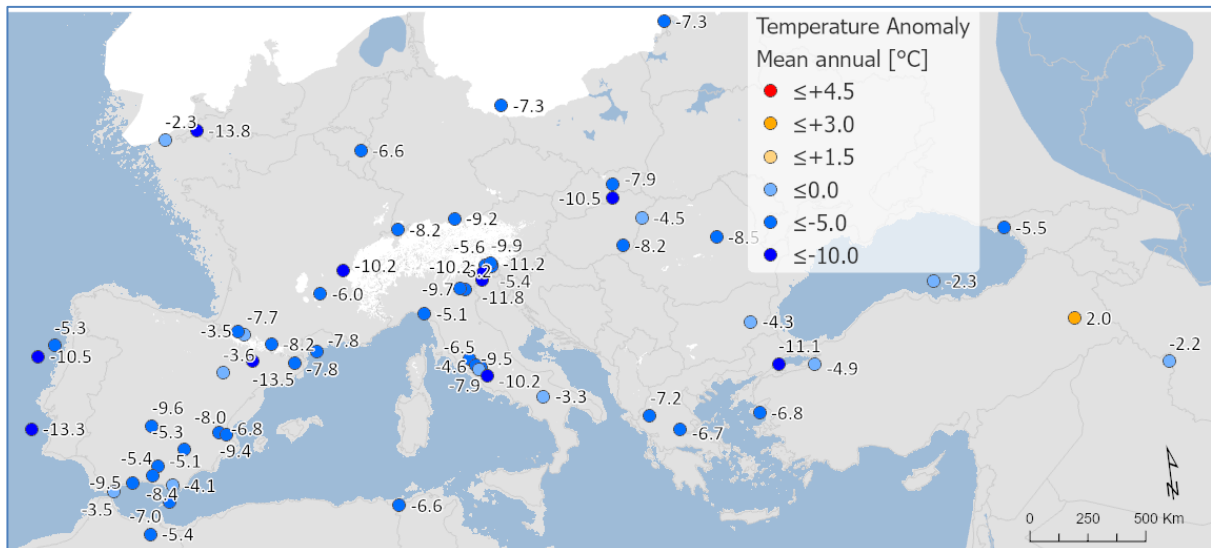
2201
2202



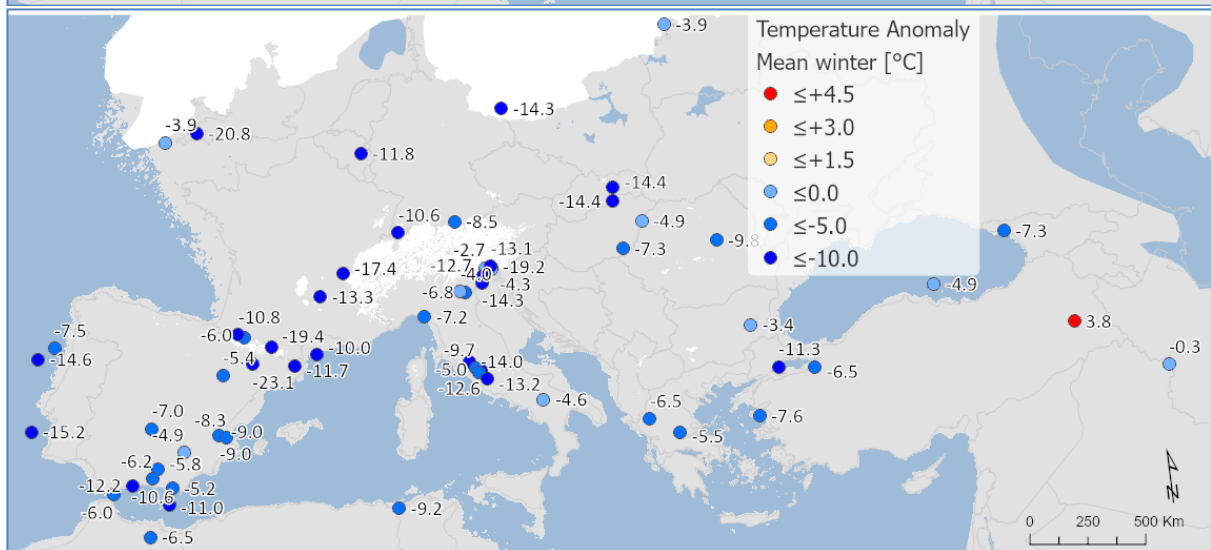
2203
2204
2205
2206
2207
2208
2209
2210
2211
2212

Figure 5. Pollen-based MAT reconstructions for LGM annual, winter and summer temperature anomalies (uncertainties represent one standard deviation). Continentality represents the difference in temperature between summer and winter, with positive anomalies indicating an increase in the temperature difference between summer and winter. All values are expressed as anomalies compared with the present day. The green line indicates the mean for all the sites.

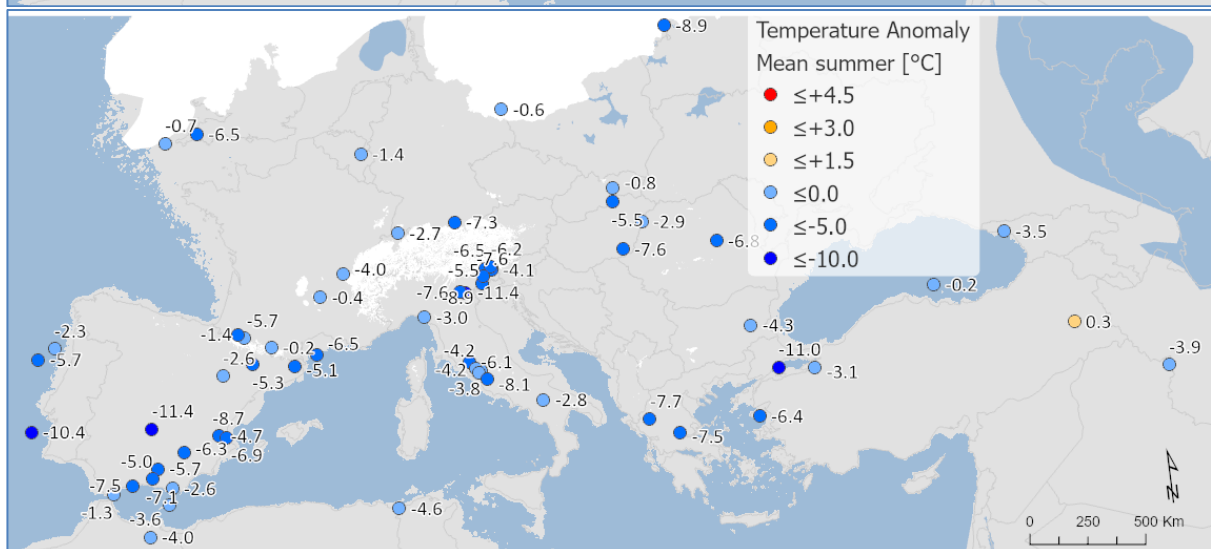
2213

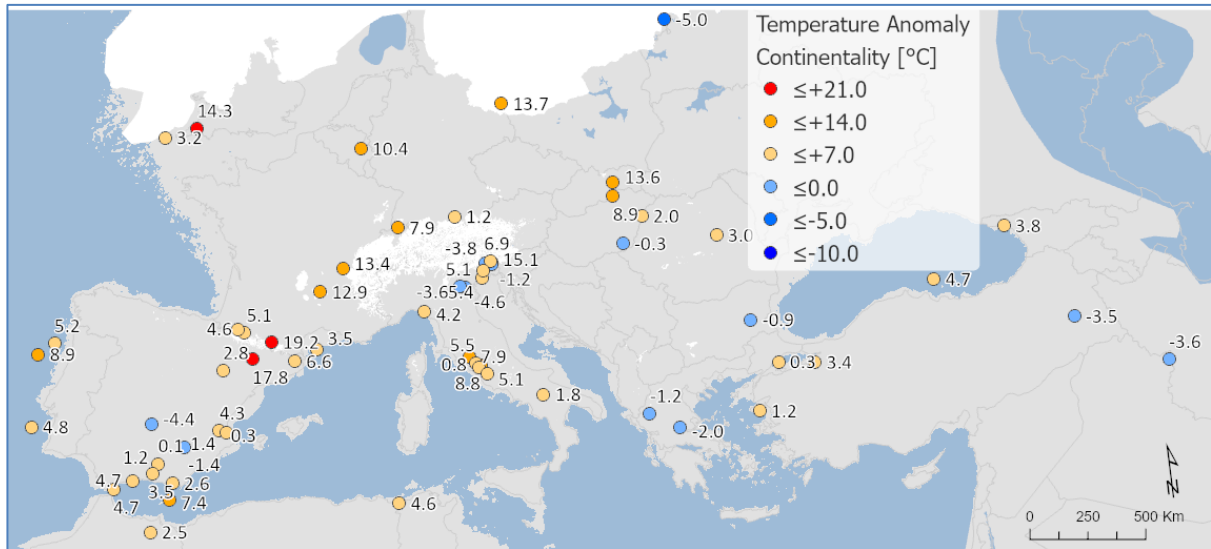


2214



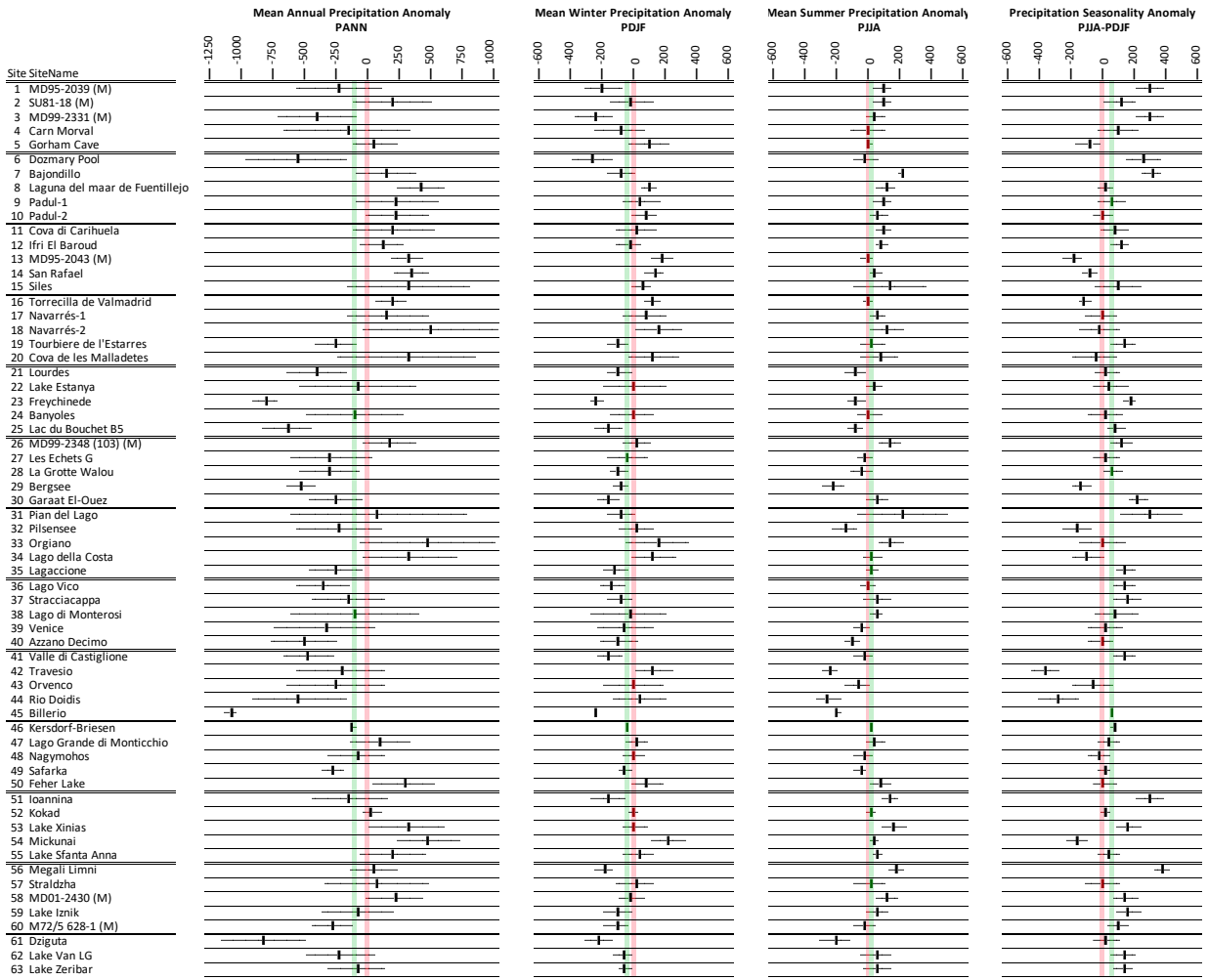
2215





2216
 2217
 2218
 2219
 2220
 2221
 2222
 2223

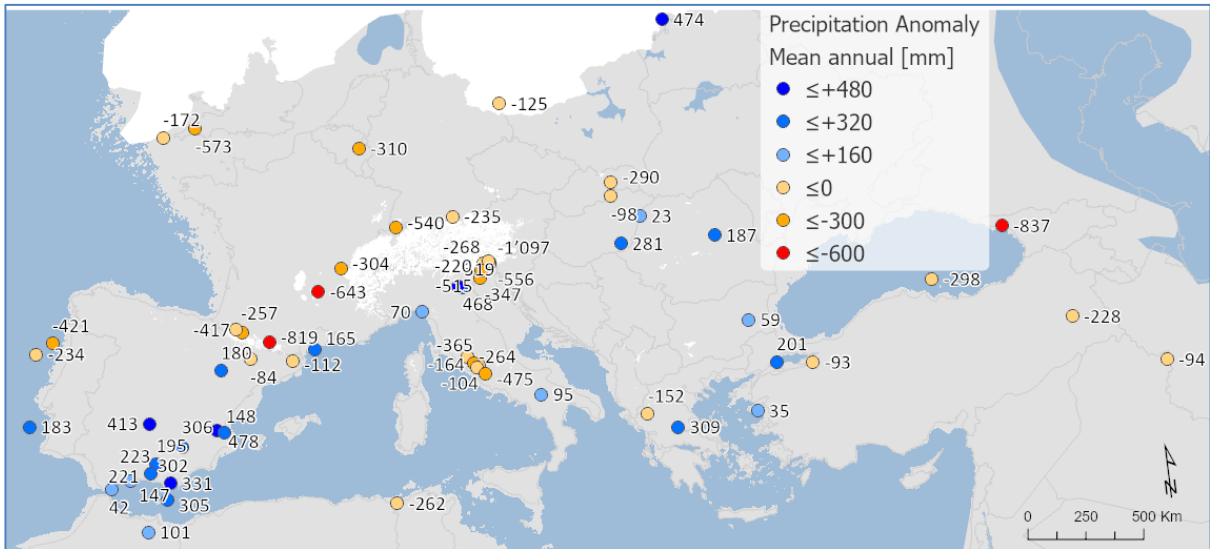
Figure 6. Maps of pollen-based MAT reconstructions for LGM annual, winter and summer temperature anomalies (as shown in figure 9). Continentality represents the difference in temperature between summer and winter, with positive anomalies indicating an increase in the temperature difference between summer and winter. All values are expressed as anomalies compared with the present day.



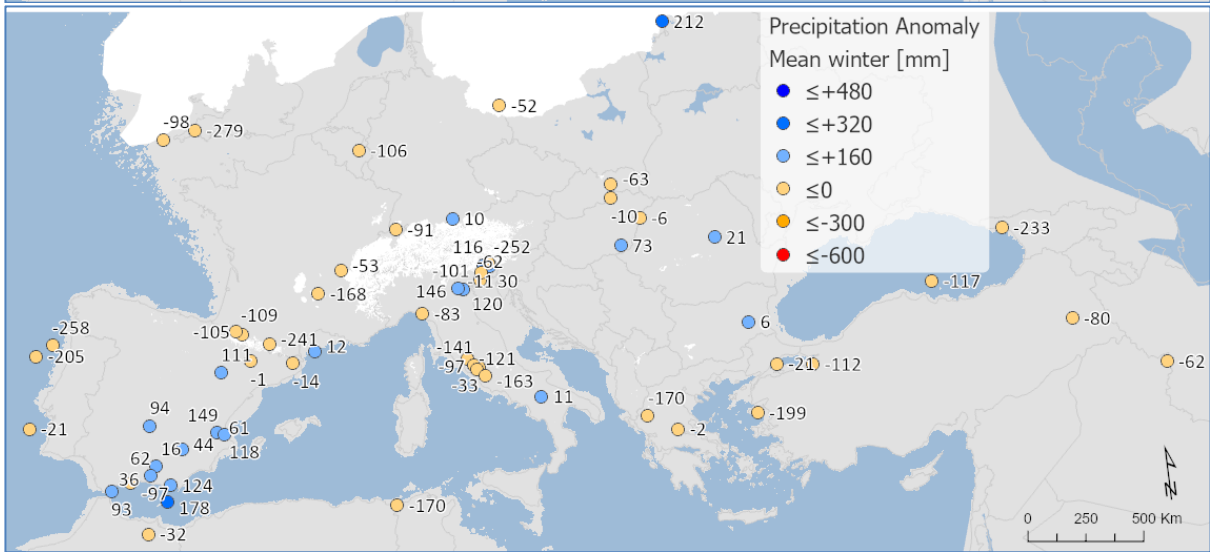
2225
2226
2227
2228
2229
2230
2231
2232

Figure 7. Pollen-based MAT reconstructions for LGM annual, winter and summer precipitation anomalies (uncertainties represent one standard deviation). Seasonality represents the difference in precipitation between summer and winter, with positive anomalies indicating an increase in summer precipitation compared to winter. All values are expressed as anomalies compared with the present day. The green line indicates the mean for all the sites.

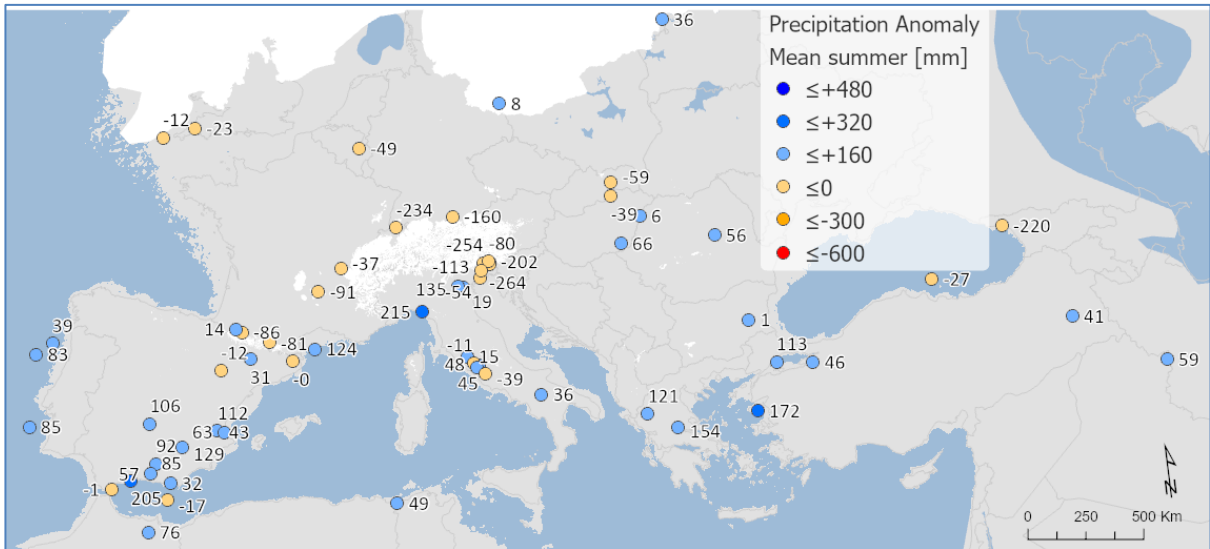
2233



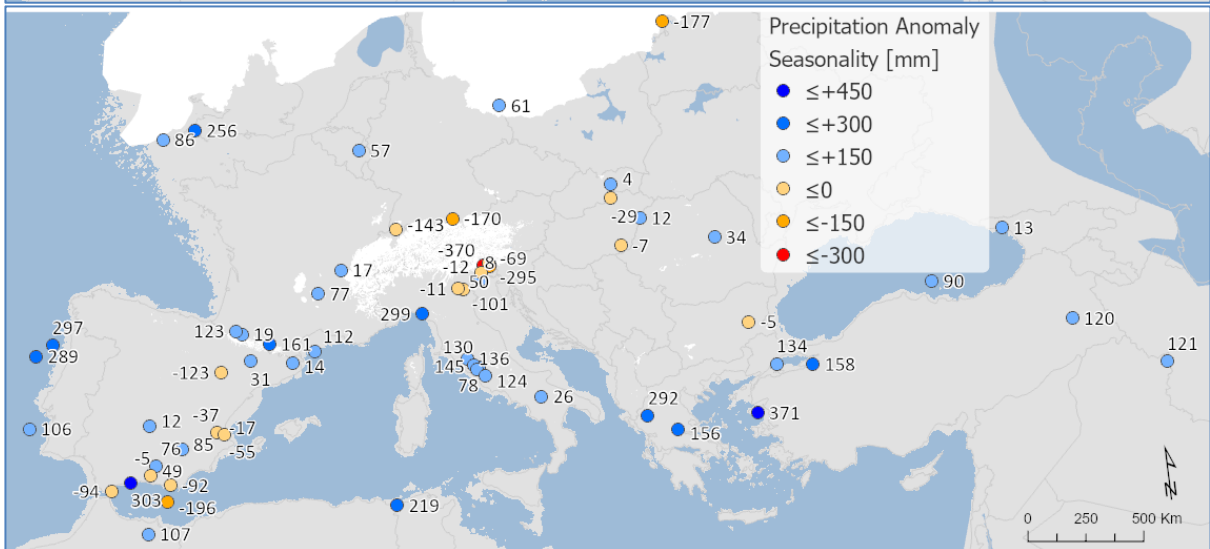
2234



2235



2236



2237

2238

2239

2240

2241

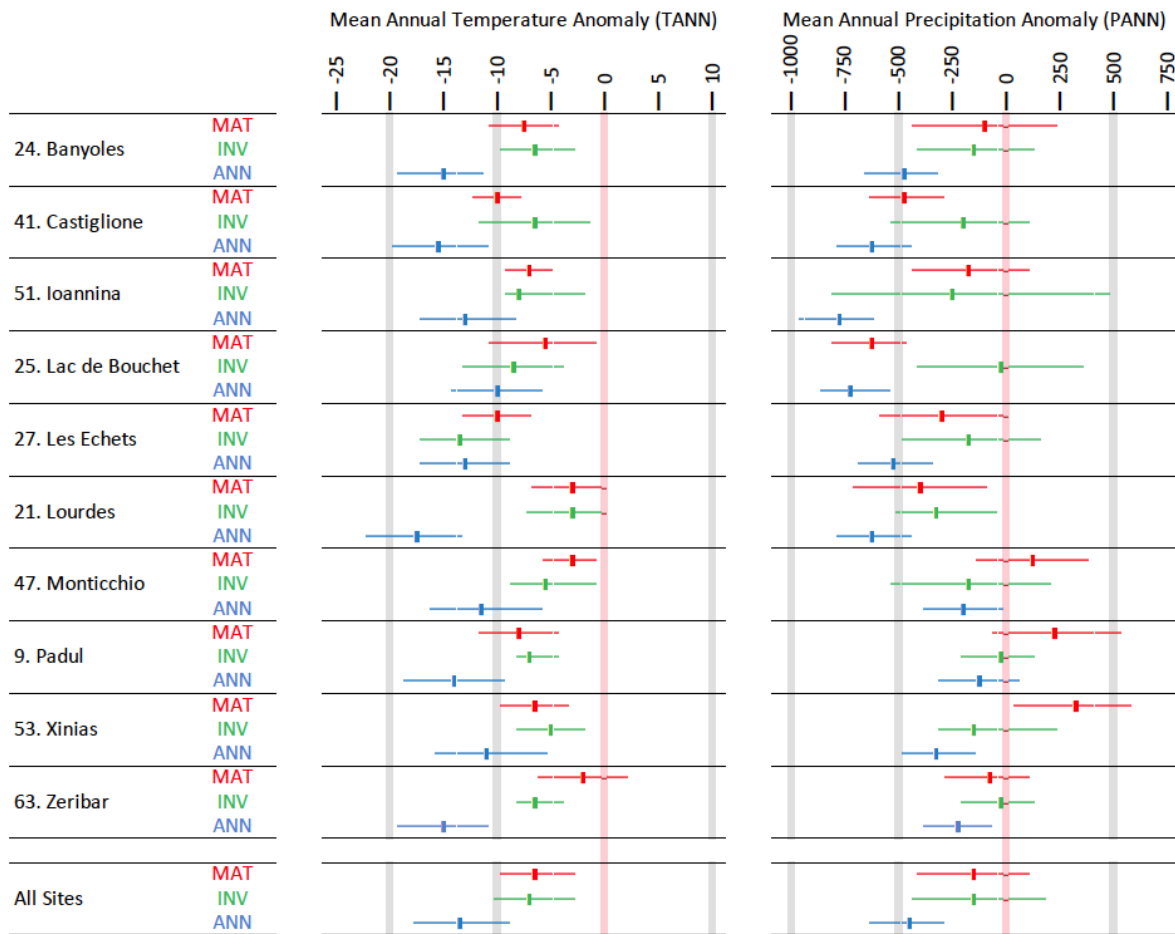
2242

2243

2244

Figure 8. Maps of pollen-based MAT reconstructions for LGM annual, winter and summer precipitation anomalies (as shown in figure 11). Seasonality represents the difference in precipitation between summer and winter, with positive anomalies indicating an increase in summer precipitation compared to winter. All values are expressed as anomalies compared with the present day.

2245



2246

2247

2248

2249

2250

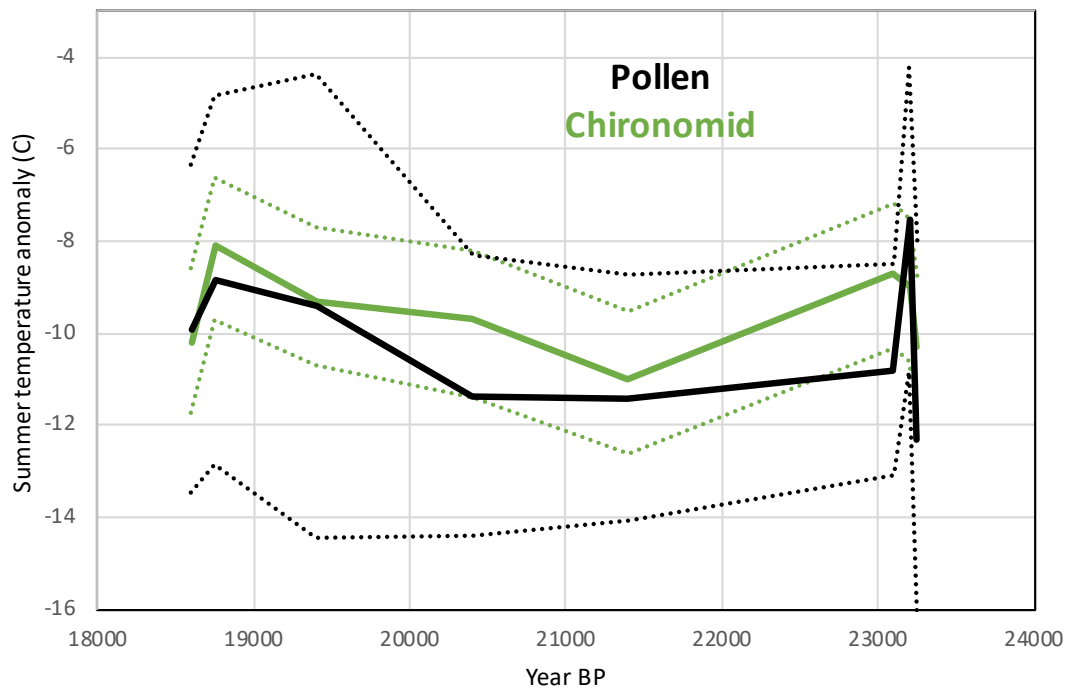
2251

2252

2253

Figure 9. A site-by-site comparison between LGM pollen-climate reconstructions based on Modern Analogue Technique MAT (this study), neural-networks ANN (Peyron et al., 1998), and Inverse Modelling INV (Wu et al., 2007). The results show that MAT and INV give similar climate reconstructions, but ANN is significantly cooler/drier.

2254
2255
2256



2257
2258
2259
2260
2261
2262
2263

Figure 10. Comparison between LGM pollen-climate MAT and chironomid summer temperature reconstructions at Lago della Costa, Italy (chironomid reconstruction and pollen data from Samartin et al., 2016). Dash lines show uncertainties.

2264
2265
2266

Appendix

| Site | Site Name | COHMAP Quality | COHMAP | | | | | | | | | | | | Upper 14C | Upper Cal. BP | Lower 14C | Lower Cal. BP |
|------|--------------------------------|----------------|--------|-----|-----|-----|-----|-----|-----|-----|-------|--|--|--|------------|---------------|---------------|---------------|
| | | | < 17k | 18k | 19k | 20k | 21k | 22k | 23k | 24k | 25k > | | | | | | | |
| 1 | MD95-2039 (M) | 3C | --- | | | | | | | | | | | | 14830±80 | 18166±269 | 19950±210 | 23883±374 |
| 2 | SU81-18 (M) | 2C | --- | | | | | | | | | | | | 17510±270 | 20952±404 | 21250±280 | 25420±441 |
| 3 | MD99-2331 (M) | 2C | --- | | | | | | | | | | | | 16170±130 | 19325±303 | 19770±170 | 23682±336 |
| 4 | Carr Morval | 4C | --- | | | | | | | | | | | | | 18600±3700 | 21500±890/800 | 25867±1127 |
| 5 | Gorham Cave | 4D | --- | | | | | | | | | | | | | | 18440±160 | 22055±341 |
| 6 | Dozmary Pool | 2C | --- | | | | | | | | | | | | 14568±129 | 17569±523 | 18325±216 | 21769±602 |
| 7 | Bajondillo | 1C | --- | | | | | | | | | | | | | 18701±2154 | | |
| 8 | Laguna del maar de Fuentillejo | 5D | --- | | | | | | | | | | | | 16540±90 | 19847±308 | | |
| 9 | Padul-1 | 3D | --- | | | | | | | | | | | | 18300±300 | 21821±412 | 19100±160 | 22922±308 |
| 10 | Padul-2 | 1D | --- | | | | | | | | | | | | | | 17450±539 | 21082±539 |
| 11 | Cova di Carihuela | 2C | --- | | | | | | | | | | | | 15700±220 | 18958±280 | 21430±130 | 25659±226 |
| 12 | Ifri El Baroud | 2D | --- | | | | | | | | | | | | 17296±87 | 20761±293 | | |
| 13 | MD95-2043 (M) | 2C | --- | | | | | | | | | | | | 15440±90 | 18533±294 | 18260±120 | 21951±335 |
| 14 | San Rafael | 3D | --- | | | | | | | | | | | | 9980±60 | 11464±133 | 16860±120 | 20083±292 |
| 15 | Siles | 2D | --- | | | | | | | | | | | | 17030±80 | 20345±351 | | |
| 16 | Torreçilla de Valmadrید | 2D | --- | | | | | | | | | | | | 17100±85 | 20456±366 | | |
| 17 | Navarrés-1 | 4D | --- | | | | | | | | | | | | 18360±195 | 22001±353 | 20700±295 | 24664±411 |
| 18 | Navarrés-2 | 5D | --- | | | | | | | | | | | | 5150±50 | 5881±85 | 16000± | 19144± |
| 19 | Tourbiere de l'Estarres | 1C | --- | | | | | | | | | | | | 17150±250 | 20522±470 | 18970±160 | 22847±317 |
| 20 | Cova de les Malladetes | 5D | --- | | | | | | | | | | | | 16300±1500 | 19686±1723 | | |
| 21 | Lourdes | 4D | --- | | | | | | | | | | | | 18510±130 | 22112±130 | 20025±175 | 23952±355 |
| 22 | Lake Estanya | 5D | --- | | | | | | | | | | | | | 9498±50 | | 19184±251 |
| 23 | Freychinede | 3C | --- | | | | | | | | | | | | 14800±800 | 17912±856 | 21300±760 | 25615±1030 |
| 24 | Banyoles | 4C | --- | | | | | | | | | | | | | 19878±100 | | 27862±3000 |
| 25 | Lac du Bouchet B5 | 2C | --- | | | | | | | | | | | | 15350±350 | 18513±435 | 19200±300 | 23006±384 |
| 26 | MD99-2348 (103) (M) | 1D | --- | | | | | | | | | | | | 17660±60 | 21065±310 | 19350±90 | 23111±271 |
| 27 | Les Echets G | 4C | --- | | | | | | | | | | | | 17530±270 | 20970±407 | 18030±250 | 21704±473 |
| 28 | La Grotte Walou | 1D | --- | | | | | | | | | | | | | | | 21200±700 |
| 29 | Bergsee | 2D | --- | | | | | | | | | | | | | | 17780±90 | 21244±306 |
| 30 | Garaat El-Ouez | 2C | --- | | | | | | | | | | | | 16010±320 | 19200±801 | | |
| 31 | Pian del Lago | 2D | --- | | | | | | | | | | | | | | | 21260±320 |
| 32 | Pilsensee | 6D | --- | | | | | | | | | | | | 15860±250 | 19073±290 | | |
| 33 | Orgiano | 2D | --- | | | | | | | | | | | | 17760±160 | 21221±373 | 19290±520 | 23141±621 |
| 34 | Lago della Costa | 2C | --- | | | | | | | | | | | | 15400±150 | 18484±330 | 19285±160 | 23052±302 |
| 35 | Lagaccione | 2C | --- | | | | | | | | | | | | 16080±450 | 19369±527 | 20615±940 | 24746±1201 |
| 36 | Lago Vico | 3C | --- | | | | | | | | | | | | 14385±140 | 17541±272 | 20500±230 | 24430±376 |
| 37 | Stracciaccappa | 4C | --- | | | | | | | | | | | | 12060±130 | 14093±281 | 19745±820 | 22675±955 |
| 38 | Lago di Monterosi | 2D | --- | | | | | | | | | | | | 17040±350 | 20398±544 | | |
| 39 | Venice | 5D | --- | | | | | | | | | | | | | | 18640±100 | 22277±336 |
| 40 | Azzano Decimo | 2D | --- | | | | | | | | | | | | 18000±300 | 21637±529 | 21025±245 | 25179±449 |
| 41 | Valle di Castiglione | 3C | --- | | | | | | | | | | | | 14220±145 | 17443±270 | 20300±700 | 24266±842 |
| 42 | Travesio | 5D | --- | | | | | | | | | | | | | | 18780±200 | 22483±406 |
| 43 | Orvenco | 2D | --- | | | | | | | | | | | | | | 19290±520 | 23141±621 |
| 44 | Rio Doidis | 5D | --- | | | | | | | | | | | | 17760±160 | 21221±373 | 18860±190 | 22390±373 |
| 45 | Billerio | 3D | --- | | | | | | | | | | | | | | 18165±200 | 21872±382 |
| 46 | Kersdorf-Briesen | 1D | --- | | | | | | | | | | | | | | 17622±94 | 21183±356 |
| 47 | Lago Grande di Monticchio | 2C | --- | | | | | | | | | | | | | 20204± | | 24014± |
| 48 | Nagymohos | 2C | --- | | | | | | | | | | | | 14246±144 | 17361±425 | 18159±247 | 21735±622 |
| 49 | Safarka | 3D | --- | | | | | | | | | | | | | | 18287±1512 | 21912±1781 |
| 50 | Feher Lake | 1D | --- | | | | | | | | | | | | 17715±250 | 21190±463 | 19911±81 | 23841±313 |
| 51 | Ioannina | 3C | --- | | | | | | | | | | | | 15330±140 | 18420±312 | 20760±230 | 24748±330 |
| 52 | Kokad | 5D | --- | | | | | | | | | | | | 14326±63 | 17433±443 | 16280±90 | 19685±538 |
| 53 | Lake Xinias | 6C | --- | | | | | | | | | | | | 11150±130 | 13049±160 | 21390±430 | 25671±648 |
| 54 | Mickunai | 1D | --- | | | | | | | | | | | | | 21000±2200 | | |
| 55 | Lake Sfanta Anna | 1D | --- | | | | | | | | | | | | 17626±96 | 20955±432 | | |
| 56 | Megali Limni | 6D | --- | | | | | | | | | | | | 19072±237 | 22906±340 | | |
| 57 | Straldzha | 6C | --- | | | | | | | | | | | | 14696±65 | 18022±364 | 23653±114 | 28580±390 |
| 58 | MD01-2430 (M) | 4C | --- | | | | | | | | | | | | 12050±75 | 14904±324 | 18310±380 | 21746±968 |
| 59 | Lake Iznik | 7D | --- | | | | | | | | | | | | 16910±100 | 19515±115 | | |
| 60 | M72/5 628-1 (M) | 2C | --- | | | | | | | | | | | | 16835±85 | 18490± | 19495±90 | 21280± |
| 61 | Dziguta | 2C | --- | | | | | | | | | | | | 12990±160 | 15839±483 | 20560±880 | 24666±1126 |
| 62 | Lake Van LG | 4C | --- | | | | | | | | | | | | | 18590±62 | | 23290±596 |
| 63 | Lake Zeribar | 4C | --- | | | | | | | | | | | | 13650±160 | 16610±399 | 22000±500 | 26462±880 |

COHMAP chronological quality classification:

- 1C: Bracketing dates within 2000 14C (2360 Cal.) yr interval about the time being assessed
- 2C: Bracketing dates, one within 2000 14C (2360 Cal.) yr and the second within 4000 14C (4682 Cal.) yr of the time being assessed
- 3C: Bracketing dates within 4000 14C (4682 Cal.) yr interval about the time being assessed
- 4C: Bracketing dates, one being within 4000 14C (4682 Cal.) yr and the second being within 6000 14C (7490 Cal.) yr of the time being assessed
- 5C: Bracketing dates within 6000 14C (7490 Cal.) yr interval about the time being assessed
- 6C: Bracketing dates, one within 6000 14C (7490 Cal.) yr and the second within 8000 14C (9681 Cal.) yr of the time being assessed
- 7C: Poorly dated
- 1D: Date within 250 14C (206 Cal.) yr of the time being assessed
- 2D: Date within 500 14C (684 Cal.) yr of the time being assessed
- 3D: Date within 750 14C (975 Cal.) yr of the time being assessed
- 4D: Date within 1000 14C (1123 Cal.) yr of the time being assessed
- 5D: Date within 1500 14C (1881 Cal.) yr of the time being assessed
- 6D: Date within 2000 14C (2360 Cal.) yr of the time being assessed
- 7D: Poorly dated

Table A1. Chronological control

2267
2268
2269
2270
2271
2272
2273
2274
2275
2276
2277
2278
2279
2280
2281
2282
2283
2284
2285
2286

2287
2288

| Site Number | Site Name | Site Type | TANN | TDJF | TJJA | PANN | PDJF | PJJA |
|-------------|--------------------------------|--------------|------|------|------|-------|------|------|
| 1 | MD95-2039 (M) | Marine | 15.7 | 10.7 | 20.8 | 1047 | 427 | 70 |
| 2 | SU81-18 (M) | Marine | 20.8 | 15.3 | 26.5 | 629 | 282 | 25 |
| 3 | MD99-2331 (M) | Marine | 14.6 | 9.8 | 19.4 | 1239 | 507 | 88 |
| 4 | Carn Morval | Lake | 12.5 | 8.7 | 16.9 | 1183 | 392 | 206 |
| 5 | Gorham Cave | Cave | 18.3 | 13.4 | 23.7 | 740 | 336 | 25 |
| 6 | Dozmary Pool | Lake | 10.3 | 6.0 | 15.2 | 1271 | 422 | 236 |
| 7 | Bajondillo | Cave | 16.6 | 10.5 | 23.4 | 542 | 223 | 27 |
| 8 | Laguna del maar de Fuentillejo | Lake | 16.1 | 8.1 | 25.4 | 474 | 156 | 47 |
| 9 | Padul-1 | Peat Bog | 16.6 | 9.6 | 24.9 | 417 | 157 | 23 |
| 10 | Padul-2 | Peat Bog | 16.6 | 9.6 | 24.9 | 417 | 157 | 23 |
| 11 | Cova di Carihuela | Cave | 15.7 | 8.1 | 25.1 | 551 | 187 | 57 |
| 12 | Ifri El Baroud | Cave | 16.9 | 10.7 | 24.0 | 457 | 184 | 22 |
| 13 | MD95-2043 (M) | Marine | 17.9 | 12.4 | 24.0 | 214.2 | 37 | 72 |
| 14 | San Rafael | Peat Bog | 18.1 | 11.9 | 24.9 | 243 | 87 | 14 |
| 15 | Siles | Lake | 14.4 | 6.8 | 23.4 | 658 | 195 | 92 |
| 16 | Torreçilla de Valmadrid | Colluvium | 14.2 | 6.6 | 22.5 | 390 | 75 | 82 |
| 17 | Navarrés-1 | Peat Bog | 17.0 | 10.9 | 23.8 | 421 | 96 | 51 |
| 18 | Navarrés-2 | Peat Bog | 17.0 | 10.9 | 23.8 | 421 | 96 | 51 |
| 19 | Tourbiere de l'Estarres | Lake | 13.0 | 6.1 | 20.4 | 1045 | 272 | 217 |
| 20 | Cova de les Malladetes | Cave | 18.1 | 12.1 | 24.8 | 478 | 117 | 60 |
| 21 | Lourdes | Lake | 12.6 | 5.5 | 20.1 | 1002 | 256 | 212 |
| 22 | Lake Estanya | Lake | 12.8 | 5.1 | 21.0 | 641 | 125 | 152 |
| 23 | Freychinede | Lake | 10.8 | 3.9 | 19.0 | 1128 | 257 | 277 |
| 24 | Banyoles | Lake | 14.3 | 7.7 | 21.9 | 698 | 157 | 139 |
| 25 | Lac du Bouchet B5 | Lake | 8.2 | 1.3 | 15.9 | 1070 | 251 | 221 |
| 26 | MD99-2348 (103) (M) | Marine | 14.6 | 8.0 | 21.9 | 618 | 158 | 95 |
| 27 | Les Echets G | Peat Bog | 11.4 | 3.6 | 19.6 | 876 | 175 | 215 |
| 28 | La Grotte Walou | Cave | 10.3 | 3.2 | 17.0 | 903 | 215 | 249 |
| 29 | Bergsee | Lake | 9.6 | 1.4 | 17.6 | 1048 | 189 | 387 |
| 30 | Garaat El-Ouez | Peat Bog | 17.3 | 11.0 | 24.3 | 830 | 360 | 33 |
| 31 | Pian del Lago | Lake | 12.4 | 5.1 | 20.0 | 995 | 266 | 149 |
| 32 | Pilsensee | Lake | 9.3 | 0.6 | 17.7 | 947 | 151 | 374 |
| 33 | Orgiano | Peat Bog | 13.0 | 3.3 | 22.3 | 907 | 200 | 228 |
| 34 | Lago della Costa | Lake | 12.9 | 3.3 | 22.1 | 888 | 196 | 224 |
| 35 | Lagaccione | Lake | 14.2 | 7.2 | 21.7 | 705 | 203 | 109 |
| 36 | Lago Vico | Lake | 13.7 | 6.4 | 21.5 | 870 | 258 | 132 |
| 37 | Stracciacappa | Lake | 14.6 | 7.3 | 22.4 | 867 | 266 | 115 |
| 38 | Lago di Monterosi | Lake | 15.0 | 7.7 | 22.9 | 837 | 248 | 115 |
| 39 | Venice | Peat Bog | 13.4 | 4.5 | 22.1 | 1050 | 221 | 277 |
| 40 | Azzano Decimo | Alluvial Fan | 13.3 | 4.4 | 22.1 | 1170 | 241 | 311 |
| 41 | Valle di Castiglione | Lake | 16.3 | 9.1 | 24.0 | 988 | 294 | 144 |
| 42 | Travesio | Lake | 12.6 | 3.7 | 21.3 | 1415 | 281 | 375 |
| 43 | Orvenco | Alluvial Fan | 13.0 | 3.3 | 22.3 | 907 | 200 | 228 |
| 44 | Rio Doidis | Lake | 12.8 | 4.1 | 21.2 | 1529 | 315 | 392 |
| 45 | Billerio | Lake | 12.8 | 4.1 | 21.2 | 1529 | 315 | 392 |
| 46 | Kersdorf-Briesen | Lake | 8.8 | -1.0 | 17.9 | 538 | 110 | 175 |
| 47 | Lago Grande di Monticchio | Lake | 11.5 | 4.1 | 19.8 | 518 | 154 | 76 |
| 48 | Nagymohos | Peat Bog | 9.5 | -1.5 | 19.1 | 616 | 103 | 230 |
| 49 | Safarka | Peat Bog | 7.0 | -3.2 | 16.0 | 755 | 119 | 280 |
| 50 | Feher Lake | Lake | 11.0 | -0.1 | 20.7 | 546 | 112 | 185 |
| 51 | Ioannina | Peat Bog | 14.7 | 6.5 | 23.3 | 1000 | 364 | 98 |
| 52 | Kokad | Peat Bog | 10.2 | -0.9 | 19.8 | 601 | 130 | 204 |
| 53 | Lake Xinias | Lake | 15.6 | 7.5 | 24.1 | 563 | 211 | 47 |
| 54 | Mickunai | Lake | 6.0 | -5.0 | 16.3 | 682 | 131 | 230 |
| 55 | Lake Sfanta Anna | Lake | 11.6 | 5.2 | 18.4 | 867 | 253 | 172 |
| 56 | Megali Limni | Lake | 15.5 | 8.2 | 23.4 | 684 | 357 | 28 |
| 57 | Straldzha | Peat Bog | 12.5 | 2.6 | 21.8 | 591 | 158 | 135 |
| 58 | MD01-2430 (M) | Marine | 18.0 | 8.7 | 27.5 | 595 | 219 | 75 |
| 59 | Lake Iznik | Lake | 13.9 | 6.1 | 21.8 | 677 | 250 | 85 |
| 60 | M72/5 628-1 (M) | Marine | 14.5 | 8.0 | 21.6 | 857 | 251 | 156 |
| 61 | Dziguta | Peat Bog | 14.1 | 6.6 | 21.7 | 1549 | 409 | 373 |
| 62 | Lake Van LG | Lake | 12.0 | 0.9 | 23.1 | 635 | 201 | 34 |
| 63 | Lake Zeribar | Lake | 17.1 | 5.0 | 29.0 | 427 | 167 | 6 |

2289
2290
2291
2292
2293

Table A2. Modern climate values for each site used in the calculation of anomalies (taken from WorldClim 2, Fick & Hijmans 2017)

2294
2295
2296

| Change in Biome compared to the Control | | | | | | | | | |
|---|-------------|-------------|--------------|---------------|---------------|---------------|----------------|----------------|----------------|
| Biome | Control | 0 Pinaceae | +5% Pinaceae | +10% Pinaceae | +20% Pinaceae | +50% Pinaceae | +100% Pinaceae | +200% Pinaceae | +400% Pinaceae |
| CLDE | 25 | 454 | 0 | 0 | 0 | -1 | -1 | -4 | -4 |
| TAIG | 1489 | -1430 | 16 | 38 | 74 | 192 | 337 | 554 | 914 |
| CLMX | 70 | 108 | 1 | 2 | 3 | -6 | -4 | 4 | 6 |
| COCO | 388 | -388 | 0 | -1 | 3 | 6 | 25 | 50 | 74 |
| TEDE | 33 | 16 | 1 | 1 | 1 | -1 | -2 | -8 | -5 |
| COMX | 2952 | -761 | 1 | 8 | 14 | -4 | -42 | -101 | -284 |
| WAMX | 418 | -28 | -1 | 0 | -1 | -6 | -11 | -29 | -62 |
| XERO | 699 | -323 | 3 | 4 | 12 | 45 | 68 | 113 | 180 |
| DESE | 0 | 0 | 0 | 0 | 0 | 0 | 0 | 0 | 0 |
| STEP | 1752 | 1388 | -14 | -39 | -83 | -173 | -296 | -468 | -663 |
| TUND | 387 | 964 | -7 | -13 | -23 | -52 | -74 | -111 | -156 |
| Total | 8213 | 5860 | 44 | 106 | 214 | 486 | 860 | 1442 | 2348 |

2297
2298
2299
2300
2301
2302
2303
2304
2305
2306
2307
2308
2309
2310
2311
2312
2313
2314
2315
2316
2317

Table A3. This shows the results of experiment to test the sensitivity of pollen Biomes to changes in the amount of Pinaceae in the pollen assemblage using 8213 modern pollen samples from the EMPD2. Pinaceae can be over-represented in marine samples, and it has been proposed that removing all Pinaceae from these samples is better than leaving the Pinaceae in the pollen assemblage. The 'Control' column on the left shows the number of samples that were classified for each Biome without changing the amount of Pinaceae (ie using the original pollen assemblage). The other 8 columns to the right show the number of samples where the Biome changed relative to the number shown in the control column as a result of either removal of all Pinaceae ('0 Pinaceae'), or by artificially increasing the amount of Pinaceae respectively from 5 to 400% of the original count ('+5% Pinaceae' to '+400% Pinaceae'). For instance, for the CLDE (Cold Deciduous) Biome, 25 pollen samples were classified as CLDE without any change in Pinaceae ('Control'), but 454 more samples were classified as CLDE when all Pinaceae was removed ('0 Pinaceae') compared to 4 fewer samples that were classified as CLDE when Pinaceae was increased by as much as 400% ('+400% Pinaceae'). The totals along the bottom show that out of the 8213 pollen samples included in the experiment, 5860 biomes changed when all Pinaceae was removed, compared to up to 2348 when Pinaceae was artificially increased by up to 400%.

2318

Temperature Anomaly

| Site Name | Site Number | TANN delta | | TDJF delta | | TJJA delta | | PANN delta | | PDJF delta | | PJJA delta | |
|---------------------|-------------|------------|-------------|------------|-------------|------------|-------------|------------|-------------|------------|-------------|------------|-------------|
| | | Pinaceae | No Pinaceae | Pinaceae | No Pinaceae | Pinaceae | No Pinaceae | Pinaceae | No Pinaceae | Pinaceae | No Pinaceae | Pinaceae | No Pinaceae |
| MD95-2039 (M) | 1 | -10.5 | -12.3 | -14.6 | -17.9 | -5.7 | -5.9 | -234.3 | -236.3 | -205.4 | -196.4 | 83.1 | 63.0 |
| SU81-18 (M) | 2 | -13.3 | -21.4 | -15.2 | -23.0 | -10.4 | -17.7 | 183.3 | 703.2 | -21.1 | 124.4 | 85.1 | 167.7 |
| MD99-2331 (M) | 3 | -5.3 | -4.8 | -7.5 | -7.0 | -2.3 | -1.4 | -420.6 | -435.6 | -257.7 | -251.1 | 39.4 | 19.0 |
| MD95-2043 (M) | 13 | -7.0 | -6.0 | -11.0 | -9.9 | -3.6 | -2.7 | 304.6 | 332.5 | 178.4 | 201.9 | -17.3 | -22.9 |
| MD99-2348 (103) (M) | 26 | -7.8 | -8.8 | -10.0 | -11.5 | -6.5 | -7.3 | 164.7 | 218.0 | 12.1 | 7.6 | 124.0 | 179.5 |
| MD01-2430 (M) | 58 | -11.1 | -13.5 | -11.3 | -14.5 | -11.0 | -12.8 | 200.6 | 349.1 | -20.8 | 31.4 | 113.1 | 127.9 |
| M72/5 628-1 (M) | 60 | -2.3 | -0.5 | -4.9 | -3.0 | -0.2 | 1.7 | -298.0 | -311.1 | -116.8 | -100.1 | -27.0 | -51.7 |
| Site Average | | -8.2 | -9.6 | -10.6 | -12.4 | -5.7 | -6.6 | -14.2 | 88.5 | -61.6 | -26.0 | 57.2 | 68.9 |

Standard Deviation

| Site Name | Site Number | TANN STDEV | | TDJF STDEV | | TJJA STDEV | | PANN STDEV | | PDJF STDEV | | PJJA STDEV | |
|---------------------|-------------|------------|-------------|------------|-------------|------------|-------------|------------|-------------|------------|-------------|------------|-------------|
| | | Pinaceae | No Pinaceae | Pinaceae | No Pinaceae | Pinaceae | No Pinaceae | Pinaceae | No Pinaceae | Pinaceae | No Pinaceae | Pinaceae | No Pinaceae |
| MD95-2039 (M) | 1 | 4.6 | 3.7 | 7.5 | 4.0 | 2.9 | 4.0 | 330.6 | 268.9 | 110.5 | 96.7 | 53.6 | 55.6 |
| SU81-18 (M) | 2 | 3.1 | 4.0 | 4.0 | 3.4 | 2.8 | 4.8 | 297.1 | 149.3 | 126.6 | 58.0 | 47.3 | 28.4 |
| MD99-2331 (M) | 3 | 2.9 | 4.0 | 3.4 | 3.8 | 2.8 | 5.0 | 302.6 | 368.6 | 103.5 | 134.2 | 57.6 | 64.3 |
| MD95-2043 (M) | 13 | 2.0 | 4.7 | 2.4 | 5.6 | 2.1 | 4.1 | 115.9 | 121.5 | 59.3 | 72.1 | 36.2 | 25.2 |
| MD99-2348 (103) (M) | 26 | 2.4 | 3.8 | 3.0 | 4.2 | 2.7 | 4.6 | 192.7 | 242.9 | 75.8 | 68.2 | 58.9 | 52.1 |
| MD01-2430 (M) | 58 | 5.1 | 2.3 | 8.1 | 2.0 | 3.9 | 2.8 | 218.7 | 182.8 | 78.9 | 58.3 | 53.4 | 45.0 |
| M72/5 628-1 (M) | 60 | 3.2 | 3.9 | 3.8 | 4.0 | 3.5 | 4.6 | 149.0 | 171.9 | 67.1 | 48.2 | 56.5 | 61.8 |
| Site Average | | 3.3 | 3.8 | 4.6 | 3.9 | 3.0 | 4.3 | 229.5 | 215.1 | 88.8 | 76.5 | 51.9 | 47.5 |

2319
2320
2321
2322
2323
2324
2325
2326
2327
2328
2329
2330
2331
2332

Table A4. A comparison of the LGM reconstructed climate for marine sites showing the effect of excluding Pinaceae (shaded) from the pollen assemblage, compared to the results of including Pinaceae (unshaded, also presented in Figures 6-8). It has been proposed that because of the potential for over-representation of Pinaceae in marine pollen samples, it is better to exclude Pinaceae completely from marine pollen samples. Comparing the two approaches, temperatures are generally 1-2C cooler, and precipitation slightly higher when Pinaceae is excluded. The differences for both temperature and precipitation are significantly less than the standard deviation of their uncertainties.

| | All surface samples | | Steppe only | |
|------|---------------------|------|-------------|------|
| | RMSE | R2 | RMSE | R2 |
| TANN | 2.28 | 0.9 | 2.51 | 0.87 |
| TDJF | 3.35 | 0.91 | 3.26 | 0.88 |
| TJJA | 2.21 | 0.81 | 2.49 | 0.82 |
| PANN | 224.94 | 0.69 | 185.7 | 0.71 |
| PDJF | 78.51 | 0.69 | 66.5 | 0.66 |
| PJJA | 52.49 | 0.75 | 43.8 | 0.79 |

2333
2334
2335
2336
2337
2338
2339
2340
2341
2342
2343

Table A53. A comparison of MAT performance statistics based on the modern pollen sample training set using all surface samples from the EMPD2 used in the LGM reconstruction (as shown in Table 3), and a subset of 1588 samples from the EMPD2 that were classified as steppe. The results show little difference between the two different types of samples. The table includes Mean Annual Temperature and Precipitation (TANN and PANN), Mean Winter Temperature and Precipitation (TDJF and PDJF) and Mean Summer Temperature and Precipitation (TJJA and PJJA).

| Site Name | Site# | Pollen Biome | Modern Analogue Biome | Modern Analogue Ecoregion |
|--------------------------------|-------|--------------|---|--|
| MD95-2039 | 1 | XERO | Mediterranean Forests, woodlands and scrubs | Iberian conifer forests |
| SU81-18 | 2 | COMX | Mediterranean Forests, woodlands and scrubs | Iberian conifer forests |
| MD99-2331 | 3 | STEP | Mediterranean Forests, woodlands and scrubs | Alps conifer and mixed forests |
| Carn Morval | 4 | STEP | Temperate broadleaf and mixed forests | North Atlantic moist mixed forests |
| Gorham Cave | 5 | STEP | Mediterranean Forests, woodlands and scrubs | Cyprus Mediterranean forests |
| Dozmary Pool | 6 | STEP | Temperate Coniferous Forest | Alps conifer and mixed forests |
| Bajondillo | 7 | STEP | Temperate broadleaf and mixed forests | Central European mixed forests |
| Laguna del maar de Fuentillejo | 8 | COMX | Mediterranean Forests, woodlands and scrubs | Northwest Iberian montane forests |
| Padul | 9 | STEP | Mediterranean Forests, woodlands and scrubs | Central Anatolian steppe |
| Padul-15-05 | 10 | WAMX | Mediterranean Forests, woodlands and scrubs | Iberian sclerophyllous and semi-deciduous forests |
| Cova di Carhuela | 11 | STEP | Deserts and xeric shrublands | Azerbaijan shrub desert and steppe |
| Ifri El Baroud | 12 | STEP | Mediterranean Forests, woodlands and scrubs | Iberian sclerophyllous and semi-deciduous forests |
| MD95-2043 | 13 | CLMX | Mediterranean Forests, woodlands and scrubs | Southern Anatolian montane conifer and deciduous forests |
| San Rafael | 14 | XERO | Mediterranean Forests, woodlands and scrubs | Tyrrhenian-Adriatic Sclerophyllous and mixed forests |
| Siles | 15 | XERO | Mediterranean Forests, woodlands and scrubs | Northwest Iberian montane forests |
| Torreçilla de Valmadrid | 16 | STEP | Mediterranean Forests, woodlands and scrubs | Southern Anatolian montane conifer and deciduous forests |
| Navarres | 17 | XERO | Mediterranean Forests, woodlands and scrubs | Iberian sclerophyllous and semi-deciduous forests |
| Navarres | 18 | STEP | Temperate broadleaf and mixed forests | Pyrenees conifer and mixed forests |
| Tourbiere de Istarres | 19 | STEP | Temperate grasslands, savannas and shrublands | Eastern Anatolian montane steppe |
| Cova de les Malladetes | 20 | XERO | Mediterranean Forests, woodlands and scrubs | Pyrenees conifer and mixed forests |
| Lourdes | 21 | STEP | Temperate broadleaf and mixed forests | Gissaro-Alai open woodlands |
| Estanya | 22 | XERO | Temperate broadleaf and mixed forests | Western Siberian hemiboreal forests |
| Freychinede | 23 | STEP | Temperate grasslands, savannas and shrublands | Mongolian-Manchurian grassland |
| Lake Banyoles | 24 | STEP | Temperate grasslands, savannas and shrublands | Gissaro-Alai open woodlands |
| Lac du Bouchet B5 | 25 | STEP | Temperate grasslands, savannas and shrublands | Gissaro-Alai open woodlands |
| MD99-2348-103 | 26 | COMX | Temperate broadleaf and mixed forests | Rodope montane mixed forests |
| Les Echets G - DIGI | 27 | STEP | Temperate broadleaf and mixed forests | Western Siberian hemiboreal forests |
| La Grotte Walou | 28 | STEP | Temperate broadleaf and mixed forests | Kazakh forest steppe |
| Bergsee | 29 | STEP | Temperate broadleaf and mixed forests | Kazakh forest steppe |
| Garaat El-Ouez | 30 | STEP | Mediterranean Forests, woodlands and scrubs | Anatolian conifer and deciduous mixed forests |
| Pian del Lago | 31 | COMX | Temperate broadleaf and mixed forests | Western European broadleaf forests |
| Pilsensee | 32 | TAIG | Tundra | Kola Peninsula tundra |
| Orgiano | 33 | COMX | Temperate broadleaf and mixed forests | Western European broadleaf forests |
| Lago della Costa | 34 | COMX | Temperate Coniferous Forest | Alps conifer and mixed forests |
| Lagaccione | 35 | STEP | Temperate grasslands, savannas and shrublands | Gissaro-Alai open woodlands |
| Lago Vico | 36 | STEP | Temperate grasslands, savannas and shrublands | Gissaro-Alai open woodlands |
| Stracciaccia | 37 | STEP | Mediterranean Forests, woodlands and scrubs | Western European broadleaf forests |
| Lago di Monterosi | 38 | STEP | Temperate grasslands, savannas and shrublands | Northwest Iberian montane forests |
| Venice | 39 | XERO | Tundra | Scandinavian Montane Birch forest and grasslands |
| Azzano Decimo | 40 | XERO | Temperate broadleaf and mixed forests | Scandinavian Montane Birch forest and grasslands |
| Valle di Castiglione | 41 | STEP | Temperate broadleaf and mixed forests | Tian Shan montane steppe and meadows |
| Travesio | 42 | XERO | Mediterranean Forests, woodlands and scrubs | Iberian conifer forests |
| Orvenco | 43 | TAIG | Temperate broadleaf and mixed forests | Western Siberian hemiboreal forests |
| Rio Doidis | 44 | XERO | Mediterranean Forests, woodlands and scrubs | Cyprus Mediterranean forests |
| Billerio | 45 | TAIG | Temperate broadleaf and mixed forests | Western Siberian hemiboreal forests |
| Kersdorf-Briesen | 46 | TAIG | Temperate broadleaf and mixed forests | Western Siberian hemiboreal forests |
| Lago Grande di Monticchio | 47 | STEP | Temperate broadleaf and mixed forests | Tian Shan montane steppe and meadows |
| Nagymohos Pleistocene | 48 | STEP | Tundra | Sarmatic mixed forests |
| Safarka | 49 | TAIG | Boreal forests / Taiga | Ural montane forests and tundra |
| Feher-to | 50 | COMX | Temperate Coniferous Forest | Alps conifer and mixed forests |
| Ioannina | 51 | STEP | Temperate broadleaf and mixed forests | Central European mixed forests |
| Kokad | 52 | STEP | Temperate broadleaf and mixed forests | East European forest steppe |
| Lake Xinias | 53 | STEP | Temperate broadleaf and mixed forests | Western European broadleaf forests |
| Mickunai | 54 | COCO | Tundra | Scandinavian Montane Birch forest and grasslands |
| Lake Sfanta Anna | 55 | COMX | Temperate Coniferous Forest | Alps conifer and mixed forests |
| Lesvos ML01 Megali Limni | 56 | STEP | Temperate broadleaf and mixed forests | Rodope montane mixed forests |
| Straldzha | 57 | STEP | Temperate broadleaf and mixed forests | Aegean and Western Turkey sclerophyllous and mixed forests |
| MD01-2430 | 58 | STEP | Temperate broadleaf and mixed forests | Euxine-Colchic broadleaf forests |
| Lake Iznik | 59 | STEP | Temperate broadleaf and mixed forests | Tian Shan montane steppe and meadows |
| M72/5 628-1 | 60 | STEP | Deserts and xeric shrublands | Azerbaijan shrub desert and steppe |
| Dziguta Core 1 | 61 | CLMX | Temperate broadleaf and mixed forests | Northeastern Spain and Southern France Mediterranean forests |
| Lake Van LG | 62 | STEP | Mediterranean Forests, woodlands and scrubs | Aegean and Western Turkey sclerophyllous and mixed forests |
| Lake Zeribar | 63 | STEP | Temperate grasslands, savannas and shrublands | Pontic steppe |

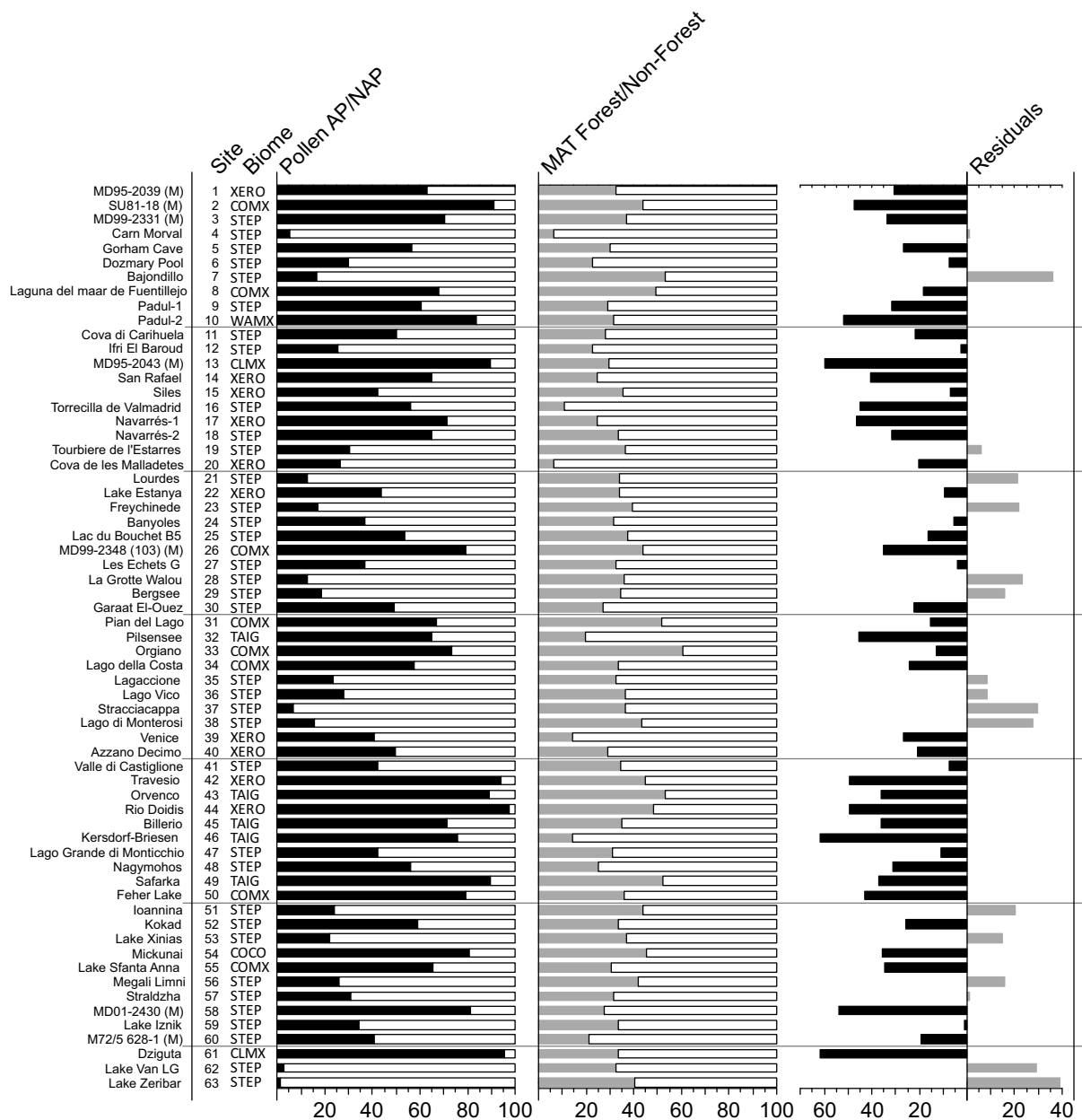
Notes: Modern analogue Biomes and Ecoregions were calculated as the most commonly occurring amongst all 6 best modern analogue pollen samples in all LGM samples for each pollen site/record. These are taken from the EMPD2 (Davis et al 2020), using the classification of Olsen et al 2001.

2344
2345
2346
2347
2348
2349
2350
2351

Table A46. The biome and ecoregion of the modern surface samples used as analogues in the pollen-climate reconstructions.

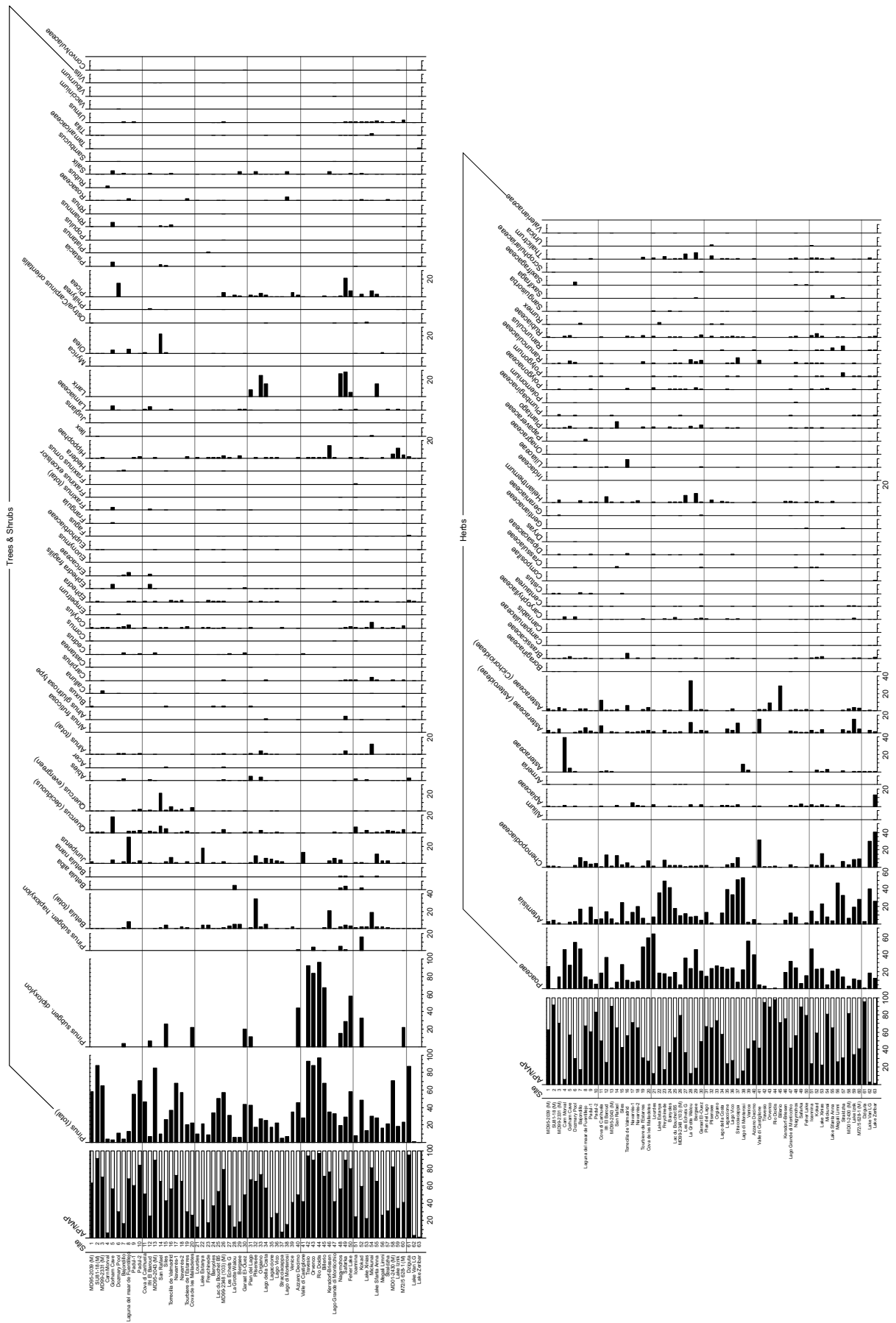
2352
 2353
 2354
 2355
 2356

Figures



2357
 2358
 2359
 2360
 2361

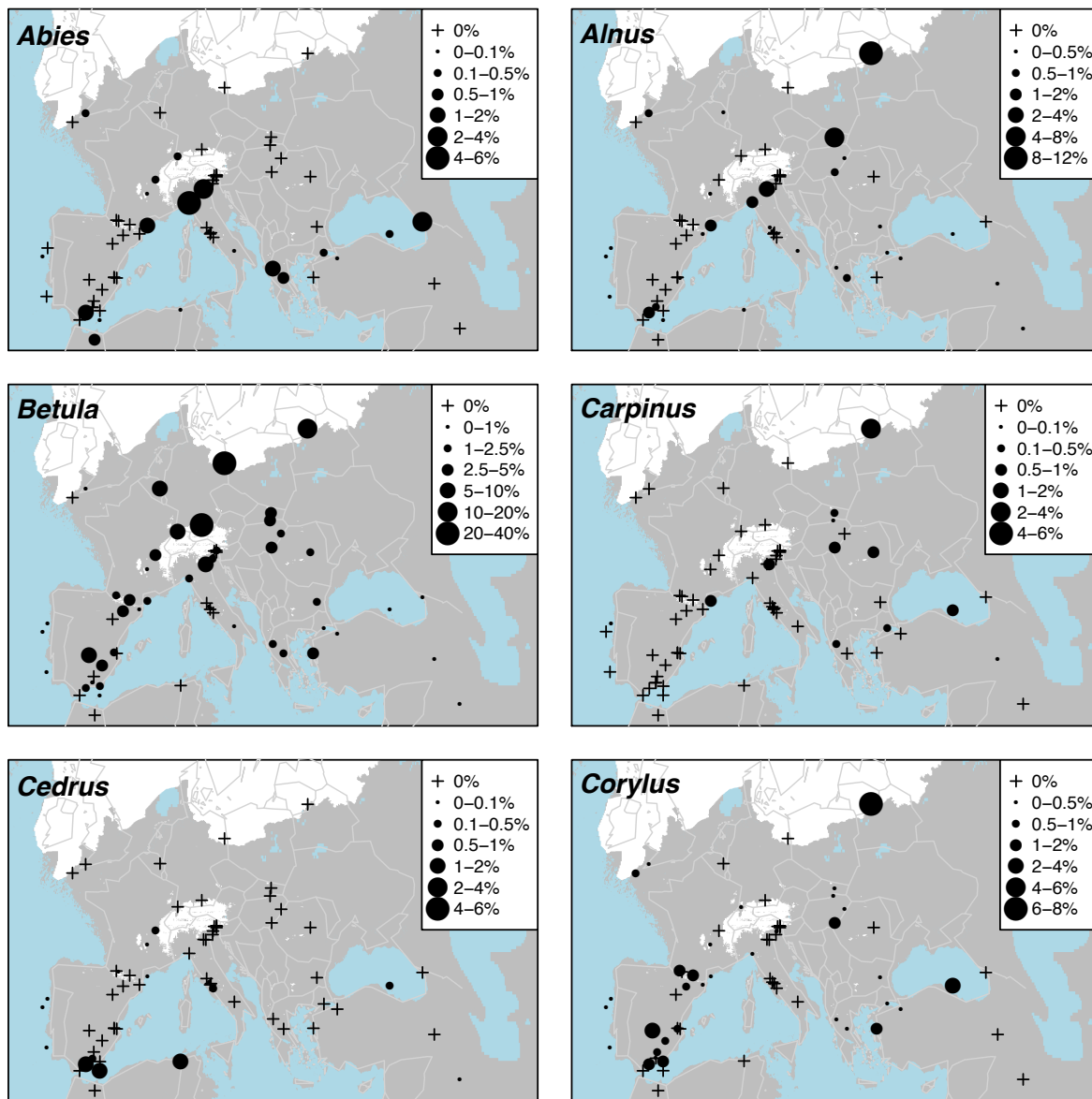
Figure A1. Pollen biomes (see figure 2 for key), Arboreal Pollen (AP) % forest cover, MAT % forest cover and residuals (AP % compared to MAT Forest %)



2362
2363

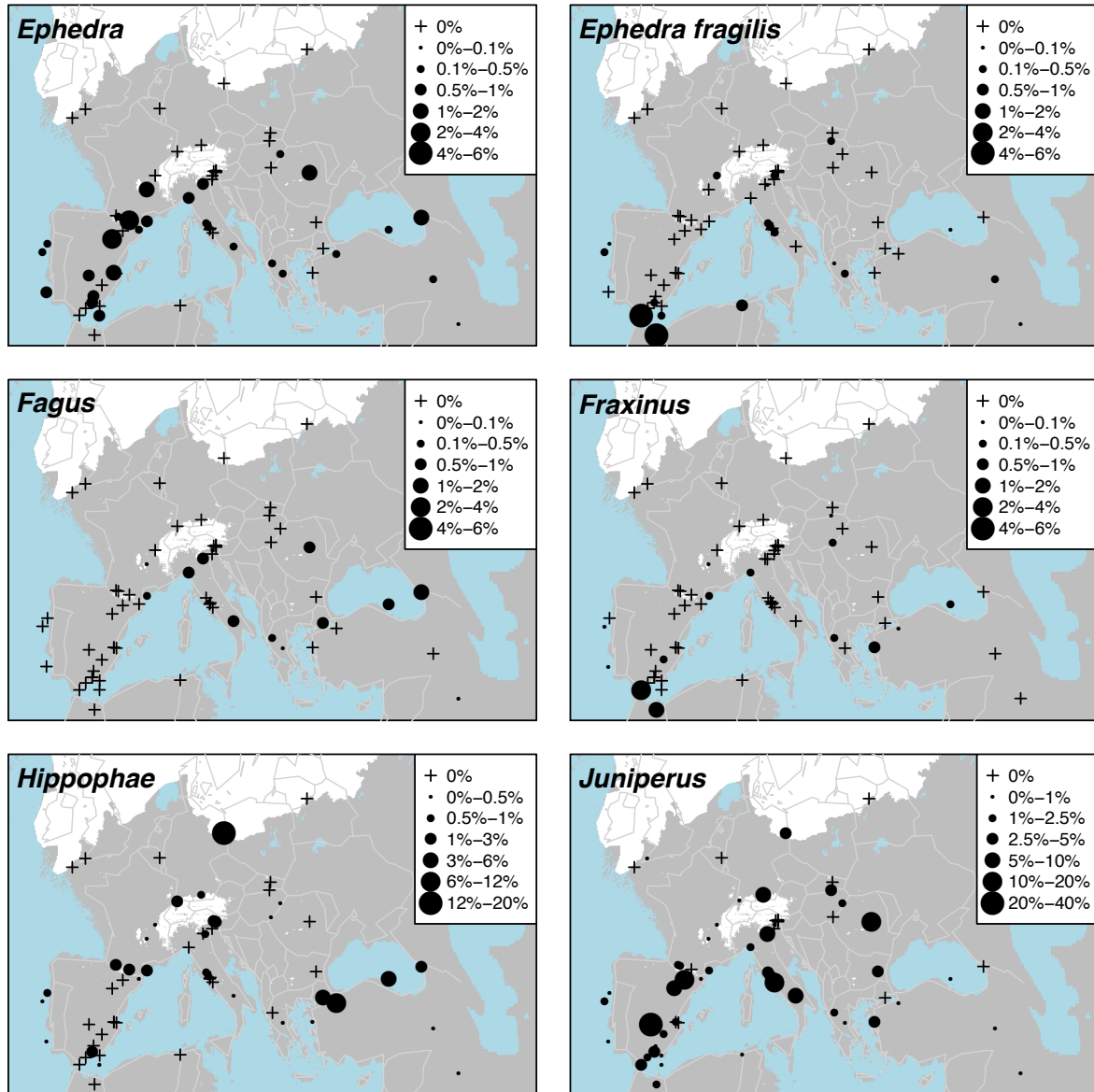
Figure A2. Pollen taxa percentages for all LGM sites/records

2364
2365
2366
2367



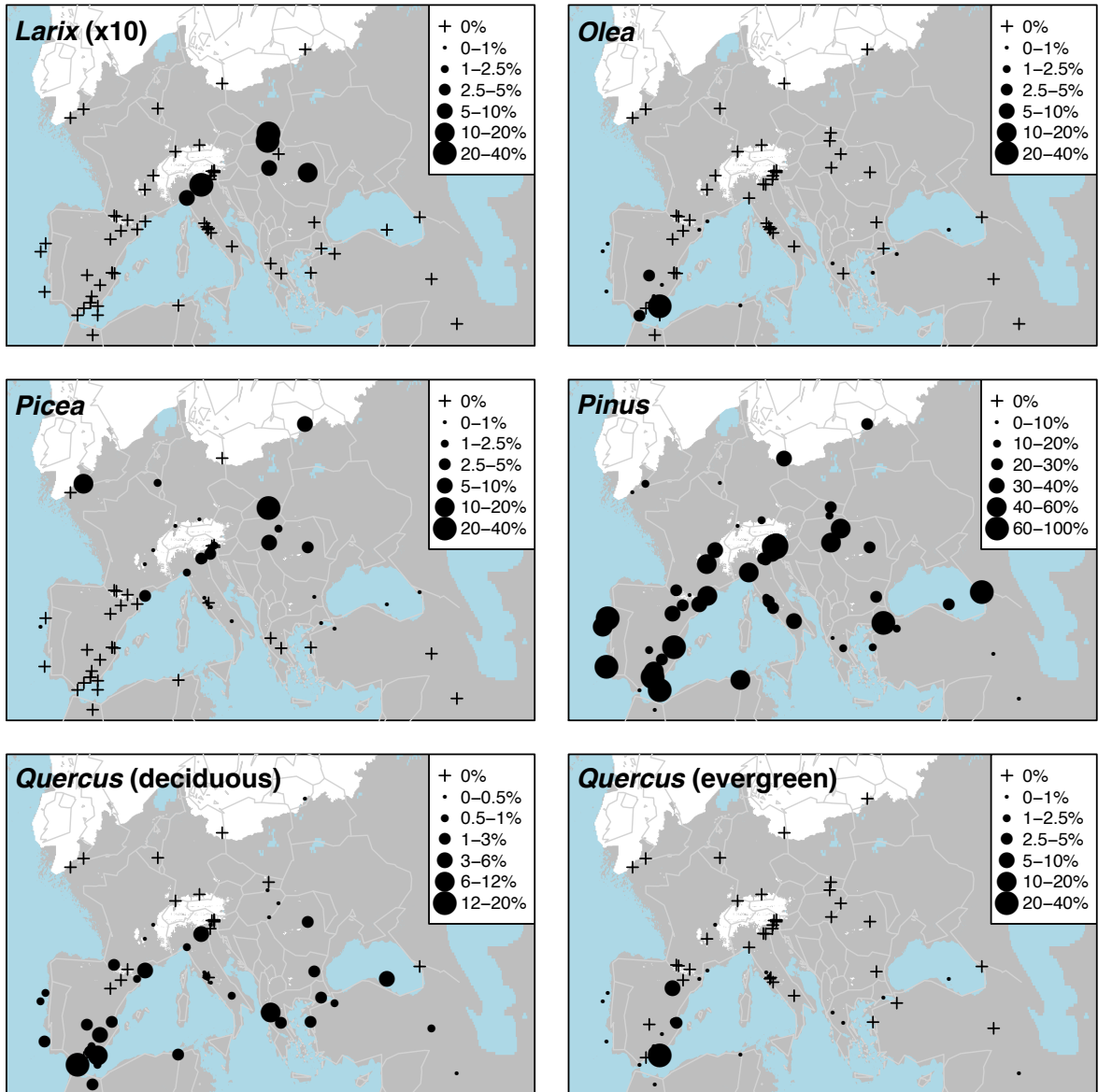
2368
2369
2370
2371

Figure A3a. Percentage maps of *Abies*, *Alnus*, *Betula*, *CarPinus*, *Cedrus* and *Corylus*



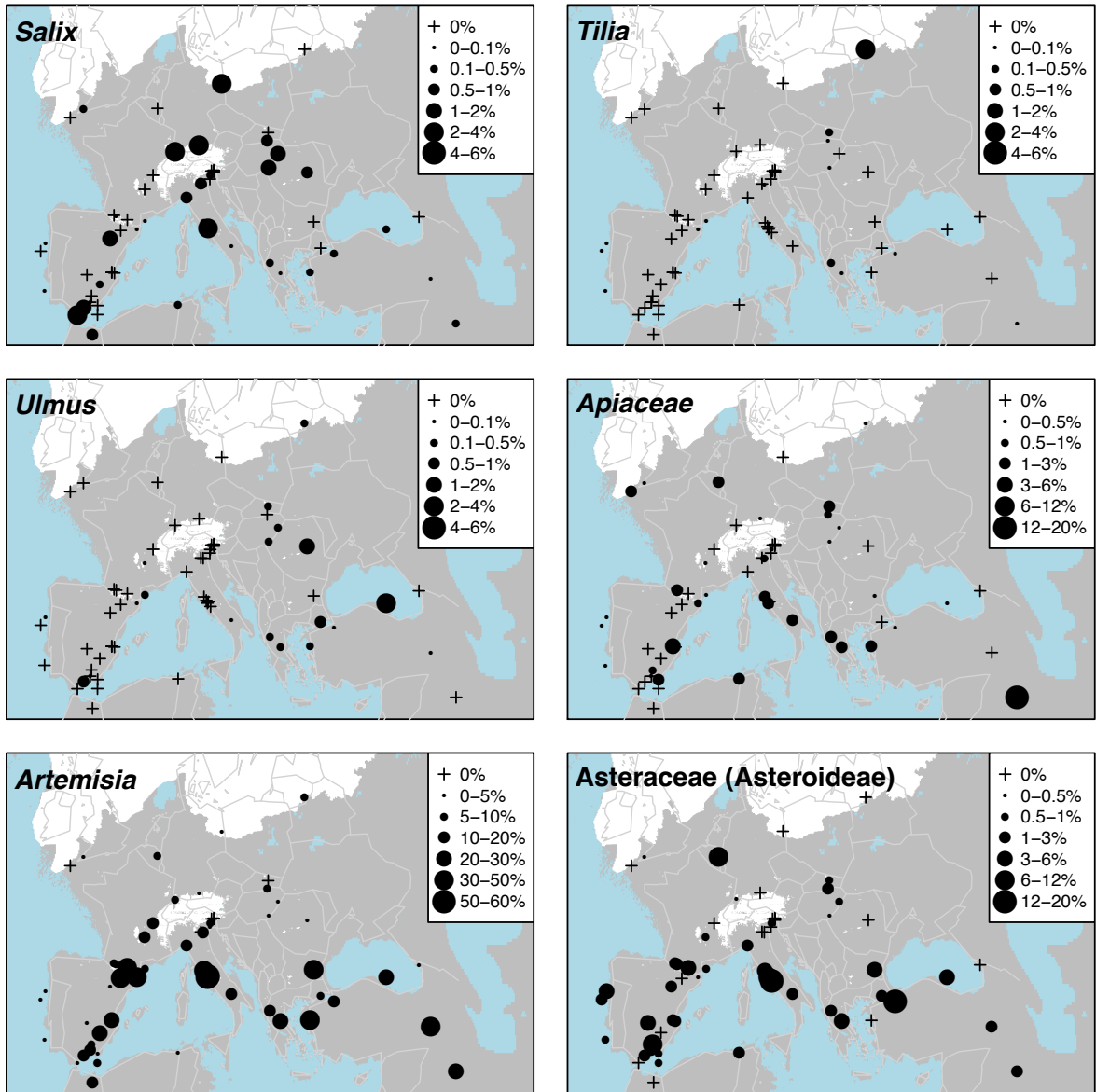
2372
 2373
 2374
 2375
 2376

Figure A3b. Percentage maps of *Ephedra*, *Ephedra fragilis*, *Fagus*, *Fraxinus*, *Hippophae* and *Juniperus*



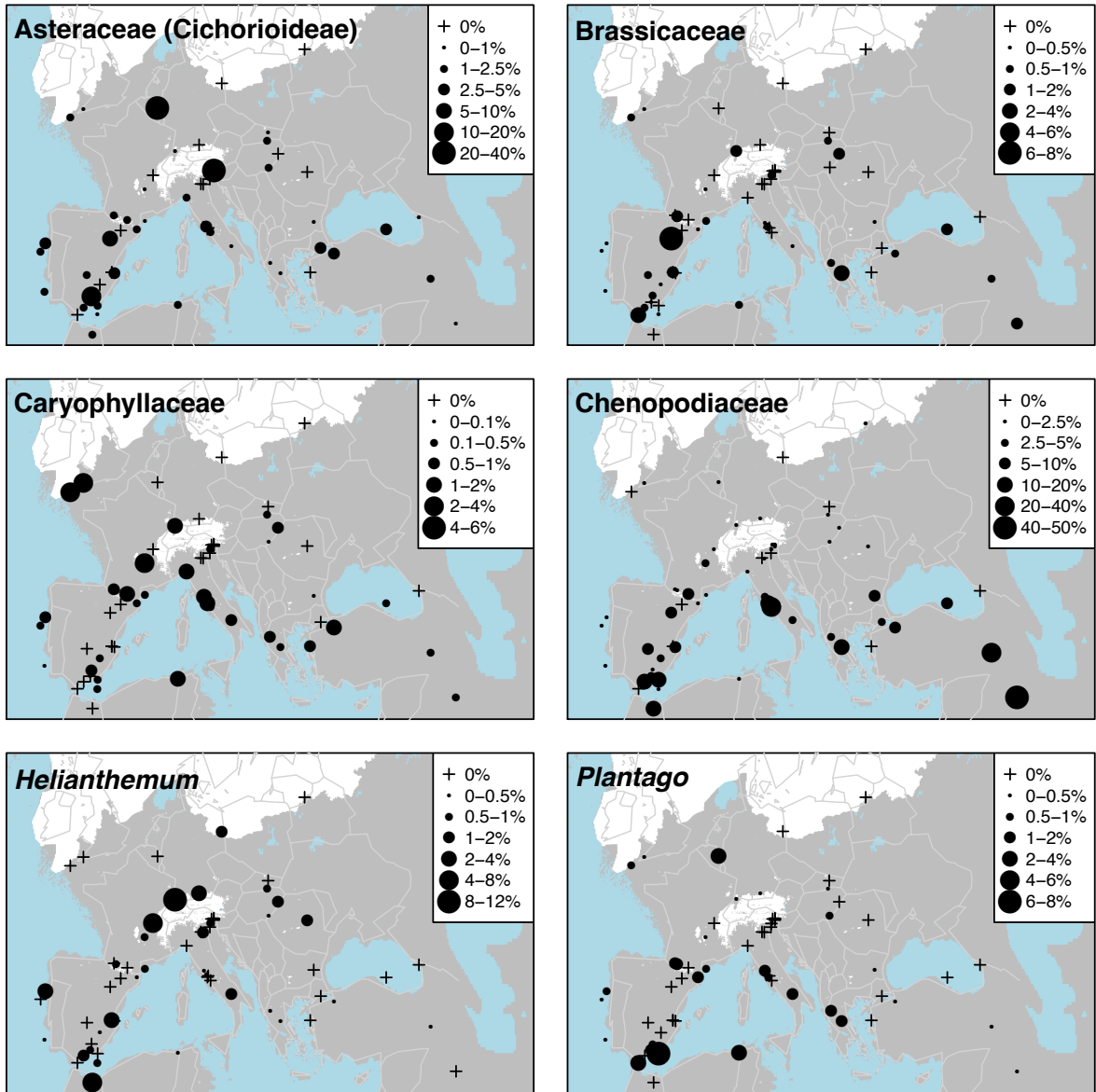
2377
 2378
 2379
 2380
 2381

Figure A3c. Percentage maps of *Larix* (x10 exaggeration), *Olea*, *Picea*, *Pinus*, *Quercus* (deciduous) and *Quercus* (evergreen)



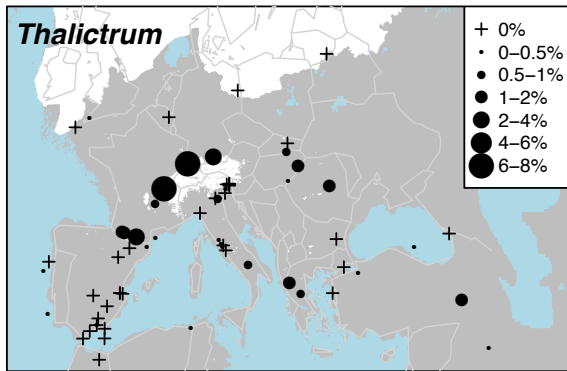
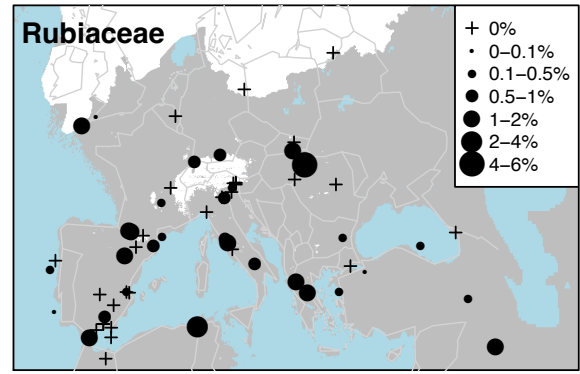
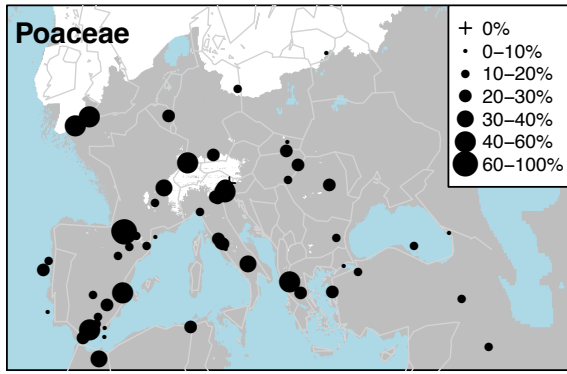
2382
 2383
 2384
 2385

Figure A3d. Percentage maps of *Salix*, *Tilia*, *Ulmus*, *Apiaceae*, *Artemisia* and *Asteraceae* (*Asteroideae*)



2386
 2387
 2388
 2389
 2390

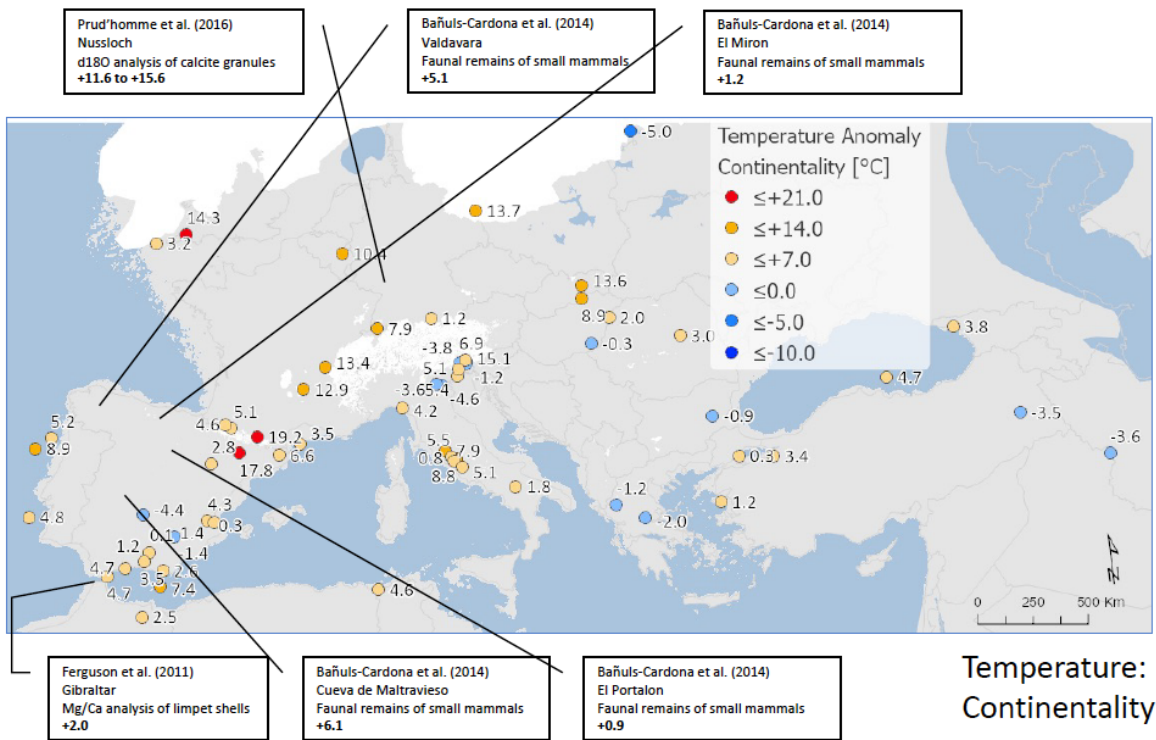
Figure A3e. Percentage maps of Asteraceae (Cichorioideae), Brassicaceae, Caryophyllaceae, Chenopodiaceae, Helianthemum and *Plantago*



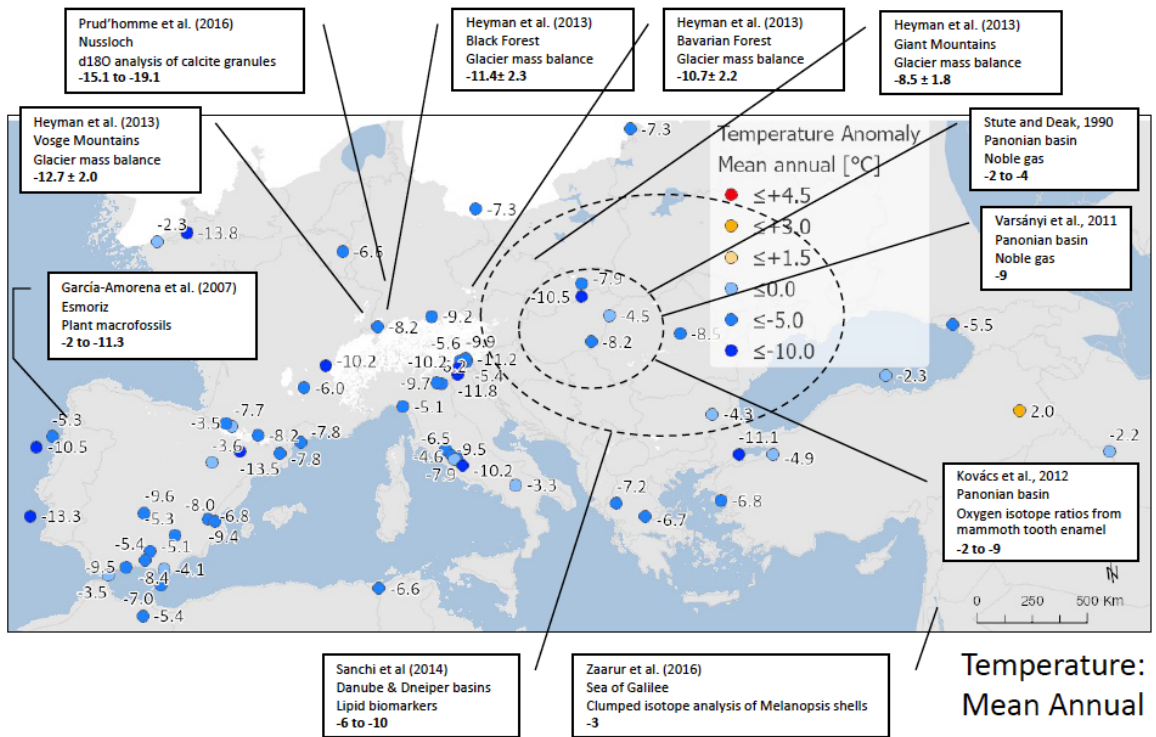
2391
 2392
 2393
 2394
 2395
 2396
 2397
 2398
 2399

Figure A3f. Percentage maps of Poaceae, Rubiaceae and *Thalictrum*

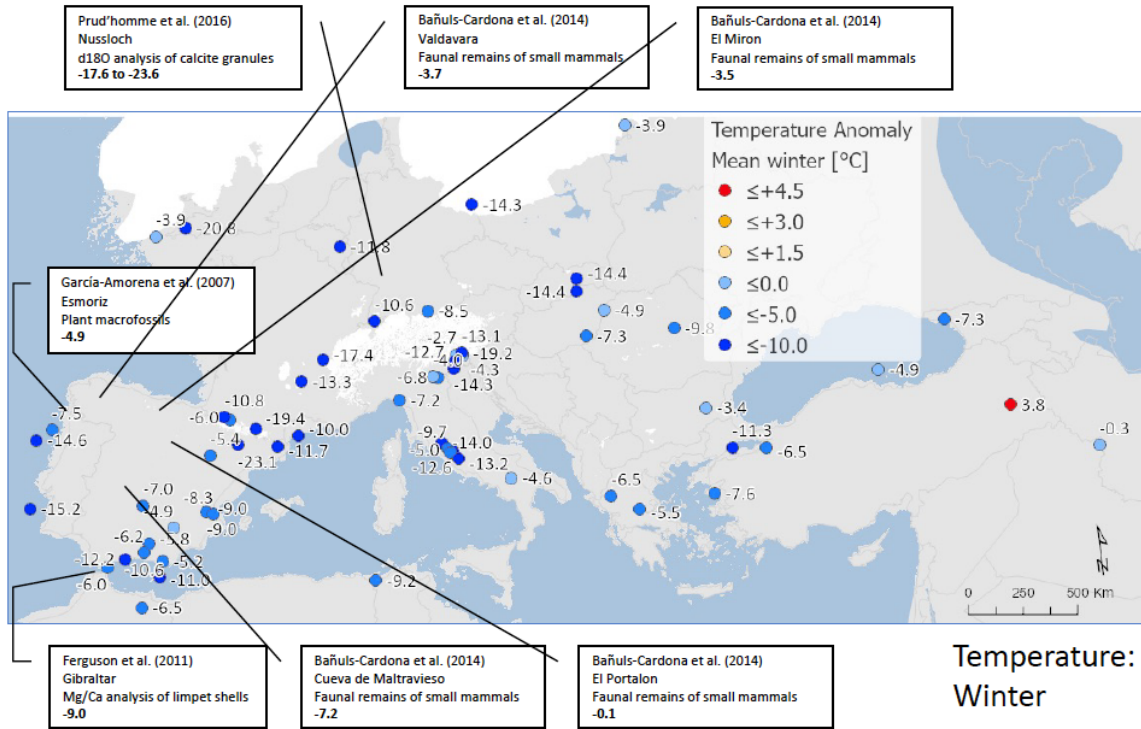
2400



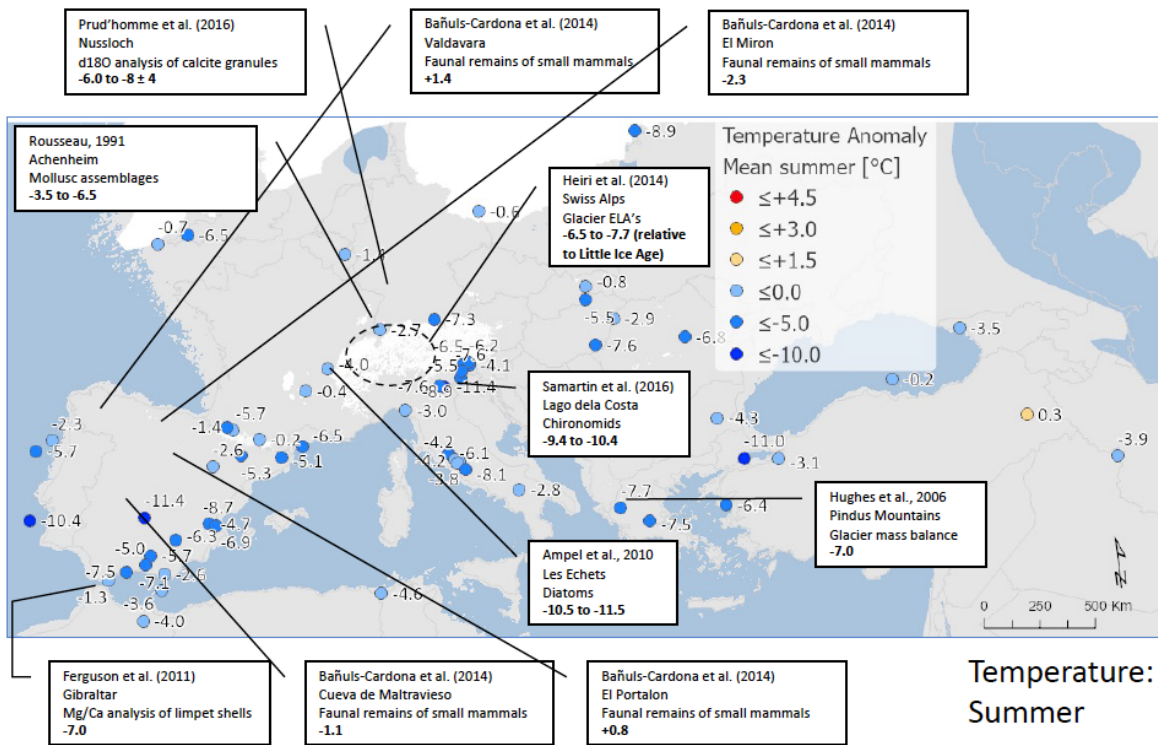
2401
2402



2403
2404
2405



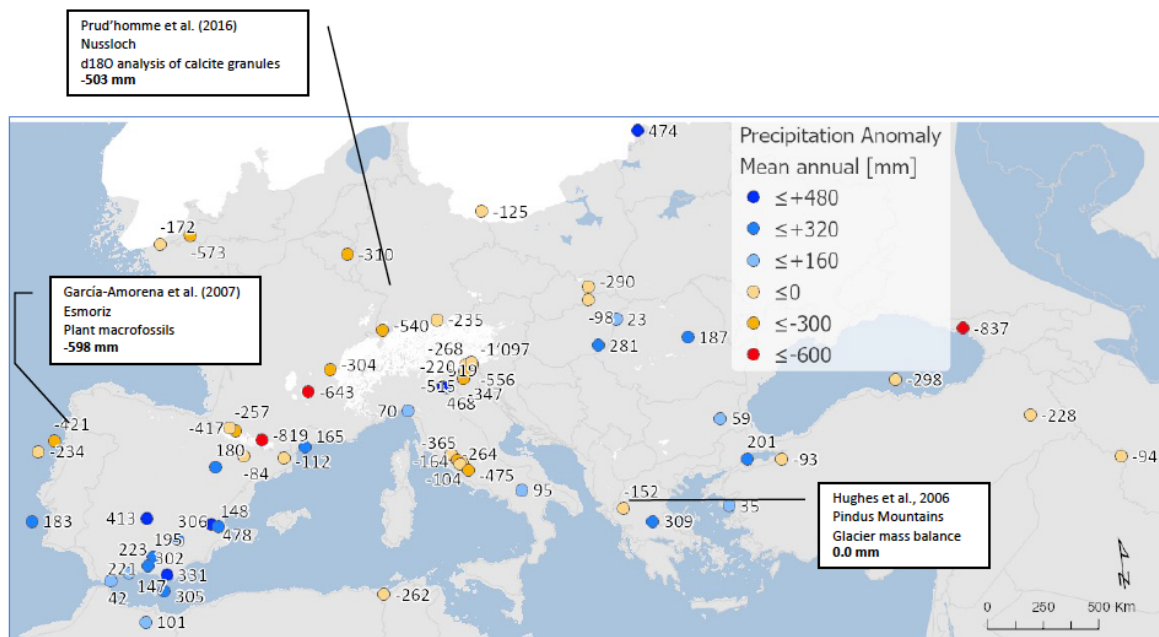
2406
2407



2408
2409

2410 Figure A4. Maps of pollen-based MAT reconstructions for LGM annual, winter and summer
 2411 temperature anomalies (as shown in figure 10), shown together with the results of other
 2412 published studies. Continentality represents the difference in temperature between summer
 2413 and winter, with positive anomalies indicating an increase in the temperature difference
 2414 between summer and winter. All values are expressed as anomalies compared with the
 2415 present day unless otherwise indicated.

2416



Precipitation:
Mean Annual

2417
2418
2419
2420
2421
2422

Figure A5. Maps of pollen-based MAT reconstructions for LGM annual precipitation anomalies (as shown in figure 12), shown together with the results of other published studies. All values are expressed as anomalies compared with the present day.

2423
2424